

Spring 1-1-2012

NSIDC Green Data Center Project: Coolerado and Modeling an Application of the Maisotsenko Cycle

Benjamin Weerts

University of Colorado at Boulder, benjamin.weerts@colorado.edu

Follow this and additional works at: http://scholar.colorado.edu/cven_gradetds



Part of the [Architectural Engineering Commons](#), and the [Energy Systems Commons](#)

Recommended Citation

Weerts, Benjamin, "NSIDC Green Data Center Project: Coolerado and Modeling an Application of the Maisotsenko Cycle" (2012). *Civil Engineering Graduate Theses & Dissertations*. Paper 19.

NSIDC GREEN DATA CENTER PROJECT: COOLERADO AND MODELING AN APPLICATION OF THE MAISOTSENKO CYCLE

Benjamin A. Weerts

B.S. Architectural Engineering

University of Colorado at Boulder 2012

A Thesis submitted to the
Faculty of the Graduate School of the
University of Colorado in partial fulfillment
of the requirement for the degrees of
Master of Science
Civil Engineering
2012

This thesis entitled:

NSIDC Green Data Center Project: Coolerado and Modeling an Application of the Maisotsenko Cycle

Written by: Benjamin A. Weerts

Has been approved for the Department of Civil, Environmental and Architectural Engineering

Michael Brandemuehl

Moncef Krarti

David Gallaher

Date_____

The final copy of this thesis has been examined by the signatories, and we
Find that both the content and the form meet acceptable presentation standards
Of scholarly work in the above mentioned discipline.

Benjamin A. Weerts (M.S., Department of Civil Engineering)

NSIDC Green Data Center Project: Coolerado and Modeling an Application of the Maisotsenko Cycle

Thesis directed by Professor Michael J. Brandemuehl

ABSTRACT

The National Snow and Ice Data Center recently replaced its traditional cooling system with a new air conditioning system that utilizes an economizer and Coolerado air conditioning units. These units represent one of the first commercially available applications of the Maisotsenko cooling cycle. A datalogging system was installed that measured the data center's power consumption before and after the cooling system was replaced. This data was organized and used to prove a 90% cooling energy reduction for the NSIDC. The data logging system also collected temperatures and humidities of inlet and outlet air of a Coolerado air conditioner. After using these data to validate a theoretical model developed by researchers at the National Renewable Energy Laboratory, the model was used to simulate slightly modified heat and mass exchanger designs of the Coolerado system to improve performance. Sensitivity analysis was performed and found a few design parameters that are important to the thermodynamic performance of the Coolerado system, while others were proved insignificant. Channel heights, sheet size and ambient pressure have the most significant impacts on the performance. Overall, it was found that the current design performs reasonably well and with minor modifications could perform optimally, as suggested by the theoretical model.

DEDICATION

This Thesis Report is dedicated to my parents, Richard and Jeri. While they may not understand much of my college academic work, they've been fully supportive for the past 17 years of my educational career, which culminates with the submission of this Thesis.

It is also dedicated to all of the building engineers in industry, who are striving to make a difference in the built environment where so many other outside factors make or break a project's success, often for reasons completely unrelated to the pursuit of the perfect engineering solution.

ACKNOWLEDGEMENTS

I'd like to thank Dave Gallaher for his support throughout the Green Data Center Project and this Thesis. Over two years ago, I was introduced to Dave and the Green Data Center Project at the NSIDC. Seeing this project move from the design stages through construction to the official grand opening in May 2012, I have gained invaluable experience with research level data collection and data logging networks, project management, web development, public educational outreach and professional conferences and awards. Thanks Dave, for these great opportunities.

To all the good people at Coolerado who are striving to change the world of cooling as we know it, and especially Daniel Zube and Lee Gillan, who have always been responsive to my questions and comments about their system, and helpful as I was writing this report. Thanks to Coolerado for partial funding for this research.

I'd like to thank Professor Michael Brandemuehl for responding to all of my questions about how to use my imperfect data to come to a conclusion, and also brainstorming what was happening when the system seemed to be operating unexpectedly.

It should be mentioned that without the help of Darren McSweeney (staff member of the ITLL), my first implementation of setting up a datalogging program would not have worked as expected. As an experienced programmer and DAQ professional, he was able to develop a program to handle minor errors and process power measurements correctly. Without his expertise, a year's worth of power consumption data of the old system would not have been reliable or consistent.

And to Eric Kozubal (NREL) for letting me use his theoretical model of the Coolerado system to perform this research.

TABLE OF CONTENTS

I.	Introduction.....	1
	Background.....	1
	Objective.....	2
II.	Motivation.....	2
	Data Centers and Energy Consumption.....	2
	National and International Efforts or Ideas to Increase Efficiencies.....	9
	NSIDC Power and Energy Use.....	11
	Old System.....	12
	New System.....	14
III.	Literature Review.....	20
	Coolerado and the Maisotsenko Cooling Cycle.....	20
	Theoretical Equations for HMX Design.....	24
IV.	Methodology.....	26
	Energy and Environment Monitoring: Data Acquisition Systems (DAQ).....	26
	Traditional AC (CRAC) Energy Use: NI/LabVIEW.....	27
	Issues with the LabVIEW monitoring setup:.....	30
	New System Energy Use: Campbell Scientific Datalogger.....	31
	One-Time Measurements.....	40
	DAQ Systems Uncertainty.....	52
	NREL MatLAB Model.....	54
	Model Description.....	54
	Basic Model Assumptions.....	61
	Discretization.....	62
V.	Analysis and Results.....	63
	Calibration with CU4 Data.....	63
	Issues with MTC's.....	67
	Sensitivity Procedure.....	73
	Optimized Design.....	92
	Inlet Condition Variance.....	92
	NSIDC Coolerado System Operation.....	94
VI.	Conclusion.....	97

Energy Use.....	97
Suggested HMX Design Improvements	97
Challenges.....	100
Future Work.....	100
References	102
Appendix.....	104

LIST OF TABLES

Table 1. ASHRAE recommended psychrometric envelope for data centers.	5
Table 2. Liebert CRAC Specifications (courtesy of University Facilities Management).....	14
Table 3. WattNode scale factors (from WattNode product manual).	29
Table 4. Monitoring system comparison: USB-6008 vs. CR10X.	32
Table 5. Summary of one-time pressure, airflow and power measurement data.	45
Table 6. Sample HMX sheet dimensions.	47
Table 7. Monitored data points summary table.....	52
Table 8. Input and Output variables for HMX MatLAB model.	55
Table 9. M50 Miscellaneous Power Consumption (Courtesy of Coolerado).	57
Table 10. Version 6 HMX "60/40 split" design dimensions.....	65
Table 11. Version 6 calibrated HMX design parameters; 65/35 split.	71
Table 12. MTC22a calibration comparison between CU4 data and model output.....	72
Table 13. Sensitivity and optimization constraints.	75
Table 14. Sensitivity simulations.....	76
Table 15. All HMX sensitivity simulations; ordered by COP.....	91
Table 16. HMX performance sensitivity to different inlet conditions data.	94
Table 17. Summary of suggested design improvements.....	99
Table 18. MTC Spreadsheet.....	105
Table 19. Divider widths used for sensitivity simulations.....	123

LIST OF FIGURES

Figure 1. 2007 EPA report U.S. data center energy use projections. [1]	4
Figure 2. ASHRAE defined psychrometric computing environments; refers to air entering the IT equipment (at sea level).....	6
Figure 3. Hot aisle / Cold aisle data center layout.	8
Figure 4. PUE and DCE definitions [6].	10
Figure 5. Schematic of new NSIDC cooling system.....	16
Figure 6. PUE comparison of CRAC system to New system.....	18
Figure 7. Monthly cooling and IT energy comparison.....	19
Figure 8. Maisotsenko process on ASHRAE psychrometric chart.....	21
Figure 9. Basic schematic of Coolerado HMX, the heart of the Maisotsenko process [8].....	22
Figure 10. Exploded schematic view of Coolerado HMX (not to scale) [9].....	23
Figure 11. Schematic view of incremental HMX cooling process, adapted from Threlkeld [10].	25
Figure 12. Screenshot of RTMC display of real-time data center performance.	35
Figure 13. Schematic of USB-6008 Monitoring System (before Coolerado installation).	36
Figure 14. Schematic of Campbell CR10X monitoring system (after Coolerado installation).	36
Figure 15. Wiring diagram for CR10X datalogger; all resistor values are in Ohms, for numbered wires, see below.	37
Figure 16. CR10X datalogger fully wired (photo taken Dec. 2011, but no changes made since August 2011).	39
Figure 17. Pressure differential measurement setup in NSIDC on CU4.....	41
Figure 18. Dimensioned image of pressure measurement setup on an identical Coolerado unit [photo courtesy of Daniel Zube, Coolerado].	43
Figure 19. CU4 inlet flow measurement diagram.	44
Figure 20. Pressure drop and airflows from Daniel Zube at Coolerado for an M50 unit [12].	46
Figure 21. Pressure vs. airflow data and regressions.	47
Figure 22. Total power vs. airflow data and regressions.....	48
Figure 23. Front (inlet) side of top HMX block.....	50
Figure 24. Front (inlet) side of HMX, close-up; Note the wide variance in open channel heights and non-uniform inlet shape due to epoxy sealant.	50
Figure 25. Screenshot of model GUI.....	56
Figure 26. Model screenshot of GUI after simulation.	58

Figure 27. Drop-down menus for changing graphical representations of results.....	60
Figure 28. Example MTC plot of steady-state conditions.	65
Figure 30. Product air temperature gradient.....	69
Figure 31. HAD temperature gradient plot.	70
Figure 32. Model calibration with 3/23/12 CU4 data.	71
Figure 33. Pressure and Airflow relationships; CU4 data, initial 60-40 model, calibrated 65-35 model.....	73
Figure 34. HMX performance sensitivity to product height ratio: 35 inlets	77
Figure 35. HMX performance sensitivity to product height ratio: 39 inlets	78
Figure 36. HMX performance Sensitivity to product height ratio: 43 inlets.....	78
Figure 38. Optimal product height ratio as a function of inlets per inch.....	80
Figure 40. HMX performance sensitivity to divider width.....	82
Figure 41. HMX performance sensitivity to hole placement.....	83
Figure 43. HMX performance sensitivity to water conductivity.	85
Figure 44. HMX performance sensitivity to Elevation (ambient pressure).	85
Figure 45. HMX performance sensitivity to Fan pressure.....	86
Figure 47. HMX performance sensitivity to additional working channels.	88
Figure 48. Airflow and wet-bulb effectiveness sensitivity to additional working channels..	88
Figure 49. HMX performance sensitivity to additional product channels.	89
Figure 50. 3D HMX performance sensitivity to different inlet conditions (locations).....	93
Figure 51. NSIDC new system operation based on inlet conditions.....	96
Figure 52. Discrete portion of cooling coil; heat transfer schematic from Threlkeld [10].....	104
Figure 53. Model vs. Field Data Comparison: MTC 1-5	119
Figure 54. Model vs. Field Data Comparison: MTC 6-10	119
Figure 55. Model vs. Field Data Comparison: MTC 11-15.....	120
Figure 56. Model vs. Field Data Comparison: MTC 16-22.....	120
Figure 58. Airflow and wet-bulb effectiveness sensitivity to product height ratio; 39 inlets.	121
Figure 59. Airflow and wet-bulb effectiveness sensitivity to product height ratio; 43 inlets.	122
Figure 60. Airflow and wet-bulb effectiveness sensitivity to hole diameter.	122
Figure 61. Airflow and wet-bulb effectiveness sensitivity to divider width.....	123
Figure 62. Airflow and wet-bulb effectiveness sensitivity to hole location.	123

Figure 63. Airflow and wet-bulb effectiveness sensitivity to waterfilm thickness. 124
Figure 64. Airflow and wet-bulb effectiveness sensitivity to water conductivity. 124
Figure 65. Airflow and wet-bulb effectiveness sensitivity to elevation. 125
Figure 66. Airflow and wet-bulb Effectiveness sensitivity to additional product channels. 125

I. INTRODUCTION

BACKGROUND

This report serves as a summary of thesis research related to data center energy use and an application of a new, unique air conditioning product from Coolerado. This narrative briefly covers current issues in data center infrastructure and power monitoring systems, and the bulk of the report is dedicated to the explanation of how performance data was collected and compared to a theoretical model of the Coolerado system. Using the model, modifications to the current Coolerado design are proposed to increase the efficiency and performance of future designs.

As the data industry is seeing an exponential growth in the bandwidth of data required by consumers in this digital age, new data centers are needed, and energy consumption in this sector is increasing. Larger data centers with more servers also need larger cooling systems. The responsibility to reduce this energy use and increase energy efficiency as much as possible falls on data center operators, public and private. Higher facility efficiencies translate into immediate energy and cost savings. However, information on how to achieve better energy performance must be readily available to operators. Both the federal government and private companies in the industry are involved in ongoing research of best practices for data center operation.

The National Snow and Ice Data Center (NSIDC) is a small data center that has transitioned from a traditional direct expansion cooling system to a new indirect evaporative system during its Green Data Center Project. This project has three consecutive phases: server consolidation and virtualization, upgrading the cooling system and installing a solar photovoltaic (PV) system on the roof. Server consolidation (completed by June 2011) saves some energy and is also a sustainable practice from an IT management standpoint. Installing a new cooling system (completed by June 2011) was expected to show the most effective savings, and once the PV system is in place

(expected by April 2012), the NSIDC may be a zero net energy data center during a clear summer day.

The new cooling system utilizes the recently patented Maisotsenko cooling cycle. Coolerado, the Denver based developer of this technology, claims significant energy savings over a conventional system. The NSIDC has served as a real-world test of these claims with 8 identical cooling units installed and operational for nearly 8 months. This study focuses on data that was collected over a 22 month period that encompasses energy use before, during and after the first two phases of the Green Data Center Project. A monitoring network was developed to determine energy use of the traditional DX system and the new Coolerado system. The Coolerado system was officially brought online in June 2011. These data showed that the new Coolerado cooling system is saving about 90% of the cooling energy previously required to cool the data center.

OBJECTIVE

The main purpose of this research was to use a model of the Coolerado system to explore design changes that may improve the system's performance. Using a complete theoretical model developed by Eric Kozubal and other researchers at the National Renewable Energy Laboratory (NREL), various internal design changes were simulated. Through a sensitivity analysis, some were found to be important because they have significant effects on the performance of the Coolerado system. Others were found to have very little effect.

II. MOTIVATION

DATA CENTERS AND ENERGY CONSUMPTION

Current expansion and the use of digital technology and communication are causing significant growth demands on the information technology (IT) industry. The worldwide capacity

for data storage and processing is increasing rapidly as more and more industries and companies must provide or store data for clients, as well as for internal business purposes. Examples include: online financial services and mobile banking; the communication and entertainment industry as they expand into social websites and internet access markets; and digital healthcare records. Almost all shipping and mail services now offer online tracking of packages. GPS technology has become smaller and more affordable, and a standard feature on many new vehicles. Real-time data processing of these geospatial data will increase exponentially. With all of these industries expanding their digital footprint, data center demand capacity for storage and processing will also grow accordingly. Data centers provide a clean, secure and stable environment for online servers and must be maintained physically and virtually at all hours of the day. Such facilities across the U.S. typically house anywhere from a few dozen to a few thousand servers and are geographically dispersed.

The data center industry has experienced trends over the past decade that can be divided into two periods: 2000 to 2005 and 2005 to 2011. During the beginning part of the decade, data center energy use in the U.S. nearly doubled [1], according to the EPA. An estimated 61 billion kWh of energy was consumed by data centers in 2006, which accounts for 1.5% of total U.S. energy consumption. In the same study, a few different projections were made based on: historical trends, current efficiency trends, improved operation, best practice, and state-of-the-art scenarios. Figure 1 shows a graph of these projected energy uses.

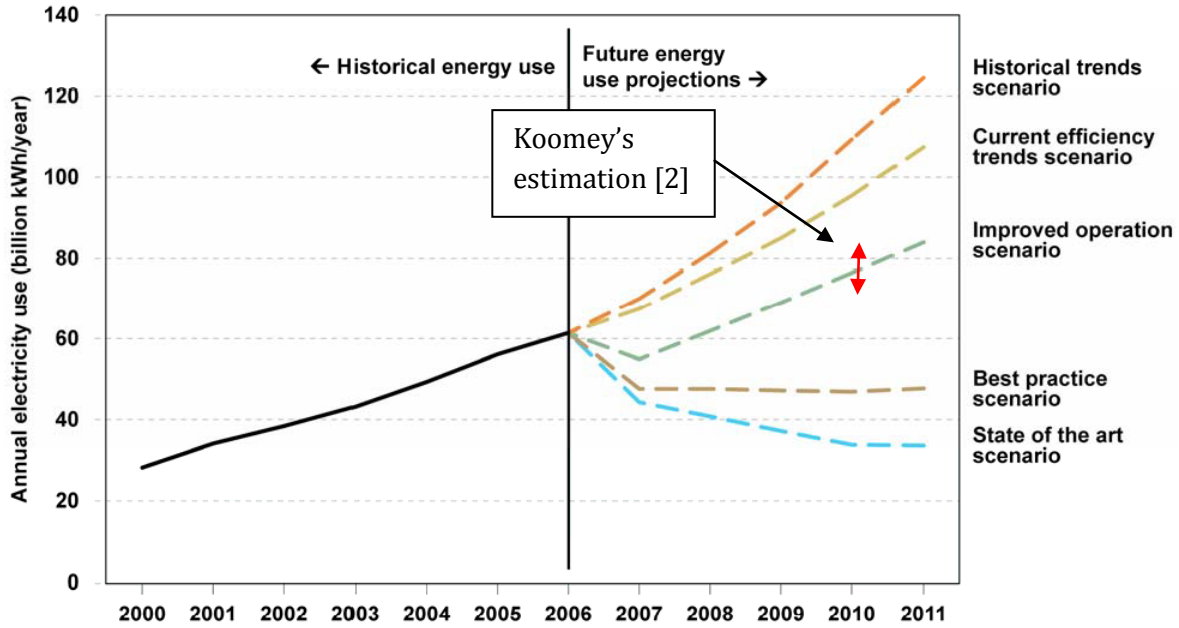


Figure 1. 2007 EPA report U.S. data center energy use projections. [1]

Note that the historical trends scenario in Figure 1 shows another doubling of energy use by 2011. And an improved operations scenario would've resulted in about 35% increase in energy use compared to 2006. Moving up to an updated report by Jonathan Koomey in 2010, it appears that data center energy use has followed the improved operation scenario and U.S. data centers now use somewhere between 70 and 85 billion kWh/year [2].

Although the data show that data center energy use has followed the improved operations scenario, it is important to point out that the 2007 EPA scenario was based on “low-cost efficiency opportunities” or simple changes that operators could implement to conserve energy within a typical budget. However, Koomey suggests that the U.S. data center energy consumption is reduced from typical 2000-2005 historical trends only because of fewer additional installed servers and not necessarily because operators have been actively improving the efficiency of their centers. The slowdown reflects some energy conservation measures like virtualization and consolidation of data centers, but also general market trends since the 2008 financial industry crash. Many companies

were struggling to balance budgets and may not have had the resources to expand their data center or IT facilities as much as expected previously [2].

Computers consume a significant amount of electrical energy. Most of this energy is converted into heat within a computer that then must be exhausted to prevent damage to the electronic components. The American Society of Heating, Refrigeration, and Air Conditioning Engineers (ASHRAE) has established temperature and humidity standards that are suitable for data centers and computer rooms [3]. The limits on this psychrometric “envelope” are shown in Table 1 and Figure 2.

Humidity control in a data center is critical to stable operation. Too much moisture in the air allows for condensation possibly leading to short circuits and damage to any part of the delicate integrated circuits, power supplies, and other hardware. Too little humidity allows for static charge accumulation and potential damage from a single, large discharge could be significant. Exceeding a certain ambient air temperature can cause thermal damage to equipment. Very low ambient temperatures can cause circuits and electricity flow to slow down, thus impeding the productivity of the computer.

It is a vital concern of data center managers to maintain an appropriate air state using heating, ventilation and air conditioning (HVAC) systems. While improvements in energy efficiency are important, machine room environment and support systems’ reliability are also critical to these data centers.

Table 1. ASHRAE recommended psychrometric envelope for data centers.

Property		Recommended	Allowable
Dry-Bulb Temperature	High	80° F	90° F
	Low	64° F	59° F
Moisture	High	60% RH & 59° F DP	80% & 63° F DP
	Low	42° F DP	20% RH

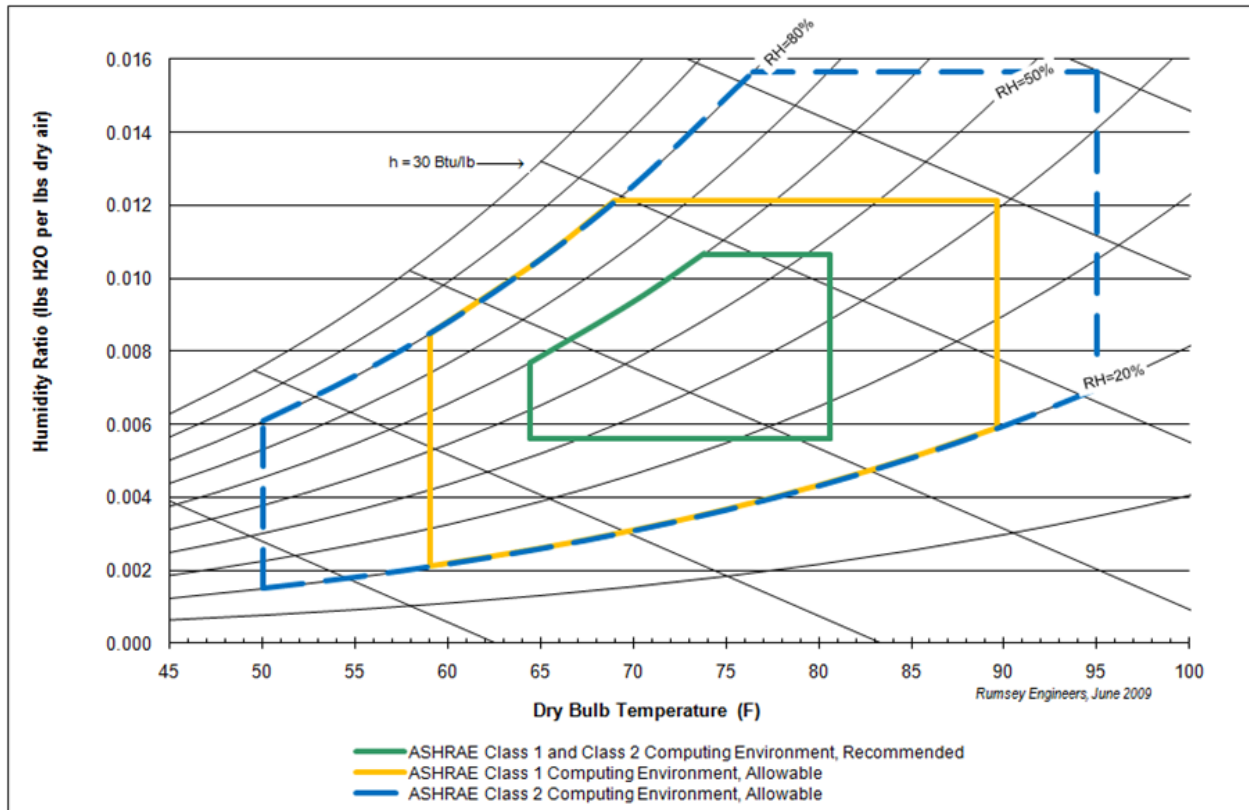


Figure 2. ASHRAE defined psychrometric computing environments; refers to air entering the IT equipment (at sea level).

All electronics produce heat as a byproduct. Exceeding a certain ambient air temperature can cause thermal damage to equipment. Very low ambient temperatures can cause bearing failures on disk drives leading to premature failure.

In order to maintain an appropriate air state within the limits as described above, the type and control of the heating, ventilation and air conditioning (HVAC) system for a data center is of vital importance. Both the HVAC infrastructure and the power distribution require a substantial amount of energy.

In 2006, total data center power consumption in the U.S. was estimated around 7 GW, and this number was closer to 9 GW in 2011 [1] as power densities increased. Power density is technically defined as server power per area (watts per square meter). Power densities are increasing as new servers use more power and require less space. A typical server in 2007 uses 251

W of peak power (EPA). If the peak power of a newer server is 351 W, and there are 10 servers per rack, then there is a 1 kW increase in peak power usage. An increase in 1 kW of power becomes significant when a full row of server racks is replaced. This change in server type can cause overall data center power efficiencies to decrease if not accompanied by a proportional change in cooling and power equipment. For this reason, a data center's design power density is very important. If cooling and power distribution equipment is designed to handle a much higher power density (as would be reasonable to assume future expansion) than is actually needed, efficiency suffers initially, and the facility costs more to operate at part load conditions. It is important to establish a reasonable design power density and ensure that future changes to servers or equipment are appropriate and do not reduce the power efficiency of the center significantly [4].

All power used by servers is essentially turned into heat that needs to be removed by cooling equipment. If a server rack uses 20 kW of power at any given time, the data center cooling load is 20 kW times the number of racks.

Another important design consideration is the *peak to average power ratio* [4]. A typical server can use up to 250 W of *peak* power. However, the *average* power use may be much lower, depending on the server details and its IT demands. The average power is the amount of power the server consumes most of the time; peak loads usually only occur for short periods. The peak to average power ratio is defined as the peak power use divided by the average power usage.

$$\text{peak to average power ratio} = \frac{\text{peak power}}{\text{average power}} \quad (1)$$

The cooling system must be designed and sized to handle the peak load. If the peak to average ratio is significantly higher than 1, then most of the time, the cooling system will be operating at a significantly reduced, partial load which is generally less efficient. The overall peak to

average ratio is also dependent on the organization and location of the different types of servers. An ideal rack would have servers that use peak power at different times so that the total power use of that rack is relatively constant.

In terms of maintaining the ASHRAE supply air state, there are a few different types of layouts that work well for introducing cool supply air and expelling hot, return air from the server racks. Many data centers separate rows of server racks with alternating hot and cold aisles. Cold air is provided on the front side of the server racks and hot exhaust air is expelled from the racks on the back side. Front sides of racks face each other, which creates this common setup. Figure 3 below shows this air distribution system.

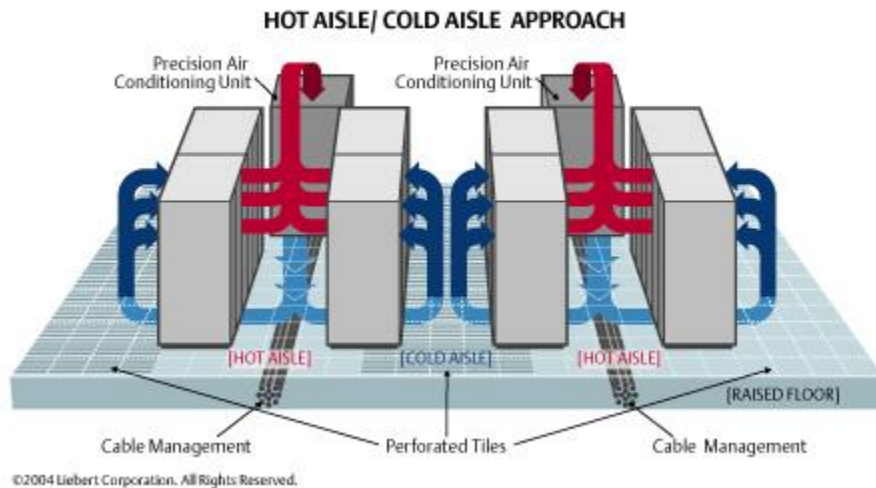


Figure 3. Hot aisle / Cold aisle data center layout.

Note the raised floor in the figure above. Most data centers use a similar system because of the ease of rearrangement to server rack layout and power distribution. However, the cooling system also utilizes this under-floor plenum to deliver conditioned air at the base of each server rack. Modular diffuser tiles can be moved or swapped out depending on rack layout. Hot aisles don't

have any diffuser tiles because the cool conditioned air (beneath) must be kept separate from hot return air (above). This hot/cold system is very common in most large data centers.

This setup can be more effective when the hot and cold aisles are physically separated by plastic curtain or other airflow barriers. Using physical separation eliminates unavoidable “short circuiting” of conditioned air over the top of the server racks and into the return air stream. Also, dedicated return air ducts or plenum and fans can reduce the pressure drop seen by the supply air fan, which would result in elevated velocities and heat transfer ratios through each rack [5].

NATIONAL AND INTERNATIONAL EFFORTS OR IDEAS TO INCREASE EFFICIENCIES

All parts of the data center system described above have room for improvements in efficiency and energy consumption. In the EPA report, some suggestions are made to increase data center efficiency.

According to the EPA, up to 2007, the rapid expansion and evolution of the data center industry has not allowed for standardized performance metrics to be established. Many variations of power densities are used which results in different reported efficiencies [4]. More recently, the Green Grid, an association of IT professionals, has developed two energy use metrics to standardize the way data centers measure efficiency. These standard metrics provide a common base for data center operators to compare different centers and determine where improvements in equipment or operation could be implemented. The Power Usage Effectiveness (PUE) and Data Center Efficiency (DCE or DCE) are defined in Figure 4 below:

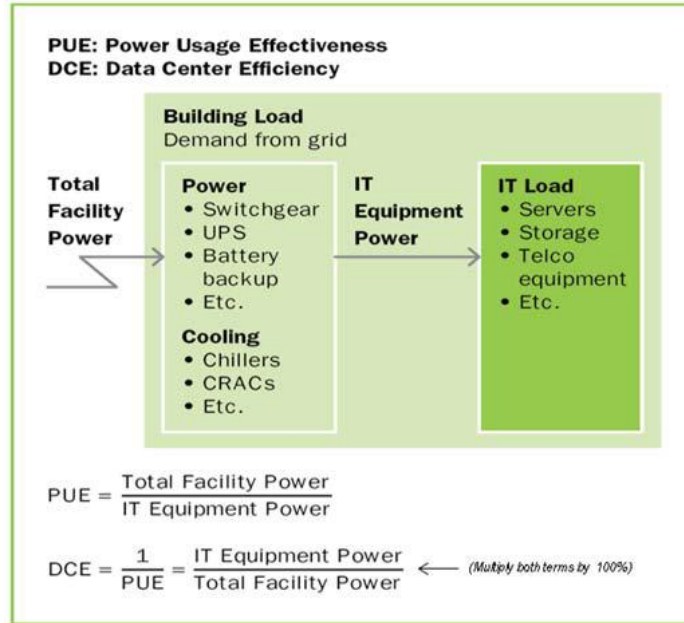


Figure 4. PUE and DCE definitions [6].

These data center performance metrics are becoming more standard within the IT and data center industry. The Green Grid has begun to engage important prominent trade organizations around the world to promote the use of these metrics with green initiatives and programs. The EPA’s Energy Star program, European Code of Conduct, Japan’s Green IT Promotion Council and others are involved in further developing and implementing the PUE and DCE metrics and calculation methods. Obviously these metrics rely on power measurements that may not be easily accessed. For example, if an office building has a data center inside, the data center power usage may be harder to determine without a submetering system. Methods and information on how to overcome this hurdle must be developed. For design purposes, ratings for IT equipment should also be established so that owner/operators can select efficient and compatible equipment for their facility. The efficiency of this equipment has an effect on the PUE and DCE. Note that IT Equipment Power is the sum of all power consumed by the servers. While Total Facility Power includes the servers, power conditioning and backup equipment, and cooling infrastructure.

Efficiency and power effectiveness metrics can help operators establish how efficiently their facility is operating, and eventually organizations like the EPA could recommend or require certain efficiency levels as a greenhouse gas reduction technique, much like is already in effect for automobiles with EPA miles per gallon (MPG) ratings.

Once standardized metrics are available, the governments (national and state or provincial levels) could act as a model for other government and private data centers by using the metrics and reporting energy consumption in their own data facilities. The government would then be in a good position to issue a private sector challenge to operators of data centers to improve the energy performance of their facility. Of course this would also require that credible, accurate information be available on efficiency improving techniques and how energy efficiency doesn't necessarily mean less data center reliability. Many operators believe that more efficient equipment translates to less reliability. Information on best practices must be readily available [1].

In order to accomplish or meet the above mentioned suggestions, more research must be completed. More information on how IT hardware, power delivery, heat removal, and facility management are related must be developed to determine best practices and equipment types for data centers. Collaboration between public and private sectors would be the best way to achieve all of suggestions above. Public developments and advancements should be shared with the private industry, and vice versa so that the overall efficiency and energy savings of the growing IT industry can be realized across the world. The National Snow and Ice Data Center, a non-profit organization funded in large part by the NSF and NASA, is an active participant in the promotion of data center efficiency, particularly over the past two years with its Green Data Center Project.

NSIDC POWER AND ENERGY USE

The National Snow and Ice Data Center (NSIDC) provides data for studying the “cryosphere”—those areas of the planet where snow or ice exist. The two most extensive regions of

study are Antarctica and the Arctic but high elevation regions are also important as they contain glaciers, and permanent ice and snow fields. The Center began operations at the University of Colorado in 1976. Some of the data held at NSIDC indicates dramatic changes in the cryosphere over the past decade and many of these changes have been attributed to global warming. NSIDC has operated a Distributed Active Archive Data Center (DAAC) for NASA's Earth Observing System since 1992. The data managed by the DAAC computer systems are distributed to scientists around the world. In order to deliver these cryospheric data to national and international clients, the data center must be available online around the clock.

The NSIDC is located at the University of Colorado's East Campus in Boulder. Room 376 on the third (top) floor in building RL-2 houses a small assortment of dedicated server racks and network equipment. Most of the servers are used for data storage and online availability. NASA and other related organizations use the satellite based climate data for simulations and other research applications. These servers must be online at all hours of the day. Access to this room is controlled, and registration is required for each visitor.

OLD SYSTEM

Traditionally, data centers have been cooled by standard (and often packaged or unitary) air conditioning systems that utilize a direct expansion (DX) heat removal process through a liquid refrigerant. This is the same type of cycle that runs the air conditioning in a car or refrigerator. Although a robust and mature technology, the DX cycle has been under scrutiny over the past few decades as other technologies capable of producing the same amount of cooling with less power requirement have entered the market and become economically viable. The DX cycle requires environmentally harmful, synthetic refrigerant (R-22) and substantial energy to run a compressor. Of all the parts in a DX air conditioner, the compressor requires the most energy. Up until the past

few years, typical data centers have been cooled by these packaged DX systems, commonly referred to as computer room air conditioners (CRAC), because they are very reliable. These systems have been economical in the past due to their off -the-shelf packaging, compact size and simple controls. However, as the need for energy use reduction and environmentally friendly technology becomes more and more prevalent, the DX systems for data centers are becoming antiquated. The NSIDC operated 2 CRAC (50 tons in total) units full time until April 2011. These units relied upon a typical raised floor for cool air and power distribution.

To maintain the space within ASHRAE standards for data centers (see Figure 2), precision cooling equipment must be included in the system design. Made by Liebert, these units were part of an air conditioning system that has a fan, a compressor, evaporator coils and controls, and these were connected to individual condenser units that were located outside on the roof (directly above the room). The specifications on these non-identical units are summarized in

Table 2 below. Note that since the new cooling system has been installed, the 20-ton CRAC has been removed and the 30-ton CRAC has been left in place for backup purposes only.

An uninterruptible power supply (UPS) is also a major piece of equipment that provides conditioned power to the NSIDC servers. The UPS also charges a large array of batteries for use during a power outage. These batteries provide emergency power to the servers and other UPS connected equipment for a few hours, which is typically long enough to allow for an expedient shutdown of computer systems, or for repair of the external electrical problem. The UPS currently installed at the NSIDC is only 87.7% efficient, which leads to a loss of 12.3% to power conditioning and conversion from AC to DC current to charge the backup battery array. Note that this loss is accounted for in the PUE by the difference between IT Equipment Power and UPS Power, as in Equation 2 and Equation 3.

$$IT\ Equipment\ Power = (UPS\ Power)(UPS\ Efficiency) \quad (2)$$

$$Total\ Facility\ Power = Cooling\ Power + UPS\ Power \quad (3)$$

Table 2. Liebert CRAC Specifications (courtesy of University Facilities Management).

Model:	Nominal Capacity	Rated Current	Nominal Power Use
DH300AHCA01	30 tons	171.6 A	61.8 kW
FH245AVCOO	20 tons	142.6 A	51.4 kW

The power system in the building had to be studied in order to determine the necessary equipment and proper method to monitor and record power usage data from the cooling and power subsystems of the NSIDC. The electrical system for the building is a basic three phase radial system. Power is delivered to the primary unit substation in the basement and transformed into 208Y/120V for distribution. Power to both of the CRAC units and the servers is delivered in separate conduits from the main distribution board in the basement of the building. The CRAC units are supplied by 2/0 AWG (THW Cu) wires. In Room 376, power for the servers comes from the UPS that is also located in the room and feeds directly to the power panels and under floor distribution network. This UPS provides power to 15 server racks (not all are full). The UPS is supplied by 400 MCM (THW, Cu) cables in 3" conduit. The wire sizes were important for monitoring equipment specification purposes.

In 2008, the Uptime Institute said that annually, global data center CO₂ emissions are poised to equal that of the airline industry if current trends persist, and it estimated that data center CO₂ emissions will quadruple between 2010 and 2020 [7]. The irony of the NSIDC's situation stems from the fact that the use of tools (the data center) necessary to study the problem (climate change) are actually contributing to the problem. When it became necessary to replace and upgrade the existing cooling infrastructure, all options were considered, and in particular, solutions that would reduce energy demand and dependency on the local utility provider were given high priority.

NEW SYSTEM

The new cooling system design includes a unique cooling system that uses both airside economization and a new Maisotsenko Cycle air conditioner. The major pieces of equipment in this system include a rooftop air handling unit (AHU) powered by a 7.5 kilowatt (10 horsepower) fan motor via a variable frequency drive (VFD), eight Coolerado M50 air conditioners and hot aisle containment. The modularity of the M50 units is a feature of this design. About 30 tons of cooling is required on a hot day. Each M50 unit is rated for 5 tons of cooling. Therefore, only 6 units are actually required to meet the full load. However, because fan power input increases as a cube of the airflow (according to fan affinity laws), running the M50 units at maximum capacity could use a lot of energy. Instead, 8 units were specified so that none of the units are ever operating at full speed for an extended period of time; in theory, the maximum would be about only 75% airflow capacity or 42% power. Including more units than necessary also allows for redundancy and the ability to operate the data center as designed even with 1 or 2 units out of commission.

Airside economization is not a new technology, but does add some complexity to the control system. Simply put, an airside economizer is a control mode that allows the air handling unit (AHU) to cool the space solely with outdoor air when the outdoor air is cooler than the air in the space. This is commonly referred to as “free cooling”. In this mode, no air conditioning (DX or other process) is required, and recirculation of room air is reduced to a minimum. As stated previously, humidity is an issue for computers and electronic systems. And in many locations, particularly the Midwest and East Coast of the United States, airside economization may not be possible due to the hot and humid climate. However, the State of Colorado (and much of the western U.S.) is much drier and cool enough for about 6 months of the year, so an airside economizer is a viable option for data centers to maintain tight control of supply air within the ASHRAE limits.

Because the data center operates 24 hours per day, there is a constant need for cooling; and without airside economization to take advantage of cold winter air, the CRAC units used to operate 24 hours per day, at near constant load. Therefore the PUE of the CRAC system at the NSIDC didn't

vary much with outdoor temperature from month to month. The new system allows the cooling power required to maintain the ASHRAE air state to decrease in correlation with the outdoor temperature.

Note that the new cooling process does not have a compressor or condenser in its cycle. Using the Coolerados, air from the AHU can now cool the data center to a cool temperature using an average of one tenth the energy that would be required by the CRAC system. Water is used in this cycle, and is only used once (single pass). Based on measurements, all eight of the Coolerado units consume an average of 1.7 liters per minute (0.5 gallons per minute) when in humidification mode, which is most of the winter. Unfortunately, similar measurements were not taken of CRAC water use, although it is expected that the CRACs use and waste more water due to an inefficient humidification process; and the CRACs used a continuous water flow regardless of whether or not they were in humidification mode.

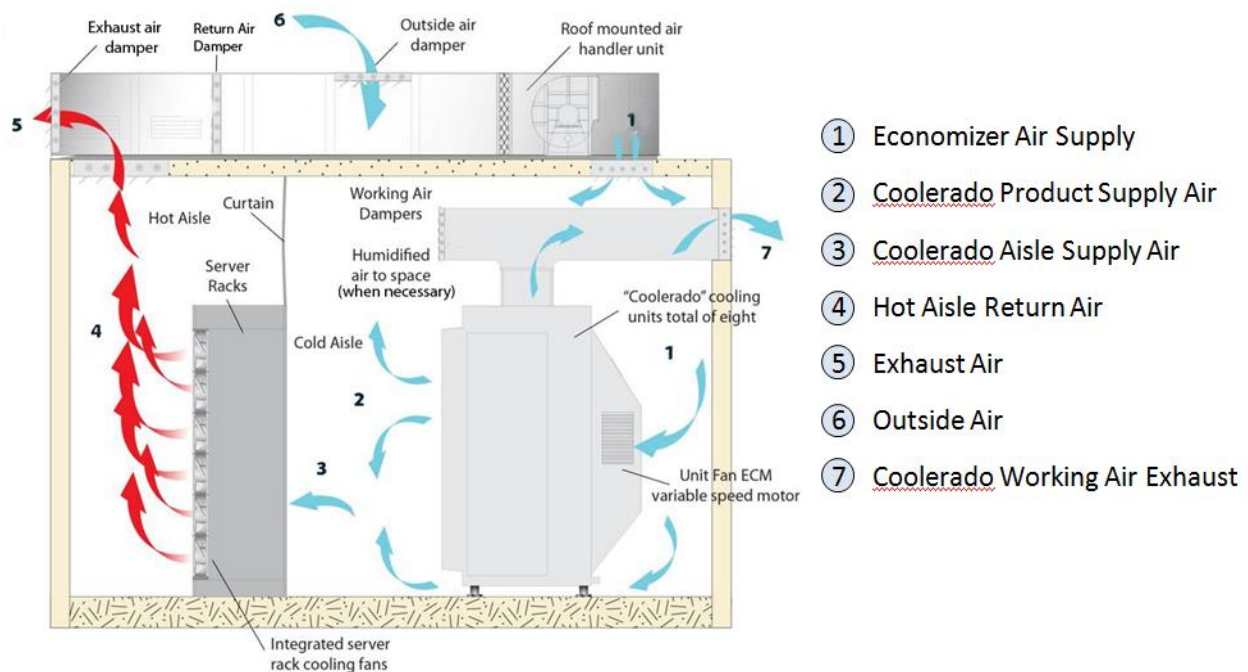


Figure 5. Schematic of new NSIDC cooling system.

Figure 5 shows a schematic of this system. On a design cooling day (hot summer day), the AHU pulls in outdoor air around 35°C (95°F) and introduces it to the front side of the Coolerado units. Then the Coolerado fans force the hot air through its HMX, splitting the airstream in half and cooling the supply air to about 12.7°C (55°F). This cool air is directed towards the front side of the server racks. After being exhausted from the backside of the server racks at around 32°C (90°F), the air is pulled out of the hot aisles by suction pressure from the return air damper in Figure 5. This slight negative pressure is caused by the same AHU fan that initially pushed the air into the room. To ensure efficiency and prevent cool air from being pulled out of the room before cooling the servers (referred to as “short-circuiting”), hot aisle containment curtains were also installed during this project.

Note that the AHU is completely responsible for the airside economization by regulating the amount of outdoor air into the space. When the outdoor air is cool enough (late fall, winter and early spring months), the AHU introduces a mixture of this cool air with some hot return air from the backside of the server racks. This mixed air is introduced into the room and allowed to flow out from beneath the Coolerado air conditioners to keep the “cool” areas of the room around 22.2°C (72°F). The Coolerado air conditioners are only used when the AHU can no longer supply cool enough air to the data center, presumably because the outdoor air temperature has climbed above the room temperature. The Coolerados are located in the room with the servers so that cool product air can be delivered directly to the front side of the servers (see 3 in Figure 5).

One CRAC unit (30-ton) was left in the room for redundancy and for dehumidification during occasional hot and humid periods in the summer. The new system (exclusive of the 30-ton CRAC) was not designed with a dehumidification mode because this is rarely necessary in Colorado’s climate.

The NSIDC computer facility meets the ASHRAE Allowable Class 1 Computing Environment (see Figure 2). Because the NSIDC is indirectly owned by NASA, this has always been a requirement, even with the old CRAC system. Internal review of manufacturer specifications revealed that all of the computer and IT equipment in the data center can operate safely (and under warranty) under the ASHRAE Allowable and Recommended Computing Environments.

Figure 6 shows the reduction in PUE compared to the CRAC system. The CRAC system had an annual average PUE of 2.03. The new system has an average PUE to date (June 2011 through March 2012) of 1.29. And this average is even lower in the winter months because outdoor temperatures in Colorado are generally cool during this time of the year. And since September 1st, 2011, the monthly PUE has been below 1.35 due to the airside economization of cool outdoor temperatures. Note that the PUE in May of 2011 was actually higher than it was in 2010 because the CRAC system was still operational as the new system was undergoing commissioning and testing. During this time, the complex control sequences for the new system were being tuned. This issue was a single occurrence and should not happen again.

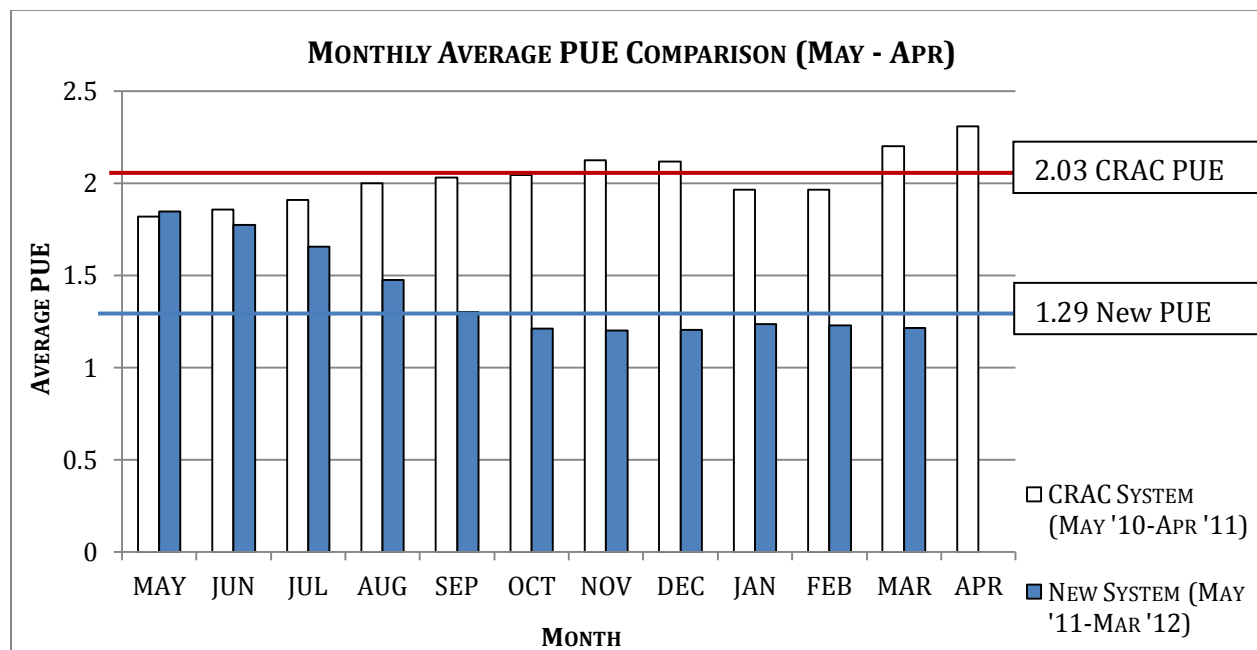


Figure 6. PUE comparison of CRAC system to New system.

Figure 7 shows the cooling energy comparison for the same total time period. The new system has used less than 2.5 kilowatts of power on average each month since October 2011. Compared to October 2010 (during which the IT load was only 13% higher and outdoor conditions were very similar), the average cooling power usage is almost 95% less. The average cooling power during the next few winter months of November 2011 through March 2012 were similar because the winters in Colorado are generally very cool. Note that there was actually a slight increase in cooling power during the winter months of 2010 while using the CRAC system. Although it is not immediately clear what caused this, it was most likely due to the CRAC active humidification process that was necessary to maintain the low humidity limit prescribed by ASHRAE. The CRACs used a series of heat lamps (inside each unit) to evaporate water into the airstream. Obviously this is inherently inefficient because the air must be cooled further to account for the heat added by the heat lamps. The new system actually produces very humid air as a byproduct (working air), and humidifying the space when necessary requires no additional energy.

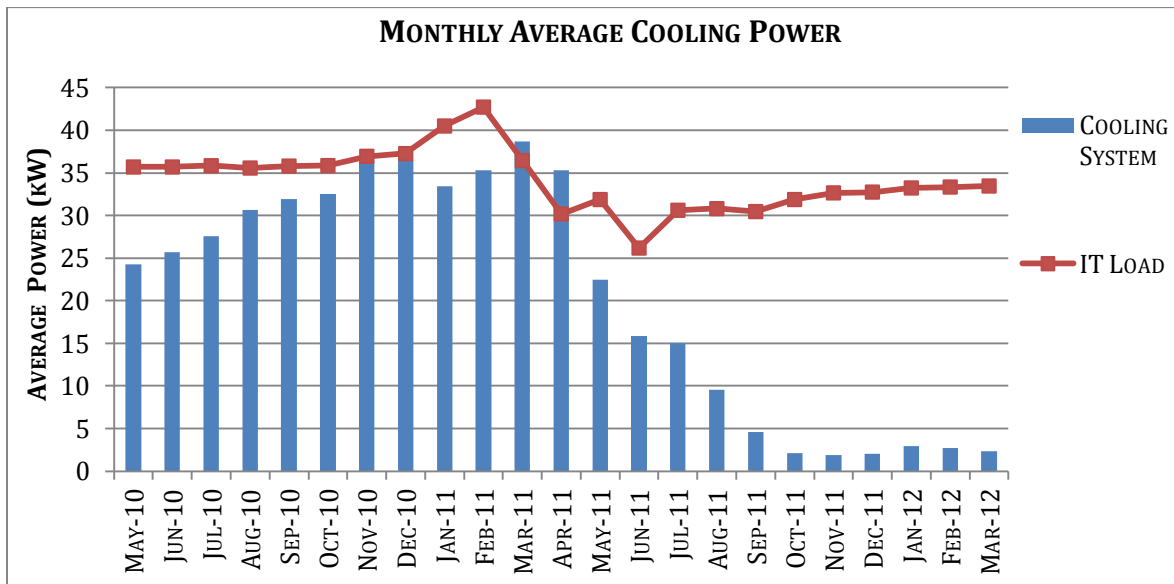


Figure 7. Monthly cooling and IT energy comparison.

The significant energy savings was accomplished while maintaining the 2008 ASHRAE standards for data center air quality, meaning warranties on servers and IT equipment are still valid. Additionally, maintenance costs have been reduced to only air filter changes and periodic check-ups on the Coolerado units. These air conditioners are very simple, without any substantial moving hardware other than a small fan.

III. LITERATURE REVIEW

COOLERADO AND THE MAISOTSENKO COOLING CYCLE

A company named Coolerado, based out of Denver, CO, has developed a high efficiency air conditioner that works well in many Western climates. Coolerado claims these units are theoretically capable of up to 80% energy savings over 2010 standards because of their use of a unique cooling cycle called the Maisotsenko cycle [8]. This cycle utilizes indirect and direct evaporative cooling in tandem to cool supply air. Incoming return air is mixed with hot, fresh outside air to produce a mixed air state. Then, the air is split into two separated air streams; a “working air stream” is used to remove heat from the “supply air stream.” The working air is cooled evaporatively as it is directed through a channel with a wetted surface in a patented heat and mass exchanger (HMX). At the same time, the supply air is directed into an adjacent channel and is cooled through conduction and contact with a membrane that separates the two air streams. Working air is rejected to the atmosphere and supply air is retained. Theoretically, the cooling limit of the supply air after one iteration of this process is the wet bulb temperature of the moist, working air. However, if this splitting and adjacent flow process is applied again to the cooled supply air, it can be cooled even more, theoretically to the *new* wet bulb temperature of the once-cooled supply air. In the Coolerado units, this process is repeated 20 times and reduces the volume of supply air by about 38% (dependent on airflow). The theoretical limit of this entire process is the dew point temperature of the original supply air. See this process in Figure 8 on a psychrometric chart.

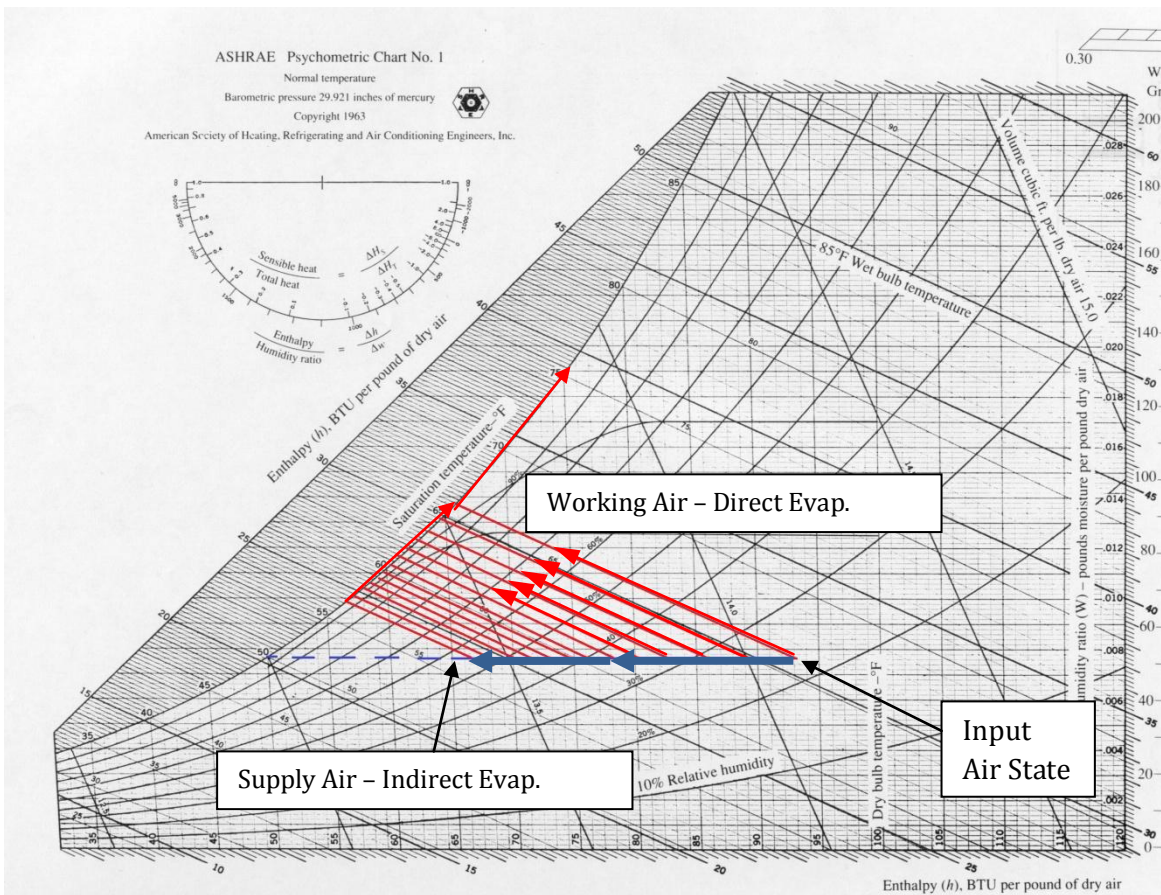


Figure 8. Maisotsenko process on ASHRAE psychrometric chart.

From **Figure 8** above, it is evident that this use of the Maisotsenko cycle does not add or remove moisture from the supply air. Moisture is added to the working air, but that air is most often rejected to the atmosphere. For this reason, the Coolerado works very well for spaces in arid climates because latent loads (moisture introduced into space, usually by occupants) can be decreased by simply mixing less return air and more dry, outside air. For spaces with very little latent load (e.g. data centers), the Coolerado works well in even more climates because there is no latent load from electrical or IT equipment and moisture removal is of less concern. Introduction of some outdoor humidity is acceptable, as long as the room air (supply air to servers) remains within ASHRAE limits.

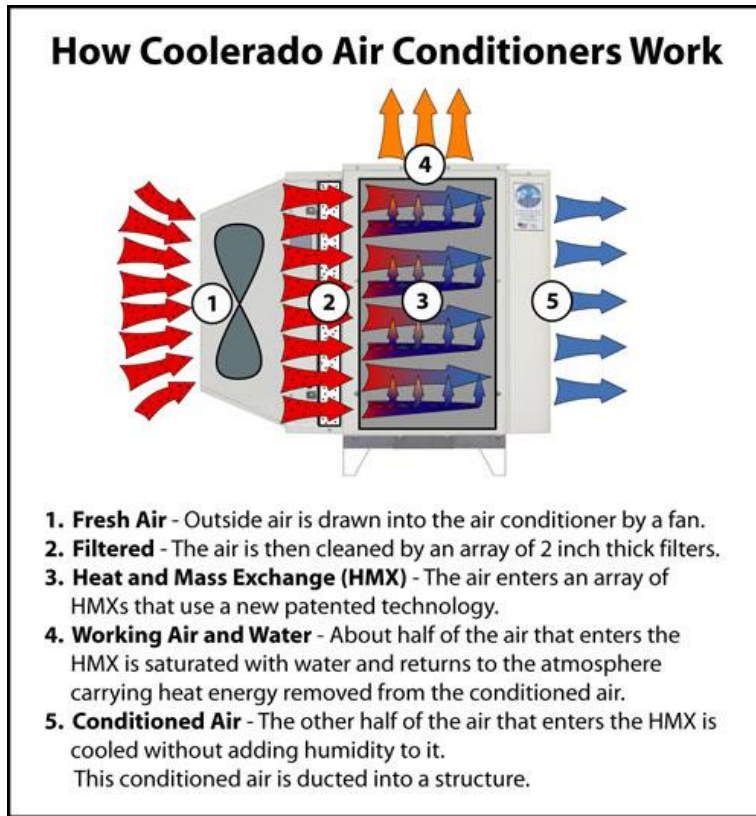


Figure 9. Basic schematic of Coolerado HMX, the heart of the Maisotsenko process [8].

Figure 9 shows an overall schematic of how the Maisotsenko process works within the Coolerado air conditioner. Note that the split between the working and process air streams occurs at step 3 of Figure 9. The device that does this is referred to as a heat and mass exchanger (HMX). A more detailed visual and explanation of the Coolerado design is provided in Figure 10.

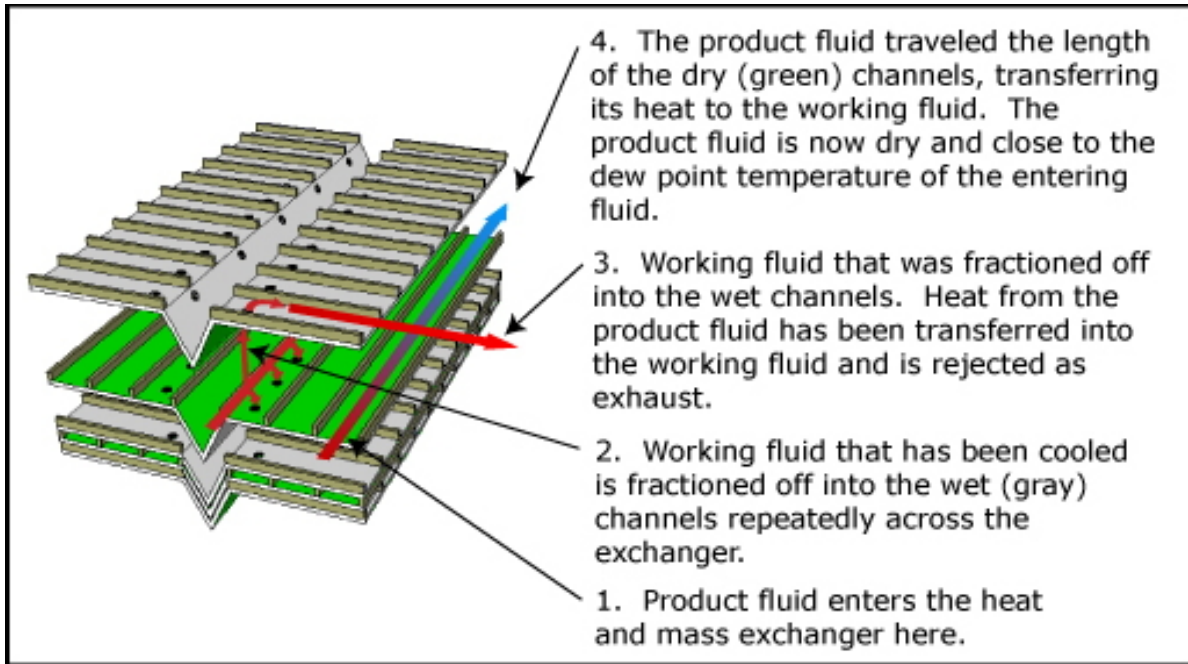


Figure 10. Exploded schematic view of Coolerado HMX (not to scale) [9].

The HMX actually divides the incoming airstream into the final supply air and working air quantities at the entrance to the HMX. The current design uses a total of 8 channels: 3 for working air and 5 for supply air. Note that the “sheets” (pliable, polypropylene sheets) in Figure 10 alternate flow directions, and each sheet has a flow direction that is perpendicular to the flow direction on the sheets above and below it. Input air flows lengthwise as working air is directed sideways on the adjacent sheet below. This configuration classifies this HMX as a crossflow exchanger. The working air sheets have a wicking surface on them and are saturated with a constant trickle of water from the V-type trough in the middle of each sheet; as working air flows over this wet surface, direct evaporation cools the working air, the sheet surface, and therefore the supply air flowing on the other side of the sheet. And as the working air travels sideways, across multiple supply air channels, it removes some heat from each supply airflow. The power of the Maisotsenko cycle, however, is realized when this process is incrementally repeated with the working air. Note that there are multiple holes in the working air channel, each corresponding to a different sideways channel. The

current design uses 20 of these channels. Since installation of Coolerado units at the NSIDC, Coolerado has made minor changes to the HMX and is now on Version 14. Because Version 6 HMX's are what is in use at the NSIDC, this report will focus on the Version 6 design.

Coolerado's M50 unit has 5 HMX's stacked vertically and, at least in theory, the flow front to back of the HMX's should be uniform, and pressure should decrease linearly in the straight sections of the channels (there may be a jump in pressure one way or the other as working air moves from the dry side to the wet side of the sheet through the hole).

THEORETICAL EQUATIONS FOR HMX DESIGN

In many ways, the fundamental, heat transfer in the HMX is similar to a cooling coil. In a cooling coil, heat is removed from the supply air stream through convection with a very cold surface and condensation. The heat is transferred to the refrigerant (typically flowing in a small tube) and absorbed into condensed water in the heat of condensation (opposite of vaporization). The water drips downward to be collected at the bottom of the coil and the refrigerant is pumped and cycled through a condenser loop to reject the heat somewhere else. The supply air leaves the coil at a much colder and often drier condition. This is illustrated in Figure 52 on page 105 in the Appendix.

The Maisotsenko cycle and the Coolerado HMX differ from this traditional cooling method because the working air acts as the refrigerant (instead of a liquid substance) and the condensation is reversed to evaporation. This evaporation occurs on the working air (refrigerant) side, which leaves the product air humidity constant. See Figure 11.

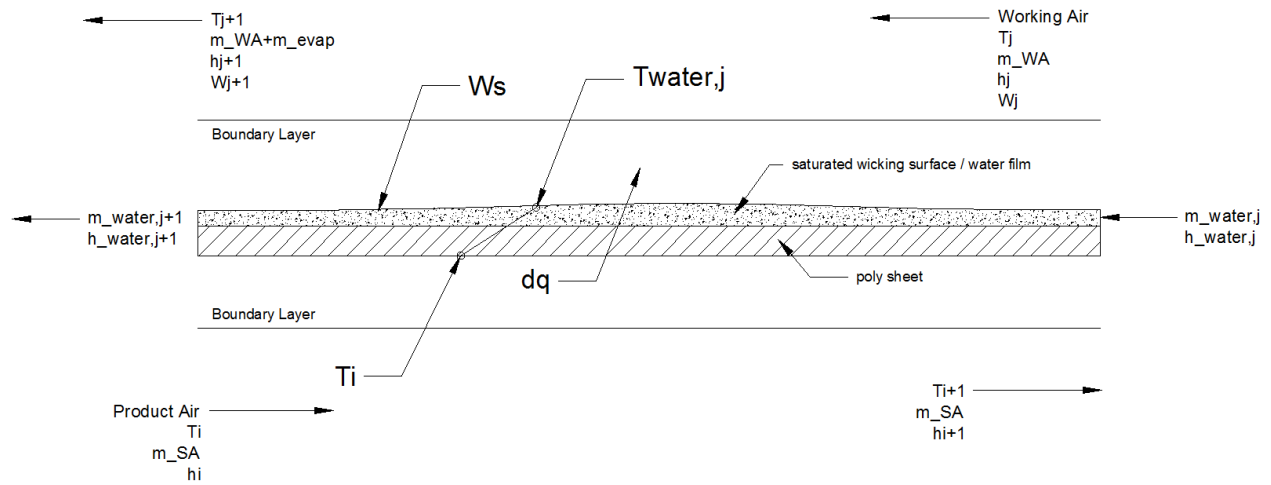


Figure 11. Schematic view of incremental HMX cooling process, adapted from Threlkeld [10].

And because this process is performed repeatedly throughout the HMX, and not just in a single pass like a cooling coil, it is appropriate to express the governing equations using a small increment of one of these processes. Equations 4 through 8 define these governing relationships. Note that Equation 4 is the basic form of Equation 5.

$$SA(\Delta sensible) = WA(\Delta latent + \Delta sensible) + water(\Delta sensible) \quad (4)$$

$$\dot{m}_{SA}(h_i - h_{i+1}) = X\dot{m}_{water,j}h_{evap} + \dot{m}_{WA}C_{p,a}(T_{j+1} - T_j) + (1 - X)\dot{m}_{WA}(h_{water,j+1} - h_{water,j}) \quad (5)$$

$$\text{where } X = h_{DO} dA \frac{W_s - W_j}{\dot{m}_{water,j}} \quad (6)$$

$$dq = h_{conv} dA (T_i - T_{water,j}) = \dot{m}_{SA}(h_i - h_{i+1}) \quad (7)$$

$$dq_{sensible,WA} = \frac{h_{conv}dA}{C_{p,a}} (h_{water,j} - h_j) = \dot{m}_{WA}C_{p,a}(T_{j+1} - T_j) \quad (8)$$

Where:

SA = Supply Air

WA = Working Air

h = enthalpy

h_{conv} = convection coefficient between wetted surface and working air

h_{DO} = evaporation mass transfer coefficient

T = dry-bulb temperature

$C_{p,a}$ = heat capacity of air

$i, i+1$ = indirect side index

$j, j+1$ = direct side index

Equation 4 is an “overview” equation simply labeling the terms in Equation 5; these equations are equal. Equation 6 defines the amount of water that is evaporated into the working air, as a fraction of total water flow. Equation 6 relates the perpendicular heat transfer from the product air surface to the top of the water film in the working air side (which must be sensible conduction only) to the sensible heat loss of the product air. Equation 8 defines the sensible heat gain to the working air, which would occur between the top of the waterfilm and the working air flowing parallel. This is in addition to evaporation (mass transfer) that also occurs.

IV. METHODOLOGY

ENERGY AND ENVIRONMENT MONITORING: DATA ACQUISITION SYSTEMS (DAQ)

One of the main goals of this research is to develop baseline energy consumption for the previous, traditional air conditioning system for comparison to energy consumption of the current new, high efficiency system that was installed in April of 2011. Determining energy consumption involved specifying power metering devices, professionally installing them with networking cables, acquiring a computer to log the data, and developing code or installing software that can interpret the data. The NSIDC required the incorporation of a monitoring network into the new system for better management and control of the critical data and servers in the data center.

For this research project, the energy monitoring can be divided into two phases: CRAC system monitoring and Coolerado system monitoring. Two different data logging systems were used because the actual energy uses of each system were different, and it was necessary to install more metering devices at additional locations when the new Coolerado system was brought online.

TRADITIONAL AC (CRAC) ENERGY USE: NI/LABVIEW

In order to quantify the actual energy savings that will be achieved by the new energy efficient system, a monitoring system had to be developed and installed to monitor all energy used by the NSIDC prior to the retrofit. Because energy is power used over a specified period of time, measuring power at given time intervals is the best way to determine energy use. It was determined that monitoring power at three locations made the most sense: at the service entrances to each CRAC (2 CRACs) and the UPS. With these three locations, all significant power that entered Room 376 was recorded. Note that lighting is not included in this calculation because the few fluorescent fixtures that are in the room are fed from an electrical panel outside the room and access to those particular feeds is difficult; these fixtures are usually off, so the unaccounted energy should be insignificant.

To monitor the power at each location, WattNode Advanced Pulse Output units made by Continental Control Systems in Boulder, CO were used in conjunction with a National Instruments USB-6008 data acquisition (DAQ) unit and LabVIEW software. The USB-6008 is a small device that can accept up to 4 differential analog inputs and 12 digital inputs/outputs. Each WattNode is located at the respective power entrance (CRAC or UPS) throughout the room and uses three current transformers to measure the current in each phase (all locations use three phase power). These devices were easily custom ordered; the current transformers are also made by Continental and are designed for use with the WattNode. Line voltage is also measured for each incoming feed.

Each device can derive the real time, total power consumption because voltage and current are known. Three phase power is commonly defined as in Equation 9:

$$P = \sqrt{3}E_L I_L PF \quad (9)$$

Where P equals phase power, E_L equals line voltage ($\sim 208V$), I_L equals line current and PF equals power factor (which is the cosine of the phase angle, nominally 0.8). The above equation is used for basic calculations of three phase electrical systems. The WattNode devices compute power using this equation internally.

Each WattNode is equipped with a 4 Hz maximum pulse output that is scaled to represent the real time power input. This output (along with two more outputs from other locations in the room) is connected to the USB-6008 data acquisition device via shielded 4-conductor, 18 AWG Cu cables. These cables were routed beneath the raised floor tiles to keep them protected and out of sight. Note that the shielding is important because the main power feeds and networking cables for the servers are also located beneath the raised floor and signal interference is a likely issue. The USB-6008 is connected to a local computer also in the room via USB 2.0 cord. The computer used for this project was borrowed from the Larsen Laboratory in the Building Systems Program in the College of Engineering at the University of Colorado. National Instruments LabVIEW software and graphical programming interface was used to process the WattNode signal, interpret the real time power use and log the data into a text file (LabVIEW software was obtained from the Integrated Teaching and Learning Laboratory in the College of Engineering). On a pulse output (digital output), more pulses means more power is being used. Each pulse corresponds to a certain number of watt-hours, as calibrated by Continental. WHpP is an abbreviation for Watt-Hours per Pulse. The values in Table 3 below were found in the WattNode Manual:

Table 3. WattNode scale factors (from WattNode product manual).

CT Rating:	WHpP
200 A	5.0
400 A	10.0

Both CRAC units used 200A CTs and the UPS uses 400A CTs. WHpP is calculated according to Equation 10:

$$WHpP = \frac{Phases * NVAC * CtAmps}{FSHz * 3600} \quad (10)$$

Where:

Phases =the number of phases included on each output (3 in this case),

NVAC = nominal voltage (208V),

CtAmps = Maximum rated current (Amps) for the CT,

FSHz = Full Scale frequency (4 Hz)

3600 converts from watt-seconds to watt-hours

The LabVIEW programming environment was researched and a program was developed to handle three inputs (one for each monitoring location) from one USB-6008 device. Once the program has been initiated by the user clicking the “run” command, each pulse output stream is sampled for 10 seconds, once every minute. This data is input into the code using a Data Acquisition Virtual Instrument (VI). Each stream is sent to a waveform measurement VI that calculates a pulse frequency (number of square wave pulses per second, Hz). It is important to note that the frequency (Hz) is per second and the sample is 10 seconds long. So this frequency is actually an average from that 10 second period. This method provides a high degree of power resolution, likely more than was necessary to determine the overall power use of the data center over many months. Any change in operating conditions will be noticeable as a gradual increase in these average frequencies over a few minutes. The UPS load is very constant with only slight variation as server load fluctuates. The average frequency is then used in Equation 11 below to find power consumption:

(11)

$$P = WHpP * 3.6 * AveFreq$$

Where:

P = average power use over 10 seconds (kW),

3.6 = conversion from pulses per second to 1000s of pulses per hour (3600 s/min x 1kW/1000 W),

WHpP = watt hours per pulse (as explained on the previous page)

Equations 10 and 11 were given and explained in the WattNode manual [11]. With power calculated, the value can be displayed to the user on a cumulative chart and an indicator readout. Average 10 second power is recalculated every minute. The process described above is looped for all three pulse streams and repeated every minute. At the start of the program, the user is asked to define a filename and location that each data entry is written to in the following order: 20 ton CRAC, 30 ton CRAC, UPS power. The program is terminated by the user clicking "STOP Data Acquisition."

After the old cooling system was removed, the power values were plotted against time using custom-developed MatLAB code (seen on pages 108-110 in the Appendix); the code had to be able to handle the data file which included over 1 year of data and 3 million data entries. The area underneath the power consumption curve represents the energy (kWh) used over each monthly time period. This energy use was calculated using trapezoidal approximation. PUE was also calculated using the methods described previously in this report (see Figure 4). The analysis of the CRAC system power and energy usage allowed the creation of Figure 6 and Figure 7.

ISSUES WITH THE LABVIEW MONITORING SETUP:

The LabVIEW system was acceptable for initial monitoring use on this project because it was free of cost and support was readily available from on-campus staff when specialize in technology research projects. However, there were a variety of issues with this system. National Instruments makes very high quality experimentation and sensor equipment for accurate

monitoring or control during experiments. But without substantial additional investment in many pieces of specialized equipment, it was evident that the combination of the USB-6008 and LabVIEW software is intended for real-time, manned operation. The simple USB interface is not robust enough for extended periods of autonomous datalogging, in part because it relies on the computer for data processing and storage. During the limited development time, the program was completed but fatal errors would often occur. Left unchecked overnight, this resulted in a loss of 1 day or more worth of data. The USB interface was also not ideal and sometimes caused issues as well.

NEW SYSTEM ENERGY USE: CAMPBELL SCIENTIFIC DATALOGGER

Due to software instability issues, hardware limitations and the rudimentary connection (USB) of the NI DAQ system, an improved, more robust and reliable monitoring system was desired to handle monitoring of the new advanced cooling system, particularly because it is expected to be more permanent. And for this research, it would be important to monitor temperature and humidity in multiple locations, in addition to adding more WattNode devices to be sure to account for all power uses in the data center. In April 2011, a Campbell Scientific Instruments CR10X datalogger and some associated temperature and humidity sensors were acquired at no cost from the Cooperative Institute for Research in Environmental Science (CIRES). These types of dataloggers are often used on many of the NSIDC/CIRES Arctic and Antarctic research expeditions, although the CR1000 has now replaced the CR10X in Campbell's current product line. This unit has 6 differential analog inputs, 2 pulse counters and 8 digital input/output ports. These additional inputs will be used to monitor 5 WattNodes and 2 temperatures, 3 humidities and 1 air velocity within the new cooling system (see Table 4). Note that 2 more WattNodes were needed in addition to the original 3. Power had to be monitored at 5 locations: UPS (as before), 30-ton CRAC (as before), air handling unit VFD, Coolerado power panel (all of the new cooling units' combined power) and Coolerado Unit 4 (CU4) individually (for coordination of localized input/output temperatures and humidities).

Table 4. Monitoring system comparison: USB-6008 vs. CR10X.

	Pre-June 2011		Post-June 2011	
	Description	Sensor	Description	Sensor
Manufacturer:	National Instruments		Campbell Scientific	
Logging unit:	USB-6008		CR10X	
Ports:	4 differential analog inputs		6 differential analog inputs	
	12 digital I/O		2 pulse counters	
	1 USB port		8 digital I/O (control ports)	
			1 Serial I/O port	
Data Points Monitored:	20-ton CRAC Power	WattNode	Coolerado Panel Power (Panel L3M)	WattNode
	30-ton CRAC Power	WattNode	30-ton CRAC Power	WattNode
	UPS Input Power	WattNode	UPS Input Power	WattNode
			AHU VFD Power	WattNode
			Coolerado Unit 4 Power	WattNode
			Coolerado Product Temperature (°F)	HMP-45C
			Coolerado Product Relative Humidity	
			Coolerado Working Temperature (°F)	HMP-45C
			Coolerado Working Relative Humidity	
			AHU Supply Relative Humidity	EE16-F3B56
		AHU Supply Air Velocity	EE65-VB5	
PC Interface:	USB		Printer/Modem Cable	SC-32A
Power:	5 V DC (provided from USB)		12 V DC	

I/O = inputs/outputs

Because the WattNodes output a digital pulse signal, the analog input channels on the CR10X are not useful; this type of square-wave signal requires a pulse counter. There are only 2 designated pulse inputs, but the digital control ports could be used as pulse inputs also. This requires some special programming steps. Unlike the USB-6008, the CR10X is a fully autonomous datalogging device, and all programming is best performed on a local computer and compiled onto the device. Once loaded, the program runs whenever the datalogger has power (which is 24/7). And because the CR10X is powered from the UPS, data will continue being collected in the event of a power failure. The datalogger is connected to the local computer via an RS-232 cable, SC-32A converter (available from Campbell), and a printer cable.

Programming the datalogger is completed using proprietary software from Campbell Scientific specifically designed for use with their dataloggers and associated sensors and equipment. LoggerNet 4.0 is used for this purpose. Although the wizard interface within this

software is appropriate for programming 2 Campbell HMP-45C Temperature and Humidity probes and 2 of the WattNodes on the dedicated pulse input channels, the remaining 3 WattNode pulse inputs require manual programming on the 3 compatible Control Ports using EdLog, Campbell's basic code editor. Essentially a glorified notepad program, documentation on EdLog and the CR10X had to be consulted to get this to work properly. Ultimately, the datalogger is programmed to sample the pulse frequency of each WattNode every 30 seconds, multiply by a combined factor to convert to power (see Equation 11), and then write the average power use of 6 thirty second intervals to a simple text file every 3 minutes. Note that this is a significantly longer sampling interval than the previous LabVIEW system called for; a recording interval of 10 seconds resulted in an excessive amount of data and was not necessary to capture system trends for this research. Using a 3 minute recording interval also significantly reduces the size of the data files, which in turn reduces the computational time to calculate the energy use over a specified period.

Using the Campbell CR10X also allows the NSIDC to easily collect and display real-time energy performance and room conditions on the Internet. LoggerNet 4.0 is designed to run on a computer in conjunction with a datalogging system to maintain the CR10X, display real-time data and act as a stable storage system for the power and room condition data. Real-Time Monitor and Control (RTMC) Development and Run-Time programs (included in the LoggerNet 4.0 software package) display the data in a user-defined graphical interface. These programs allow a novice user to easily create a simple and effective display of live data from the datalogger. Unfortunately, these displays can only display data directly from the CR10X, which holds about 4 days of data if it is logged at 3 minute intervals (note this is also dependent on the number of data points stored at each timestamp). RTMC cannot display data that is stored locally on the computer for reasons unknown. Separately, LoggerNet is set up to download data from the CR10X to be stored every 3.5 minutes, a period just barely longer than the 3 minute recording interval. The data is then manually collected and organized into one large spreadsheet file about every week.

In addition to displaying the data locally, the NSIDC also desired to display the data to the public on its website. Fortunately, Campbell also makes an RTMC WebServer application that is designed to do exactly this, but this software is not included in the LoggerNet package and must be purchased separately. The WebServer application is relatively simple; it captures the same display available locally through RTMC (or another, separate user arranged display), and publishes an image at a user-defined interval. The NSIDC is currently publishing a new image every 2 minutes. As with the RTMC display, the displayed data is pulled in real-time from the CR10X, not the local computer. A screenshot of the RTMC display (both local and online) can be seen in Figure 12.

Past to Present Comparisons

Cooling Power Reduction: **92 %**

Old Cooling = 30.3 kW
New Cooling = 2.4 kW

Minimum Observed PUE: 1.16 with existing 88% UPS
1.09 with 94% efficient UPS

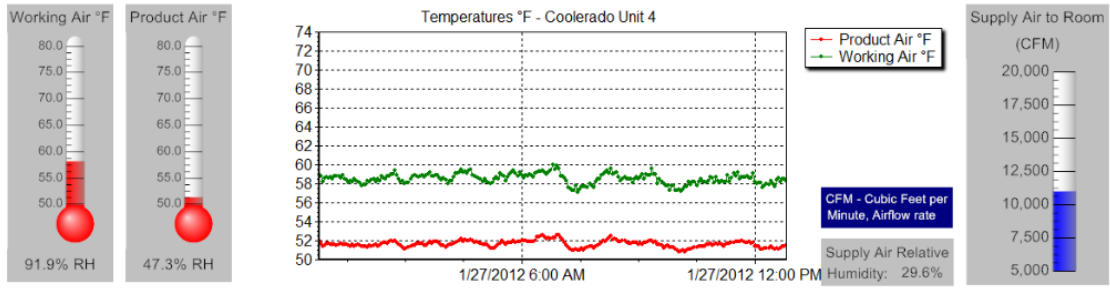
Old Air Conditioning PUE: 2.03

The Uninterruptible Power Supply (UPS) provides power to the servers and charges large batteries for use during a power failure; servers should be able to remain online for about 3 hours.

The Power Utilization Effectiveness (PUE) is simply total data center power divided by computer equipment power. This metric allows for easy comparison of energy efficiency between different sized data centers.

	August	September	October	November	December
PUE:	1.47	1.30	1.21	1.20	1.21

Current Temperatures



Power In Use

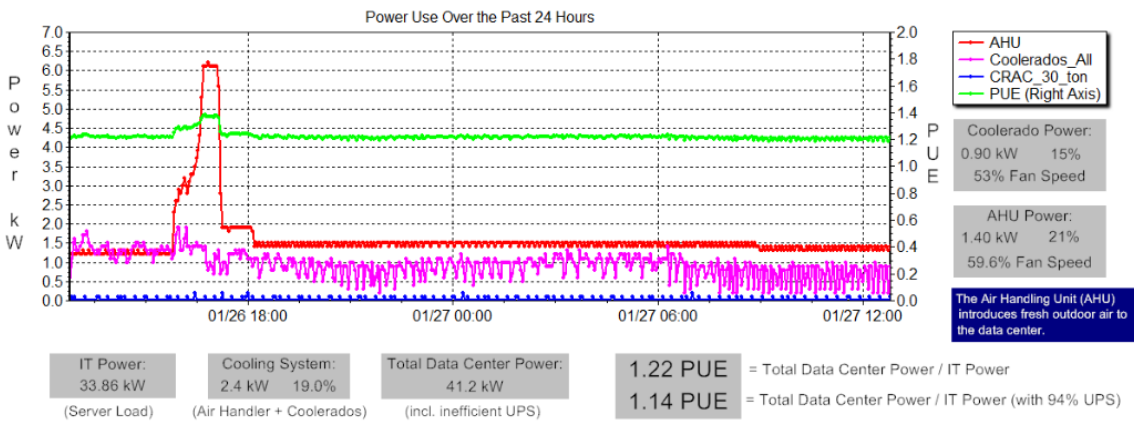


Figure 12. Screenshot of RTMC display of real-time data center performance.

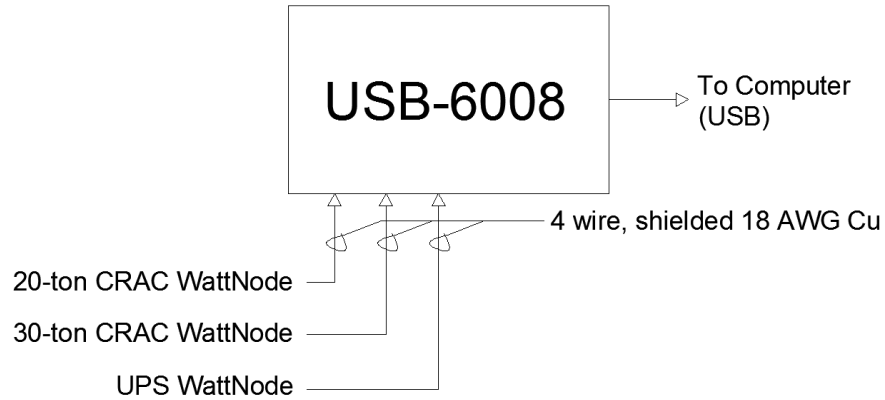


Figure 13. Schematic of USB-6008 Monitoring System (before Coolerado installation).

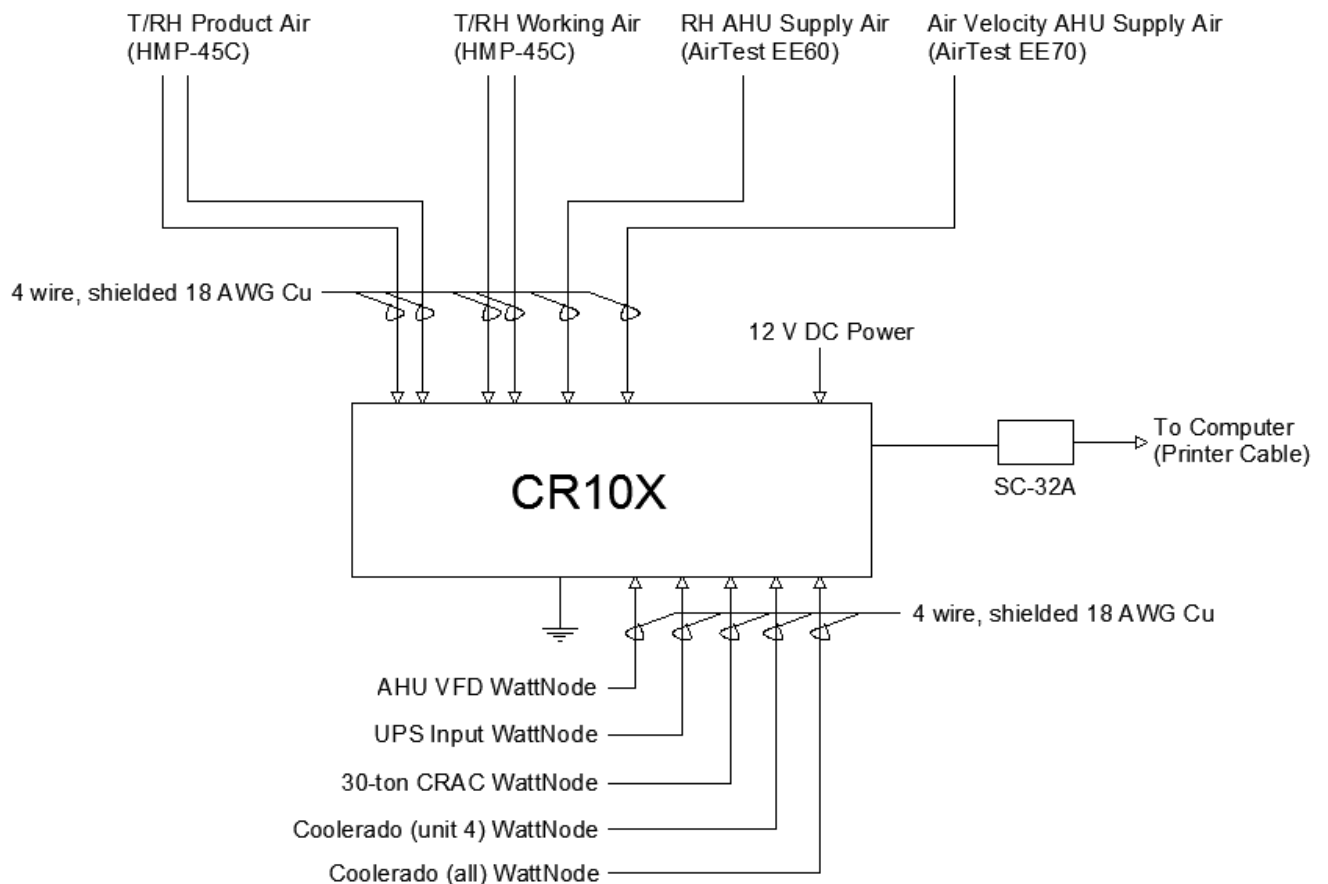


Figure 14. Schematic of Campbell CR10X monitoring system (after Coolerado installation).

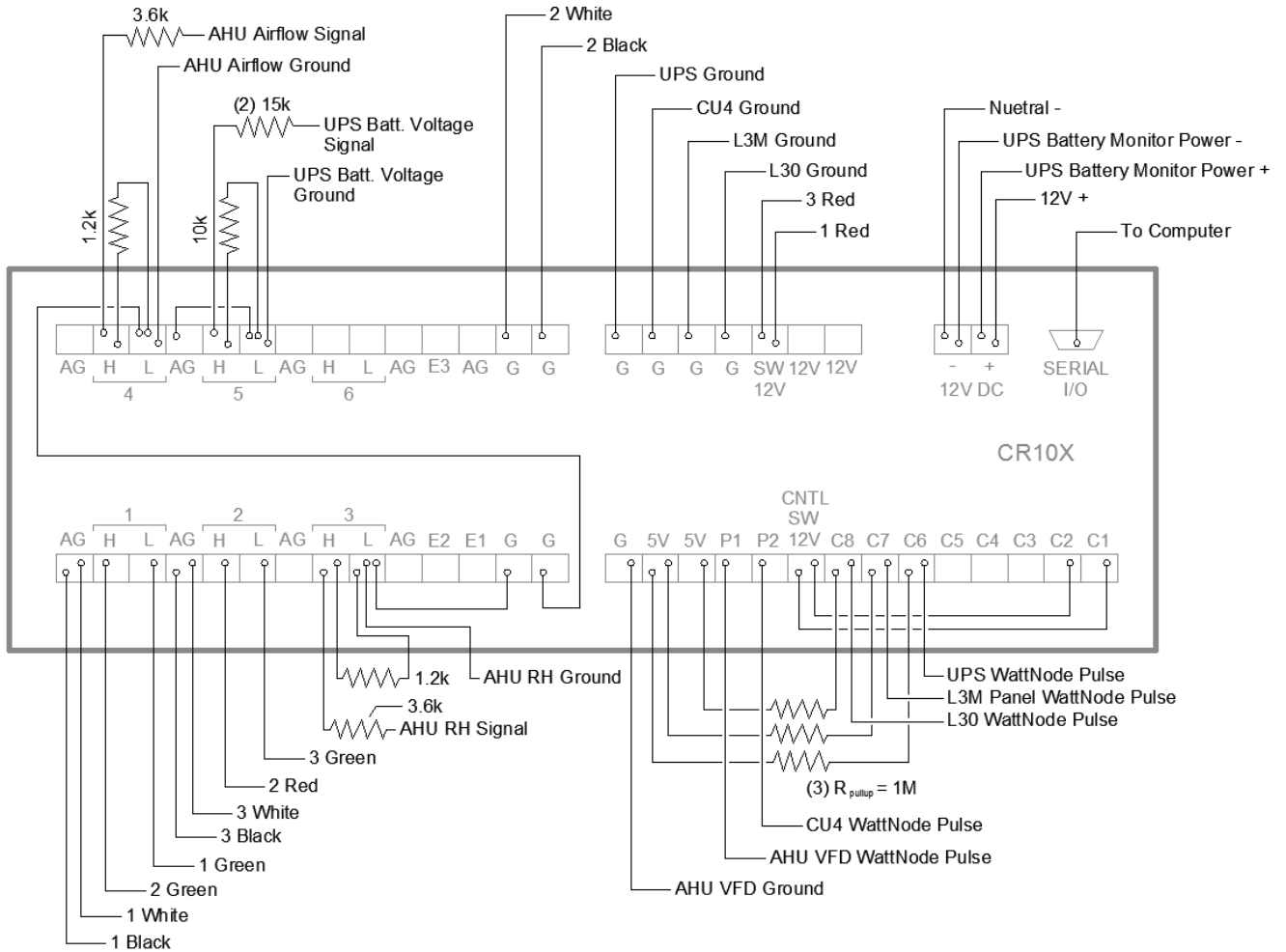


Figure 15. Wiring diagram for CR10X datalogger; all resistor values are in Ohms, for numbered wires, see below.

A more detailed wiring diagram for the CR10X datalogger can be seen in Figure 15. Note that some of wires are labeled 1, 2 or 3. Because the T/RH sensors have 6-wire leads and only 4-wire conductors were available, the two 6-wire leads (one from each T/RH sensor; 12 wires total) were divided between three 4-wire conductors for transmission to the CR10X datalogger. The wire re-assignments are defined below:

Campbell HMP45C (2) – Temperature and Relative Humidity Sensors (6 wires each)

Located on Coolerado Unit 4 (CU-4)

Working (Exhaust) Air Sensor in the Humid Air Damper of CU-4:

Red → 3 Red

Blue → 3 Green

Black → 3 Black

Yellow → 2 Red

White → 3 White

Clear → 2 White

Product Air Sensor in the back plenum of CU-4:

Red → 1 Red

Blue → 1 Green

Black → 1 Black

Yellow → 2 Green

White → 1 White

Clear → 2 Black

** Numbers refer to the 3 gray, shielded, 4-conductor wires beneath the raised floor. They are labeled with numbers 1,2,3. There is junction box where these connections are made in front of CU-1 beneath the floor tiles.*

The wiring diagram was necessary because of the small space and large number of wires required to monitor all of the appropriate points. Figure 16 demonstrates this necessity.

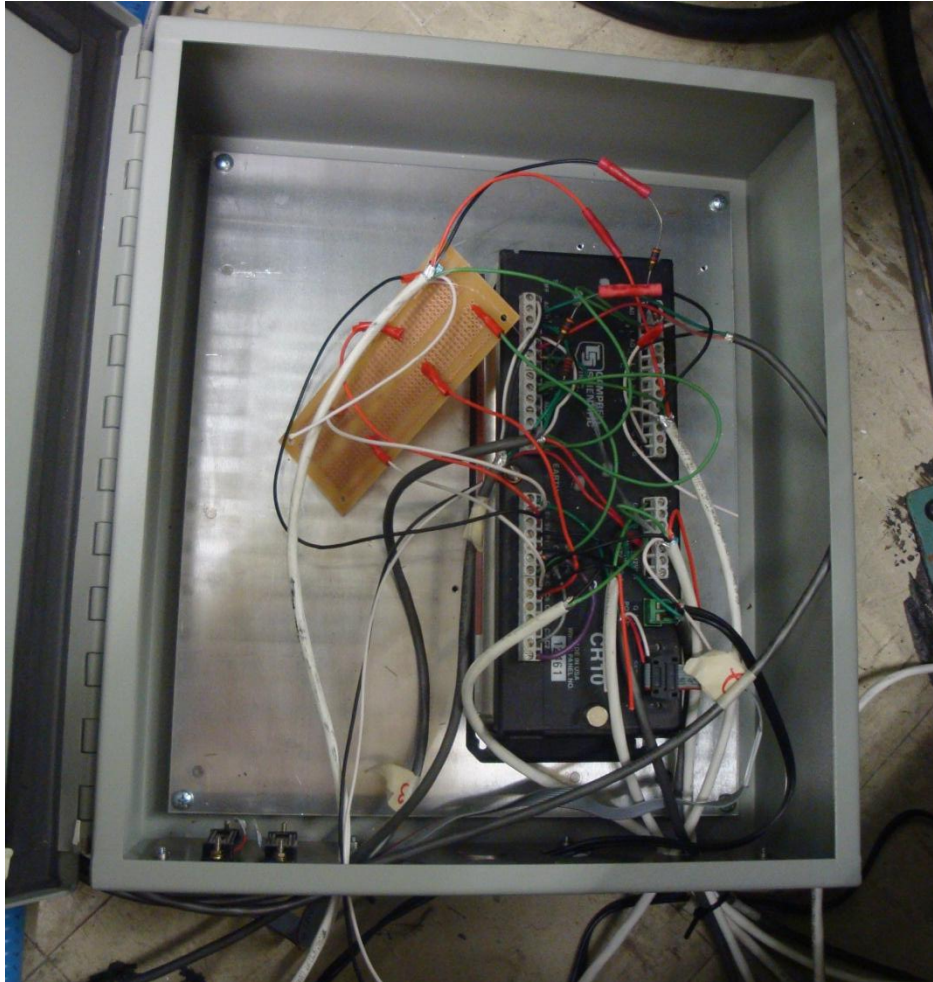


Figure 16. CR10X datalogger fully wired (photo taken Dec. 2011, but no changes made since August 2011).

Note that there is a small electronics board as seen in Figure 16. This board was used to organize the pull-up resistors necessary for using the Control Ports as pulse inputs for 3 of the WattNode devices. Other voltage dividers were installed directly inline with the signal wires, as shown in the wiring diagram. Note that all of these are 4:1 voltage dividers to step down the 0-10V signal to a 0-2.5V signal, which is the maximum range the CR10X can measure.

The data collected from the CR10X was later merged with other temperature and humidity data collected with a completely separate Onset HOBOnode network, arranged in the data center by NSIDC staff member Ron Weaver. Data points collected by this HOBOnode network include: East Wall T/RH, West Wall T/RH, AHU supply air T/RH, CU4 input temperature, north hot aisle temperature,

west hot aisle temperature, north Coolerado supply air temperature, south Coolerado supply air temperature, north wall temperature, and building voltage. Most of these data were only used for IT and data center management purposes; although CU4 input temperature is used in model validation.

All of the data from both the Campbell CR10X and the HOBO network were combined into one large dataset using custom MatLAB programs and a few Excel spreadsheets.

ONE-TIME MEASUREMENTS

Some measurements can only be obtained at a single point in time due to expensive instrumentation or impractical permanent setup arrangement. Most of these measurements are only relevant to the calibration of the theoretical model and were not a requirement of nor relevant to the IT management team of the NSIDC.

The one-time measurements needed for this project were pressure differentials across CU4 (the same unit that exhaust and product air temps and humidities are measured by the CR10X datalogger; see Figure 15) and airflow at the inlet to CU4 and at the supply inlet the room. Power consumption of the unit was also recorded manually from the datalogger display throughout the experiments. These on-time measurements were performed on February 17, 2012 at 11:00AM. Measurements were taken at 4 different fan speeds, which were manually adjusted with a built-in potentiometer on the new system's control board.

Pressure Differentials across CU4

The theoretical model developed by NREL requires two static pressure differentials as inputs: product air pressure drop and exhaust air pressure drop. Due to the unique design of the HMX, the two airstreams (supply and exhaust) must be measured separately. The product air

pressure drop is defined as the difference between the point just before the HMX (within CU4) and the point immediately after the HMX at the supply air outlet of CU4. The exhaust air pressure drop is defined as the pressure difference between the point just before the HMX and the point at the exhaust air exit of the HMX (within CU4). Both of these differentials are directly related to the fan speed of the unit, which is continuously variable. These measurements were performed with a self-averaging setup and a Dwyer manometer borrowed from the Larsen Laboratory in the Building Systems Program area of the Engineering Center.



Figure 17. Pressure differential measurement setup in NSIDC on CU4.

Because both outlets on CU4 are open to the room or the outdoor atmosphere (supply air or working air, respectively), the pressure differentials are very close to the same and very close to the fan pressure. However, because this data was to be compared with similar pressure measurements taken by Coolerado, the pressure measurement setup on CU4 (seen in Figure 17) was installed with the exact same arrangement that Coolerado used. Figure 18 shows the dimensions used for the same test run by Coolerado. Inlet pressure taps were placed 7" behind the front vertical seam of the unit. Exhaust pressure taps were placed 1.5" in front of the rear vertical seam of the unit. And supply air pressure taps were placed roughly in the middle of the supply plenum. Note that three pressure taps were installed at each location (for a total of 9). This measurement is trying to quantify the pressure differential across each of the two air paths within the HMX. Note that because the Coolerado unit has 5 HMX's in it, these pressure measurements are an average across all 5 HMX's.

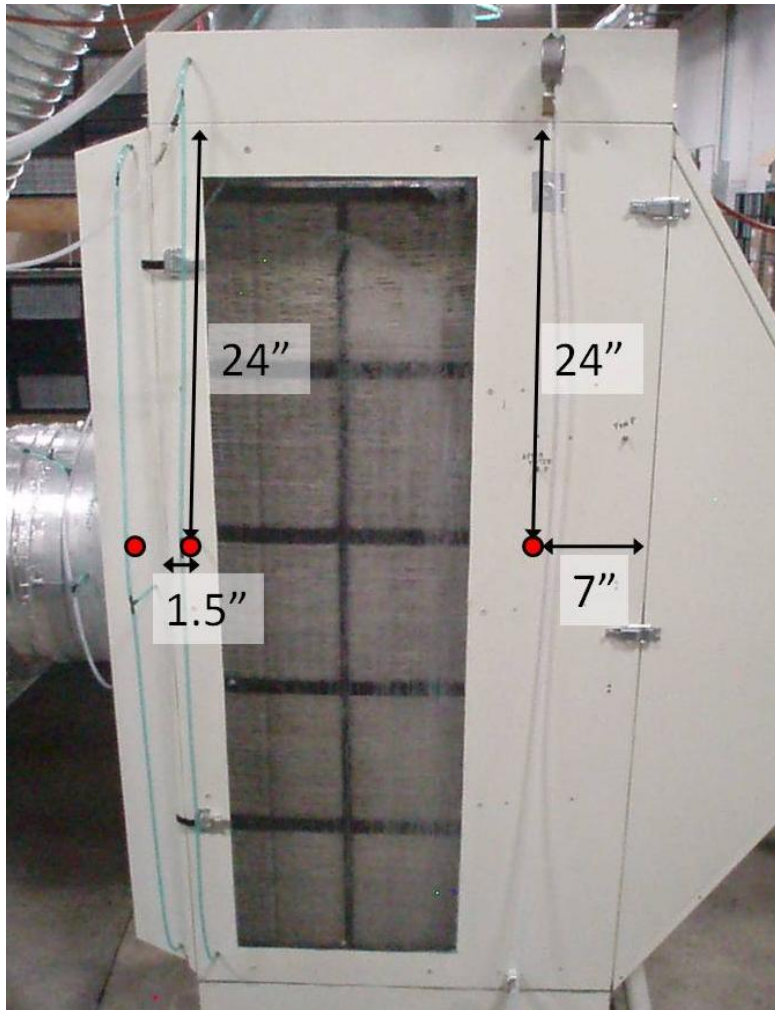


Figure 18. Dimensioned image of pressure measurement setup on an identical Coolerado unit [photo courtesy of Daniel Zube, Coolerado].

The pressure, airflow, and power measurements are given in Table 5 below. Note that the pressure drops across both airstreams were about equal for a given power. This was also the case in Coolerado's test data. Although in some installations, radically different duct arrangements on either airstream could affect this relationship, in the NSIDC, both airstreams are released to near atmospheric pressure, and this explains the similarity. Product air is directed directly out the back of the unit and working air is directed vertically up through the roof about 10' to the outside. The room pressure is kept slightly positive, but the setpoint is only 0.015" which is a very small amount and likely not noticeable in these measurements, at least relative to the fan pressure.

Airflows

Airflows at the inlet of CU4 and the air inlet to the room had to be measured to more precisely quantify the airflow profile at each location. Due to the asymmetric introduction of air to the inlet of all 8 Coolerado units, simply dividing the total airflow into the room (which is measured with the CR10X datalogger) would not provide enough accuracy for comparison to the theoretical model. A hot wire anemometer was used to determine the velocity profile for both of these measurements. Each velocity measurement must be made to represent an equal area of flow. When this condition is met, a simple average of all measurements will provide an accurate average velocity. This velocity can easily be converted to volumetric flow by multiplying by the total area of the inlet. A diagram of the measurement locations can be seen in Figure 19.

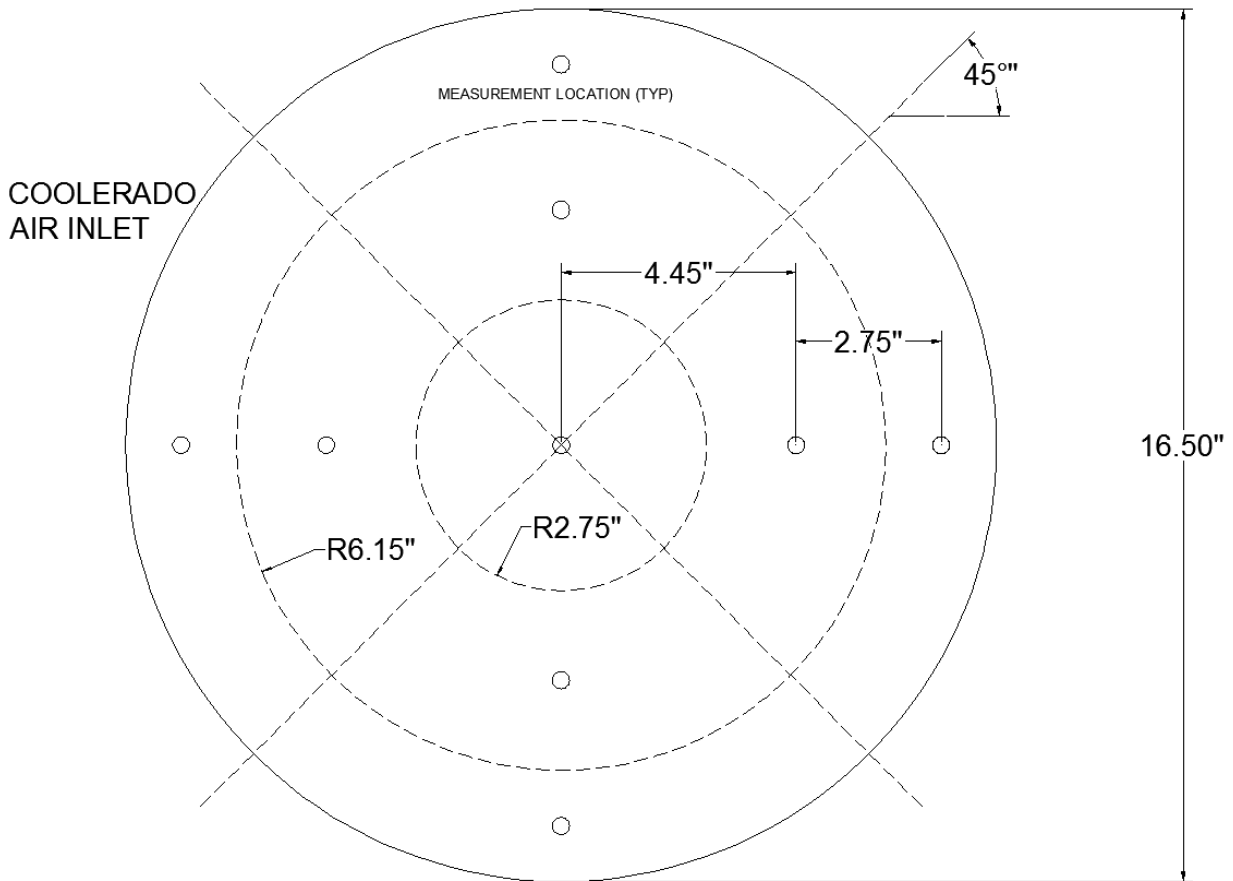


Figure 19. CU4 inlet flow measurement diagram.

Note that all flow measurements were taken perpendicularly to the inlet. And although there are probably some velocity vectors that are not perpendicular to the inlet plane (especially around the edge), these were not considered in this measurement due to time constraints and the number of measurements required. Nine measurements were taken at 4 different fan speeds, for a total of 36 measurements. Table 5 below shows all of the pressure and airflow data collected from CU4.

Table 5. Summary of one-time pressure, airflow and power measurement data.

Power (kW)	Pressure (in W.C.)	Airflow (CFM)
0.033	0.05	438
0.150	0.24	1319
0.400	0.55	2144
0.500	0.68	2488

The one-time pressure and airflow data collected were used to develop correlations and regressions between power, airflow and pressure. Pressure and airflow data was also received from Daniel Zube, a Test Engineer at Coolerado. Zube was able to run a similar test on the same day using Coolerado’s test M50 unit at their facility in Denver. Additionally, Coolerado’s test unit is equipped with separate Venturi flow devices for accurately measuring airflows of the product and working air separately. Zube’s data shows that approximately 62% of the total air flow becomes product air (and 38% of the total air becomes working air). This data is summarized in Figure 20.

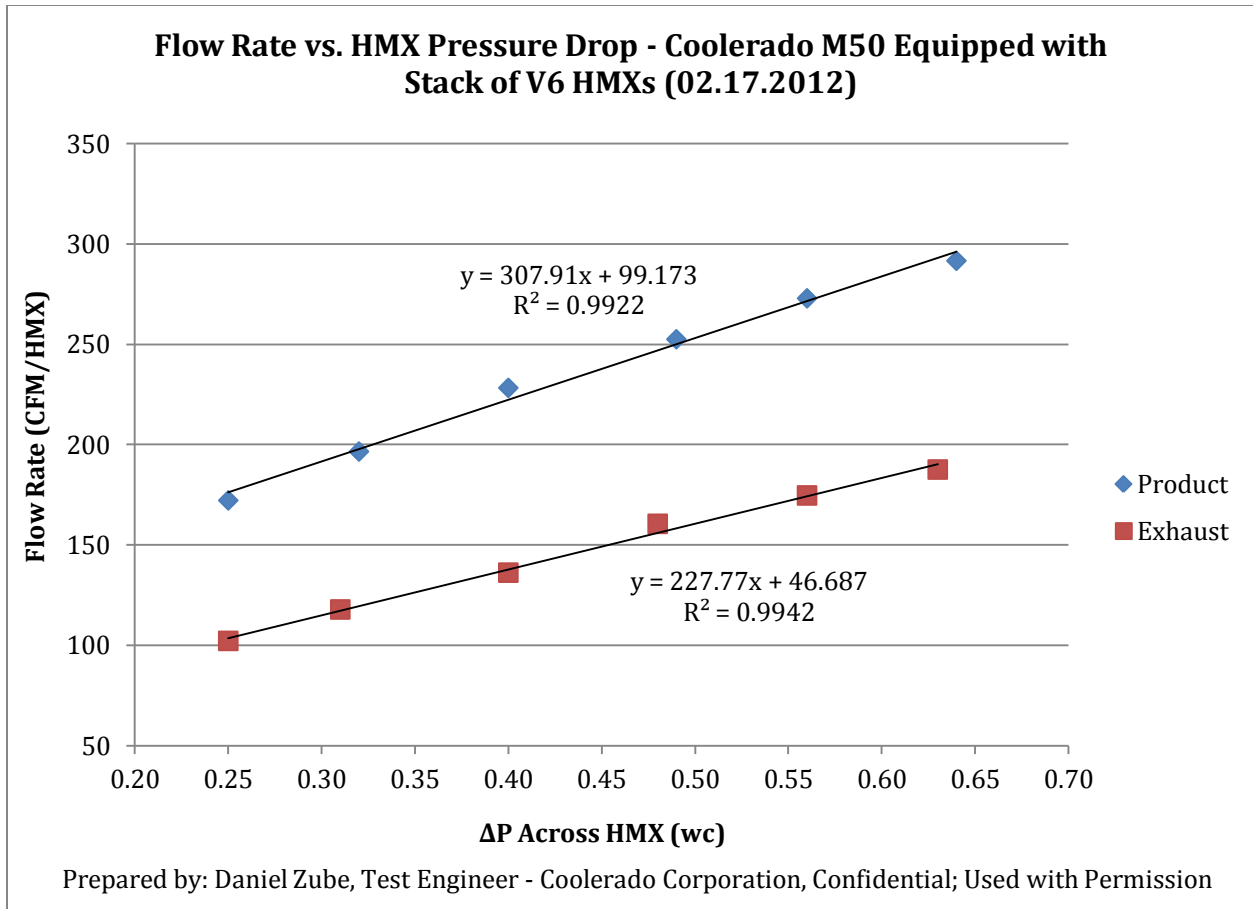


Figure 20. Pressure drop and airflows from Daniel Zube at Coolerado for an M50 unit [12].

Zube's product and working air flows were summed to determine a total airflow for each pressure drop in Figure 20. It is important to note that the pressure drops across both airstreams were about equal for each step; this is a similar finding to what was seen on the NSIDC CU4 unit. Also note that the airflow in Figure 20 is in units of CFM/HMX. For comparison to the CU4 data, these values were multiplied by 5 because there are 5 HMX's in the M50 units at the NSIDC. Figure 21 below shows the data and regressions for pressure vs. airflow for the one-time measurements on CU4, Zube's data, and the MatLAB model predictions. Note the error bars for the CU4 data nearly encompass all of Zube's data.

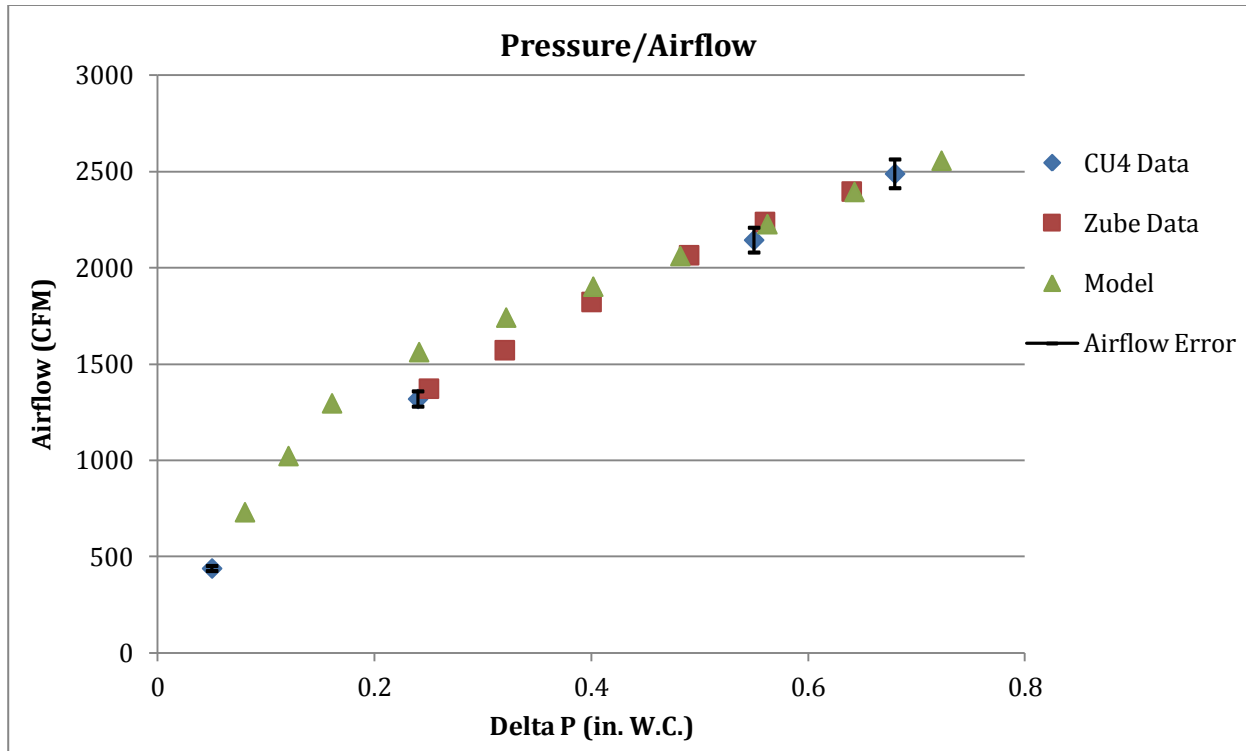


Figure 21. Pressure vs. airflow data and regressions.

The model pressure and airflow predictions were based on simply running the model at pressure differences (Delta P) ranging from 20Pa to 180Pa in 20Pa increments. All other model inputs were held constant at values derived from an HMX sample sheet. It was later discovered that this sample sheet was from a previous HMX version and the dimensions used for model verification and optimization were adjusted. The adjusted model's pressure and total airflow correlation did not differ more than 100 CFM from the correlations seen in Figure 21. Figure 22 shows that the MatLAB model is reasonably suited to predict the airflows through an HMX, even before calibration.

Table 6. Sample HMX sheet dimensions.

	Width (mm)	Height (mm)	Wall Thickness (mm)	Hole Diameter (mm)
Indirect Channel	23.4	3.18	1.9	4.75
Ind/Dir Channel	23.4	3.18	1.9	4.75
Direct Channel	23.9	2.25	1.6	4.75

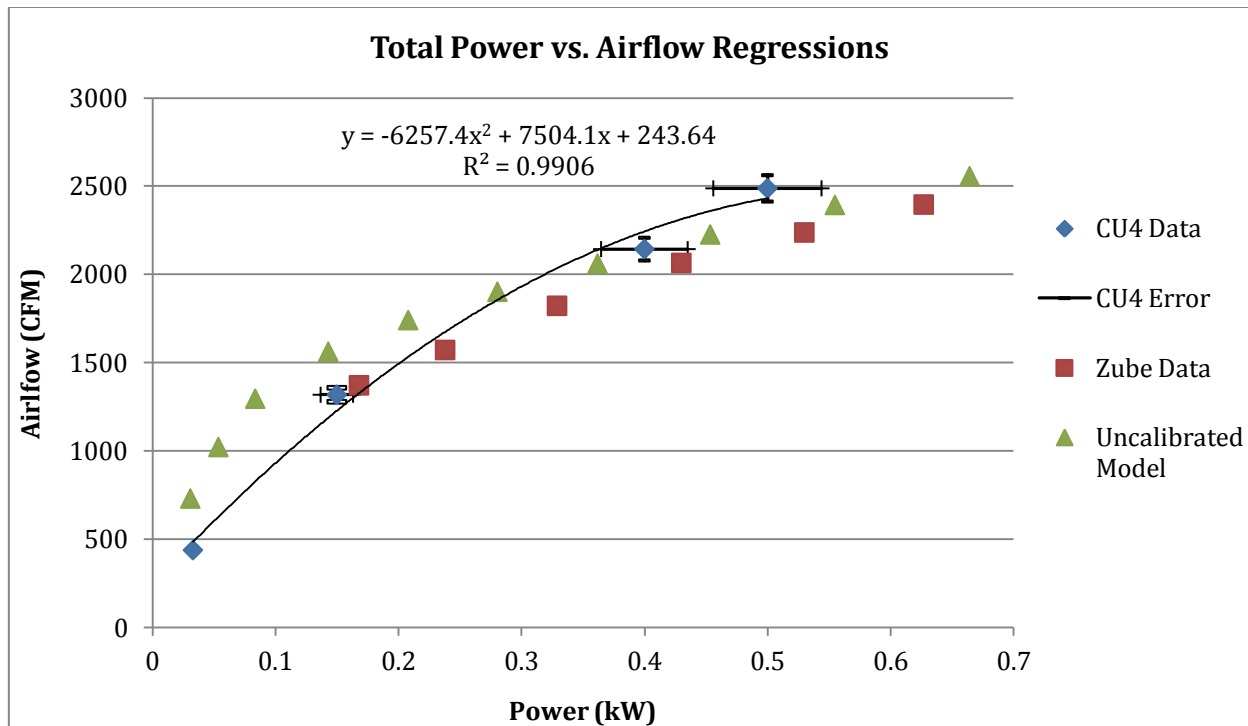


Figure 22. Total power vs. airflow data and regressions.

The relationship between power and airflow can be seen in Figure 22. Note that the correlation between the different datasets and the model isn't as close as it was for the pressure and airflow relationships in Figure 21. During Zube's test, a slightly different fan and motor were used in Coolerado's test M50 unit; hence the difference between Zube's test data and the data from CU4 in the NSIDC. The model total power was calculated from model output; hydraulic power divided by fan and motor efficiency. For this plot, the combined fan and motor efficiency of 35% combined placed the model predictions reasonably between Zube and CU4 data. The model total power and airflow relationship exhibits a similar shape to the other datasets, but with a flatter curve on the top end. It is also interesting that the model airflow has a very steep slope at low power levels. It is evident that the methods used to measure total power are not very precise. However, because this report is focused of the performance of the CU4 unit at the NSIDC, the regression from that data could be used to predict the approximate total airflow through an M50 unit at any point in time (if the total power is known).

Version 6 HMX Dimensions

Due to limitations in Coolerado's current manufacturing methods, the HMX sheet dimensions are not exact and have tolerances associated with them. The channel dividers are made from beads of polyethylene plastic and are attached to the sheet using a mechanical system similar to a hot glue gun. The flow rate of the warm polyethylene and the speed of the machine affect the bead thickness and height. And adjusting this device to produce a specified bead dimension is a trial and error process. Note that the working air sheets and product air sheets can be different heights, but on any one sheet, the heights are consistent. Because of significant variation in the inlet channel heights (visible in Figure 23), measuring this dimension would be difficult and likely inaccurate. However, the front face of the frame has an open height of 10.0" (254mm). This total dimension ultimately controls the number of sheets and therefore average channel height available in any given HMX block. Coolerado claims to stack somewhere between 39 and 43 product air sheets into an HMX frame; the exact number varies in this range because of current manufacturing tolerances. There are 39 product air channels in each of the top 3 HMX blocks of CU4. It is assumed that the bottom 2 HMX blocks also have 39 product air channels. With an open face height of 10.0", this results in a combined value of 6.51mm for a product air channel, working air channel and two polypropylene sheets with wicking material. There is 1 working air channel for every product channel; and the working air channel is not open to the inlet directly because it flows sideways out either side of the HMX. Instead, the end working air channel dividers are sealed on the front and back of the HMX with hard epoxy. See Figure 23.

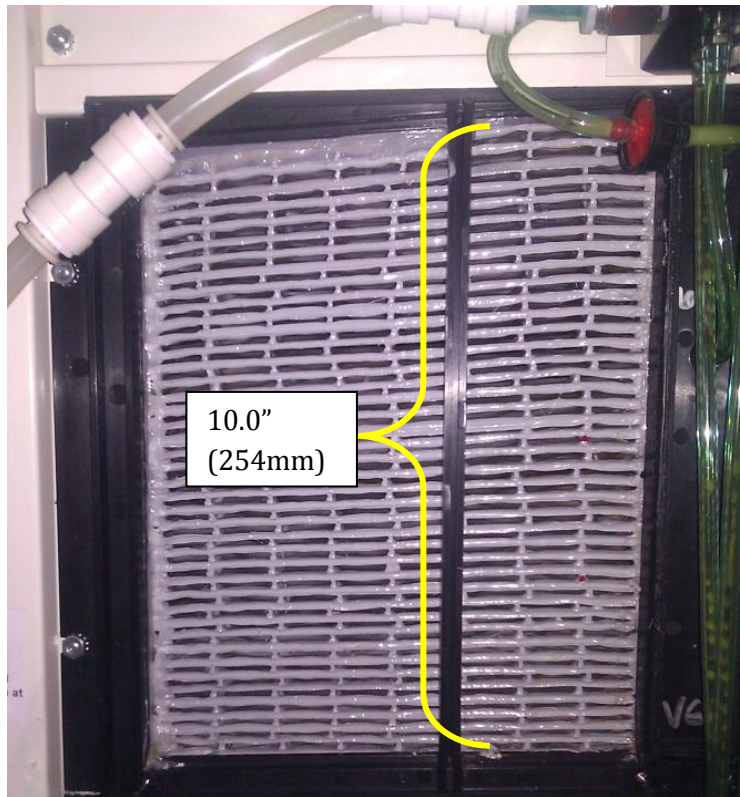


Figure 23. Front (inlet) side of top HMX block.



Figure 24. Front (inlet) side of HMX, close-up; Note the wide variance in open channel heights and non-uniform inlet shape due to epoxy sealant.

This sealing process is not exact and often causes significant deformation to the otherwise rectangular product channel inlets. The irregular inlets may have a negative impact on the performance of the HMX.

Also according to Coolerado, the sheet material and thickness has been consistent throughout the past few years. The average sheet thickness is 0.566mm. Because 2 sheets are included in the 6.51mm, the actual combined channel height of product and working air channels is 5.38mm. As stated previously, the product air and working air channels can have different heights, so it is not realistic to assume a perfect split of this total value for each channel height. Coolerado claimed that the product and working air channels had nominal heights of 0.15" (3.81mm) and 0.10" (2.54mm) respectively. However, if these values are used, the total height of 39 product channels is 11.27" which is above the maximum of 10.0". So, rather than use those nominal values, the ratio between the product and working air channels is used with the 5.38mm total to determine product and working air channel heights respectively. The product to working air channel height ratio is 0.15:0.10 or 3:2. Therefore the product air channel height should be about 60% of the total and the working air channel height should be about 40% of the total, or 3.23mm and 2.15mm respectively.

Nominal channel width is limited to 1.0" O.C. from divider to divider. According to Coolerado, using a channel width wider than 1.0" does not leave enough support for the pliable sheets and causes the HMX to lose structural rigidity. Yet for a given total width, wider channels result in more heat transfer surface area and therefore better performance (both thermally and hydraulically) in theory. So the actual channel width is the maximum 1.0" minus bead thickness, or about 23.4mm (assuming a channel divider width of 2.0mm).

DAQ SYSTEMS UNCERTAINTY

Each measurement taken using each different measurement system is subject to some degree of uncertainty. It is prudent to document the uncertainty in every measurement in order to attempt to quantify the accuracy of the measurement, particularly if the data will be used for in depth analysis or simulation. Table 7 shows the uncertainty in each measurement. These uncertainties were taken in to account during the calibration and modeling of the Coolerado HMX, as discussed in the next section.

Table 7. Monitored data points summary table.

Measurement	Sensor	Manufacturer	Accuracy	Notes	Sensor Output
Product Air RH	HMP45C	Campbell Scientific	2.0%	0-90% RH	0-2.5V Diff. Voltage direct to CR10X
Product Air Temp		Campbell Scientific	0.05% /°C	Temp Dependence	
Working Air RH	HMP45C	Campbell Scientific	0.20 °C	@ 20°C	0-2.5V Diff. Voltage direct to CR10X
Working Air Temp		Campbell Scientific	0.30 °C	@ 0 or 40°C	
AHU Supply Air RH	EE16	Airtest	3.0%	90-100% RH	0-2.5V Diff. Voltage direct to CR10X
AHU Supply Air Velocity	EE65	Airtest	0.05% /°C	Temp Dependence @ 45% RH	
Coolerado Unit 4 Power	WNB-3Y-208-P	Continental Control Systems	40.0 fpm	+ 3% of diff. voltage	0-10V Diff. Voltage to hand-made voltage divider then to CR10X
	CTS-0750-200	Continental Control Systems	< 3.0%	@ Delta_alpha < 10° (angular dependence)	
INPUT Air Temp	ZW-007	HOBO	3.0%	@ 20°C	(direct to HOBOnode network and local MacBook)
INPUT Air RH			0.50%	of voltage measurement	
Coolerado Unit 4 Input Temp	ZW-001	HOBO	1.00%	of current measurement (each CT)	0-33V Diff. Voltage direct to WattNode
			2.0 °	phase angle accuracy (each CT)	
Datalogger	CR10X	Campbell Scientific	0.21 °C	0 - 50°C	(direct to HOBOnode network and local MacBook)
One-time CU4 Inlet Air Velocity	407123	Extech Instruments	2.5%	10-90% RH	(direct to HOBOnode network and local MacBook)
One-time CU4 Pressure Differentials	200	Dwyer Instruments	0.21 °C	valid 0 - 50°C	(direct to HOBOnode network and local MacBook)
			0.05%	of FSR (for diff. voltage measurements; 1.25mV)	Serial / RS232 to local PC
			3.0%	Basic Accuracy	(LED screen)
			2.0%	Basic Accuracy (although mostly dependent on user interpretation of reading)	(gage fluid level)

The uncertainty in any measurement (or group of measurements) can be determined by the square root of the sum of the squares of systematic error and random error, as seen in Equation 12.

$$Error = \sqrt{systematic^2 + random^2} \quad (12)$$

Manufacturer’s published error bounds (seen in Table 7) typically represent systematic error. Random error is defined as error that is introduced due to fluctuations in the reading or experimenter’s interpretation. Random error is more difficult to quantify. But for a group of repeated measurements that should be the same, the average should represent the true value. Then the difference between each value and the average can be calculated. The sum of the squares of these differences is the random error. For error in calculated values (as in Equation 9 for power), the error in the calculated value is defined as seen in Equation 13.

$$\text{Error in Calculated Value } C = \left[\sum_1^i \left(\frac{\partial C}{\partial X_i} \Delta X_i \right)^2 \right]^{\frac{1}{2}} \quad (13)$$

Where X_i represents the input variables to the calculation and ΔX_i represents the combined error in each variable as defined by Equation 12. Equation 14 defines this specifically for power, as calculated by the WattNodes. The partial derivatives are derived from Equation 9.

$$\Delta W = \sqrt{\left(\frac{\partial W}{\partial I} \Delta I \right)^2 + \left(\frac{\partial W}{\partial V} \Delta V \right)^2 + \left(\frac{\partial W}{\partial \phi} \Delta \phi \right)^2} \quad (14)$$

This method is used for determining the error in all power measurements taken by the WattNodes. This method is a basic uncertainty calculation method for “pure product form” equations, like Equation 9, and is documented in [13].

NREL MATLAB MODEL

MODEL DESCRIPTION

In 2009, an effort was made to model the Coolerado HMX cooling performance using purely theoretical relations and equations. Much of Coolerado's in-house design work is currently based on mostly experimental data and curve fit relations. NREL had received funding to develop a MatLAB model. MatLAB was the chosen platform because it is very flexible as a generic programming language and handles iterations and matrix calculations very efficiently; both of these functions are critical to solving the fundamental heat and mass transfer equations within a Coolerado HMX described in the previous chapter.

The model was packaged neatly and organized with all related m-files and functions and can be run on any computer with MatLAB 7 or newer. It is fully equipped with a graphical user interface (GUI) that shows the simulated sheet designs (direct, wet side and indirect, dry side) as well as numeric inputs for the user to adjust this design. Input and output values are highlighted in Table 8.

Table 8. Input and Output variables for HMX MatLAB model.

INPUTS:	OUTPUTS:
• Number of Ind/Dir Channels:	• T_DB Process Outlet:
• Number of Dir Channels:	• T_WB Process Outlet:
• Number of Ind Channels:	• Process Humidity Ratio:
• Width Ind/Dir Channels (mm):	• Process Relative Humidity (%):
• Width Dir Channels (mm):	• Process Enthalpy (kJ/kg):
• Width Ind Channels (mm):	• Process Density (kg/m ³):
• Width Ind/Dir Sep. Wall (mm):	• Process Dry Mass Flow (kg/s):
• Width Dir Sep. Wall (mm):	• T_DB Exhaust Mean:
• Width Ind Sep. Wall (mm):	• T_DB Exhaust Mixed:
• Height Ind/Dir Sep. Wall (mm):	• Exhaust Humidity Ratio:
• Height Dir Sep. Wall (mm):	• Exhaust Relative Humidity (%):
• Height Ind Sep. Wall (mm):	• Exhaust Enthalpy (kJ/kg):
• Paper Thickness (mm):	• Exhaust Density (kg/m ³):
• Waterfilm Thickness (mm):	• Exhaust Dry Mass Flow (kg/s):
• Number of Process Layers:	• Water Evaporation (kg/s):
• Number of Holes (each Ind/Dir Channel):	• Cooling Power (kW):
• Hole Dia (each Ind/Dir Channel):	• Process WB Effectiveness (%):
• Paper Conductivity (W/m-K):	• Process DP Effectiveness (%):
• Waterfilm Conductivity (W/m-K):	• Exhaust WB Effectiveness (%):
• Ambient Pressure (Pa):	• Exhaust DP Effectiveness (%):
• T_DB Process Inlet:	• Process Hydraulic Power (W):
• T_WB Process Inlet:	• Exhaust Hydraulic Power (W):
• Process DeltaP (Pa):	• Hydraulic Power (W):
• T_DB Exhaust Inlet:	• COP:
• T_WB Exhaust Inlet:	• EER:
• Exhaust DeltaP (Pa):	

Screenshots of the GUI can be seen in Figure 25 and Figure 26. Note the inputs seen in Table 8.

appear on the right side of the images, and the outputs can be seen near the bottom of the images.

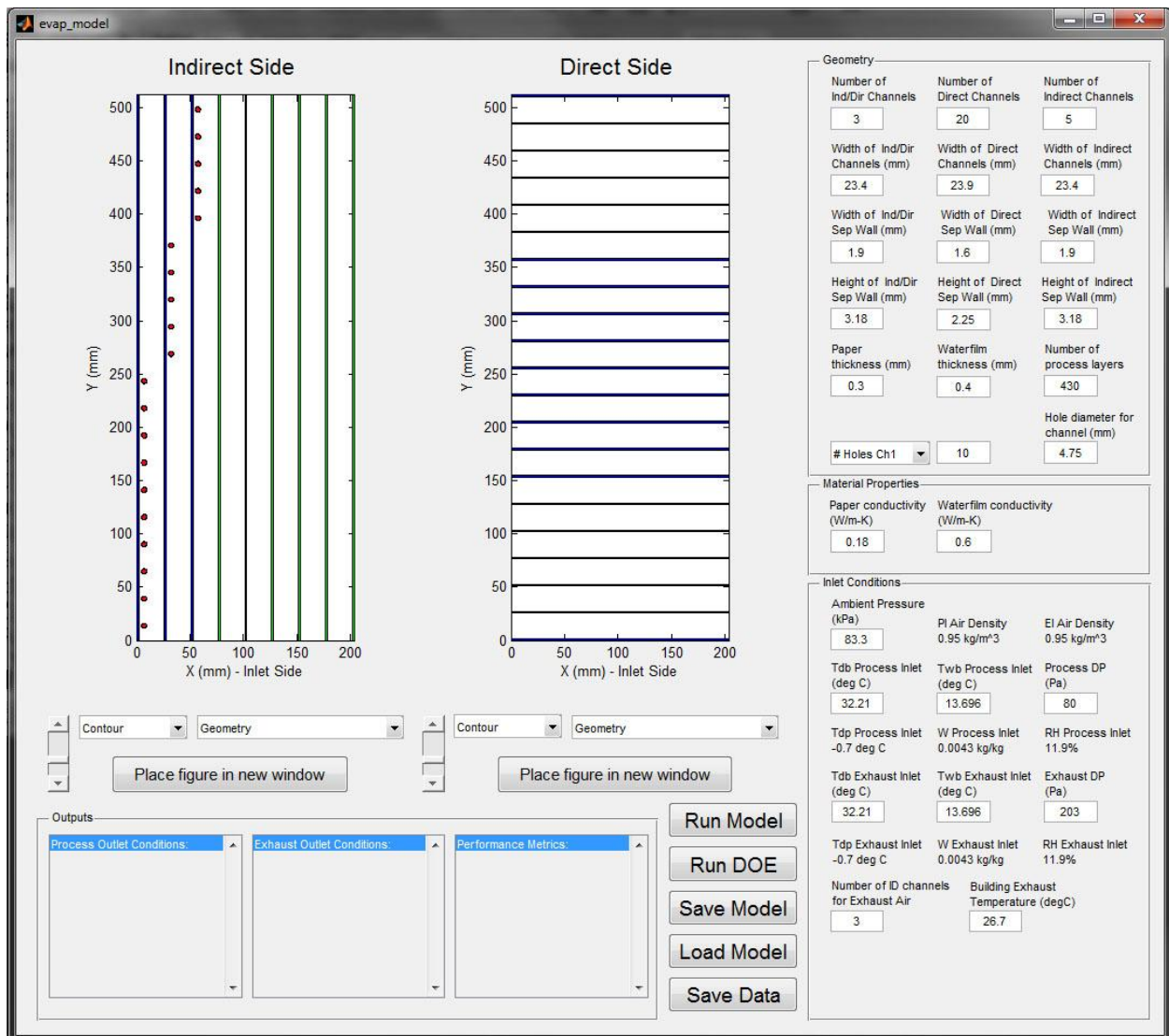


Figure 25. Screenshot of model GUI.

It is important to note that the model includes input pressures (Process and Exhaust DP; separately) and not airflow or fan power. The model does not simulate performance of the M50 unit as a whole, including fan power and other miscellaneous power (control board, soap pump, etc.). It is only designed to simulate the internal HMX performance because that is the unique centerpiece of the Coolerado air conditioner, and well-known understanding or correlations between fan efficiency and total power consumption can be used to determine the total power use of an M50 unit. Note that the model outputs hydraulic power, which is the power defined by Equation 15 and Equation 16.

$$\text{Hydraulic Power} = \dot{V}_{\text{total airflow}}(\Delta P) \quad (15)$$

$$\text{Hydraulic Power} = \frac{\dot{m}_{\text{exhaust air}}}{\rho_{\text{exhaust air}}} (\Delta P_{\text{exhaust}}) + \frac{\dot{m}_{\text{process air}}}{\rho_{\text{process air}}} (\Delta P_{\text{process}}) \quad (16)$$

$\dot{m}_{\text{exhaust air}}$ = exhaust air flow rate (kg/s), calculated by the model

$\rho_{\text{exhaust air}}$ = density of exhaust air (kg/m³), calculated by model

$\Delta P_{\text{exhaust}}$ = pressure differential (Pa) from HMX inlet to the exhaust outlet

$\dot{m}_{\text{process air}}$ = process air flow rate (kg/s), calculated by the model

$\rho_{\text{process air}}$ = density of process air (kg/m³), calculated by model

$\Delta P_{\text{process}}$ = pressure differential (Pa) from HMX inlet to the process outlet

Hydraulic power is the power that must be provided to the airflow by the fan in order to achieve the flowrate and pressure differential. Total power consumption of an M50 unit is related to hydraulic power through the fan and motor efficiencies as seen in Equation 17.

$$\text{Total Power} = \frac{\text{Hydraulic Power}}{\text{Efficiency}_{\text{fan}} * \text{Efficiency}_{\text{motor}}} + \text{Misc. Power Uses} \quad (17)$$

Fan efficiency is obtained from the fan specifications and an average value of 60% is reasonable for this analysis. Motor efficiency is unknown.

Miscellaneous power consumption includes the M50 internal controls, pumps and other equipment. See Table 9. Note that the soap pump and solenoid only run periodically; therefore they were not included when calculating the total instantaneous power consumption.

Table 9. M50 Miscellaneous Power Consumption (Courtesy of Coolerado).

M50 Power Consumption Summary	
<i>Component</i>	<i>Power Consumption (W)</i>
Board	8.6
Thermostat	1.2
Fan	618.2
Soap Pump	6.5
Solenoid	14
Total	648.5

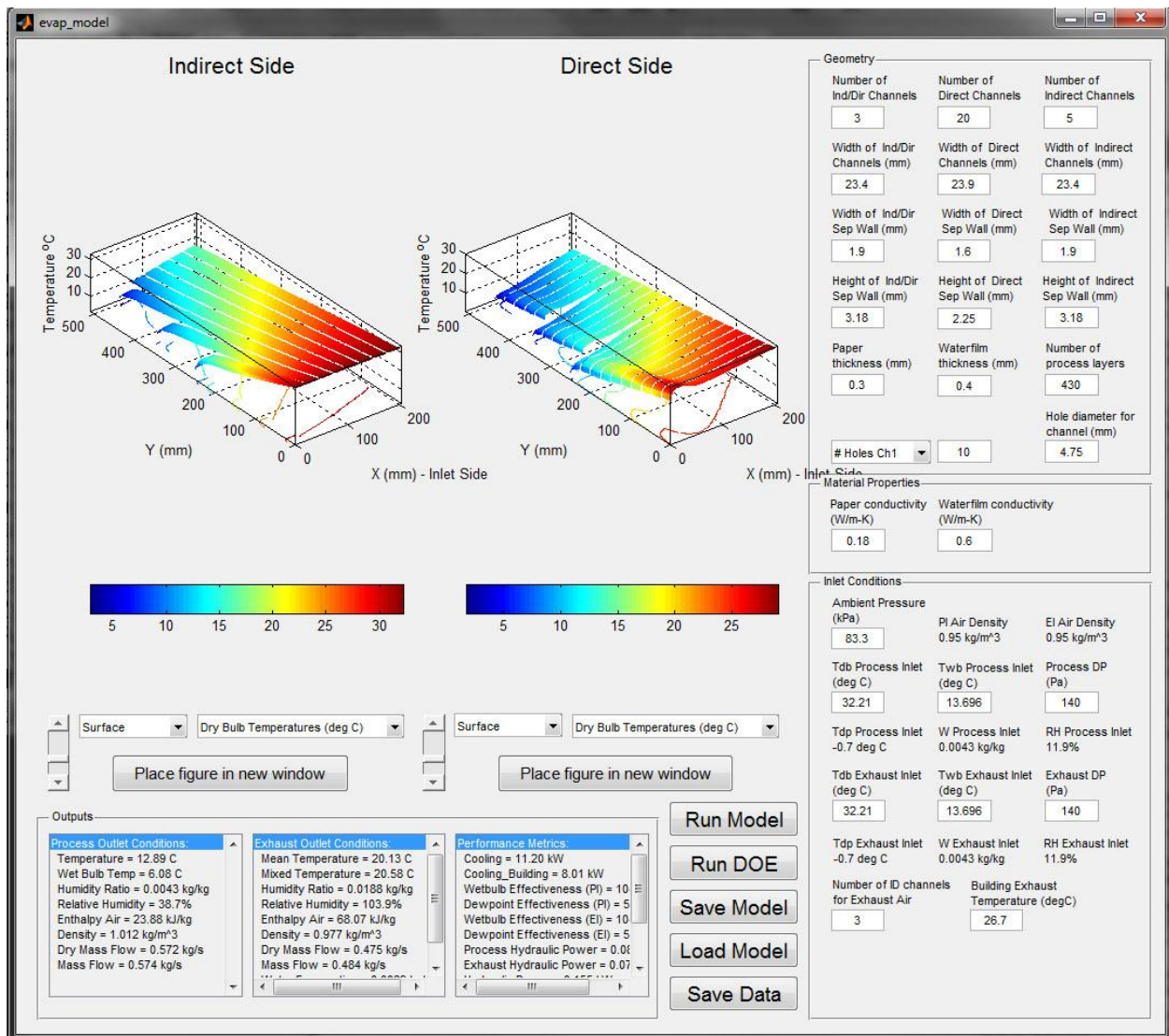


Figure 26. Model screenshot of GUI after simulation.

The model interface displays most of the output conditions near the bottom of the screen; outputs are divided into Process Outlet Conditions, Exhaust Outlet Conditions and Performance Metrics (see Figure 26). As expected, Process Outlet Conditions includes information on the air state and flow out of the process (supply) channels. The Exhaust Outlet Conditions includes air state and flow information for the humid, exhaust (working) air channels out the side of the HMX. Performance Metrics includes efficiency (COP and EER) of the HMX unit for the given input conditions. It also includes wet-bulb and dewpoint effectivenesses for both Process (supply) and

Exhaust (working) air. Because the model has the input capability of different process inlet and exhaust inlet air conditions, these effectivenesses can be calculated separately; although the basic M50 Coolerado units that the NSIDC employs are not equipped with this capability.

The GUI also has a few different ways to view the outputs graphically. After running a model, the user can use the drop-down menus to choose the type of display as well as what data to display (see Figure 27). The best plots to look at dry-bulb or wet-bulb temperatures are the “surface” plots or “filled contour”. Note that the model calculates air state properties throughout the HMX sheet on both the direct and indirect sides. The Process Conditions and Exhaust Conditions boxes on the GUI are the combined outlet values from all supply or exhaust channels, respectively.

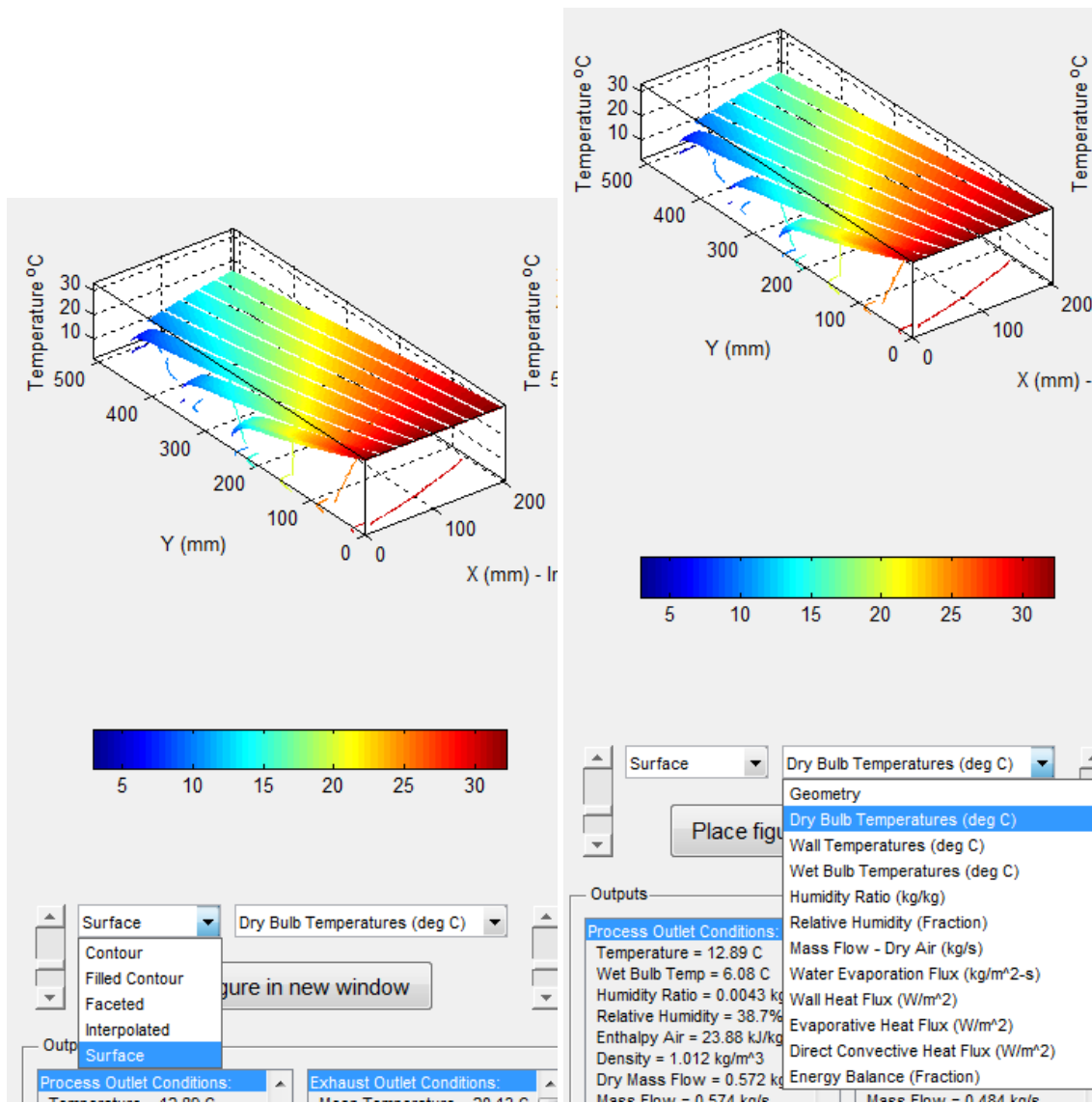


Figure 27. Drop-down menus for changing graphical representations of results.

The model GUI, in addition to simply running the model, includes buttons to save the current model design, load a previously saved design, or save the output data directly to a text file. This last feature was especially important for comparing the model predicted outputs to CU4 data as well as other previous simulations; it was easiest to perform the comparison with spreadsheet software (Microsoft Excel). Although the plots produced by the model GUI are great for visualizing the general temperature or humidity or heat transfer trends, for comparing small changes between

designs, actual performance outputs are needed because many of the changes didn't have obvious or noticeable impacts on the 3D or 2D plots.

BASIC MODEL ASSUMPTIONS

Before the model could be used for testing different HMX designs, it had to be validated; it had to be shown that appropriate assumptions were made, where necessary, and that most of the theoretical fluid dynamics and heat transfer phenomena are correctly simulated. Simply inspecting the model code Solve.m revealed that the very same equations defined by Equations 4-8 are used in the model. It was relieving confirmation to see that the model was theoretically sound and included the right level of detail to produce realistic results. Upon further inspection, it was evident that the model made a few other assumptions that may not be realistic but were necessary to allow the theoretical computations to work:

1. **Rigid sheet structure** – In reality, the polypropylene sheet material is very thin (like paper) and pliable. This means that most of the structure of the HMX blocks comes from the outer frame (rigid polypropylene/glass material) and the polyethylene separation walls between each channel. Because the actual sheets are pliable, varying flows and pressures would likely have an effect on the geometry of each channel; they would not be perfectly rectangular like the model assumes.
2. **Airflow knob factor** – The developer of the model calibrated the airflows with experimental data that was taken at a limited number of performance points. The experiment was performed at NREL facilities. “knob factors” were used to adjust the theoretical, calculated friction factors within the model to fit this data.
3. **Hole Placement** – The actual HMX design has holes in the first 2 ind/dir channels only (10 holes each); the 2nd and 3rd ind/dir channels are connected through 2 breaks in the separation wall. The concept behind this is to direct more air into the last 5 holes, which

otherwise may be limited due to pressure resistance. The model does not have the capability to place breaks in the separation wall. The default model design simply has 10 holes in the 1st ind/dir channel and 5 holes in each of the next ind/dir channels (see Figure 25).

4. **Number of Process Layers** – The model assumes that the heat and mass transfer phenomena that occur within an HMX block is symmetrical; each sheet has two sides that are asymmetrical across the trough in the middle. Version 6 HMX blocks are 39 inlet channels tall, and the M50 air conditioner has 5 HMX blocks in it. Therefore, the “number of process layers” input on the model should be 390. $(39)(2 \text{ sides})(5 \text{ blocks}) = 390$. This also assumes that thermodynamic and fluid flow performance is the same for each HMX block stacked on top of each other.
5. **Steady-state conditions** – The model can only simulate steady-state Coolerado conditions. It is not designed to simulate varying fan speeds or dynamic inlet conditions, although the actual M50 units are equipped with VFDs and are rarely maintained at a constant speed.

Also included with the model code were basic psychrometric functions that are called upon by the code while it iteratively solves for air states across the HMX sheet. These functions were developed and written in MatLAB at the same time the Coolerado code was developed. Most of the psychrometric functions were derived from the 2005 ASHRAE Handbook of Fundamentals.

DISCRETIZATION

The NREL model uses a basic discretization scheme. Although official documentation or information about the method used in this model is unavailable, inspecting the code reveals the simple method. The model selects the smaller of two dimensions as the length and width of each discretization square: minimum divider width or minimum channel width divided by 6. If the

divider widths are larger than channel width divided by 6, the model forces each channel (product and working) to have at least 6 cells perpendicular to the flow path to account for a temperature and heat transfer gradient perpendicular to the airflow path. This is expected in a cross-flow heat exchanger design like the Coolerado HMX. For all of the simulations and analysis performed in this research, the channel divider width defined the discretization size because the minimum divider width (1.6mm) is significantly smaller than the channel width divided by 6 (which would be about 4.0mm). Most of the simulations have about 15 cells across each channel and 320 cells along the length of the product (dry) channels. This results in a 320 by 128 grid, or 40960 cells.

V. ANALYSIS AND RESULTS

CALIBRATION WITH CU4 DATA

The first step to calibrating the model and ensuring its results were reasonable was to adjust the model default geometry to reflect the actual Version 6 HMX in use at the NSIDC. The model automatically loads a default design on startup. However, these values had to be updated to reflect the Version 6 design and to calibrate the model.

Some inputs had to be verified with Coolerado, like paper thickness and waterfilm thickness. The sheet material is made by Fiberweb and consists of two parts: impermeable polypropylene membrane and a poly wicking material. The membrane is about 0.003" (0.076mm) thick and the wicking material is about 0.49mm thick; the combined total is 0.56mm. For modeling purposes, it is assumed that the waterfilm is completely absorbed into the wicking material, so is therefore 0.49mm. The model uses the waterfilm thickness and water conductivity to calculate the heat transfer rate through the water, and the paper thickness and paper conductivity to calculate the heat transfer rate through the membrane. Note that the model doesn't have an input for wicking material thickness. By assuming the wicking material is completely saturated (which is Coolerado's

design intent), it is assumed that the heat transfer through the fully saturated wicking material is similar to heat transfer through an equal thickness of water. This may or may not be true, and the effect of modifying the “water conductivity” input was explored in the model sensitivity analysis. Essentially, as far as the model is concerned, there is a very thin, 0.076mm poly material layer that has a 0.49mm waterfilm on it. Heat transfer through these layers is quantified by multiplying by respective conductivities and a temperature difference, as solved by Equation 7.

The number of process layers was set 390 to calculate the flow, heat transfer and power usage of an entire M50 unit, thereby attempting to model the performance of CU4 (see list of assumptions on previous page). The model simply uses this value to multiply the performance (heat and mass transfer) of 1 set of sheets (1 product air and 1 working air). All of these validated design dimensions were saved into a new default file for the model to automatically load on startup (default_adjusted2_40deg.mat).

As explained in the One Time Measurements section, the combined channel height of 1 product and 1 working air channel is 5.38mm. And according to Coolerado’s nominal design values, there should be a 60/40 split between product channel height and working channel height.

Estimated channel widths, channel heights and hole diameters of the Version 6 HMX are given in Table 10. All dimensions except for the heights were measured from a sample HMX sheet; these measured values were initially assumed to be close enough to the Version 6 HMX values, although the sample sheet was known to be an even earlier version HMX. The channel height values, however, have a significant impact on the HMX performance and it would not be acceptable to simply use measurements from the old sample sheet.

Table 10. Version 6 HMX "60/40 split" design dimensions.

	Width (mm)	Height (mm)	Wall Thickness (mm)	Hole Diameter (mm)
Indirect Channel	23.4	3.23	1.9	4.75
Ind/Dir Channel	23.4	3.23	1.9	4.75
Direct Channel	23.9	2.15	1.6	4.75

Before optimization of HMX design could be performed, model performance should ideally be verified by comparing its results to CU4 data collected since late June 2011. The extensive amount of data collected on CU4 (from both the CR10X and the HOBO network) had to be organized and consolidated; this made MatLAB the preferred system for this task. (Microsoft Excel slowed significantly when processing and graphing datasets this size). MatLAB code was developed to process data and plot any or all of the different data points against time on the same plot (see this code on pages 118-119 in the Appendix). This was important to aid in steady-state condition selection. It was important to choose operating conditions that were relatively steady-state because the Coolerado model is not capable of simulating dynamic conditions. Steady-state conditions were initially selected by visual inspection of plots of the data. See below.

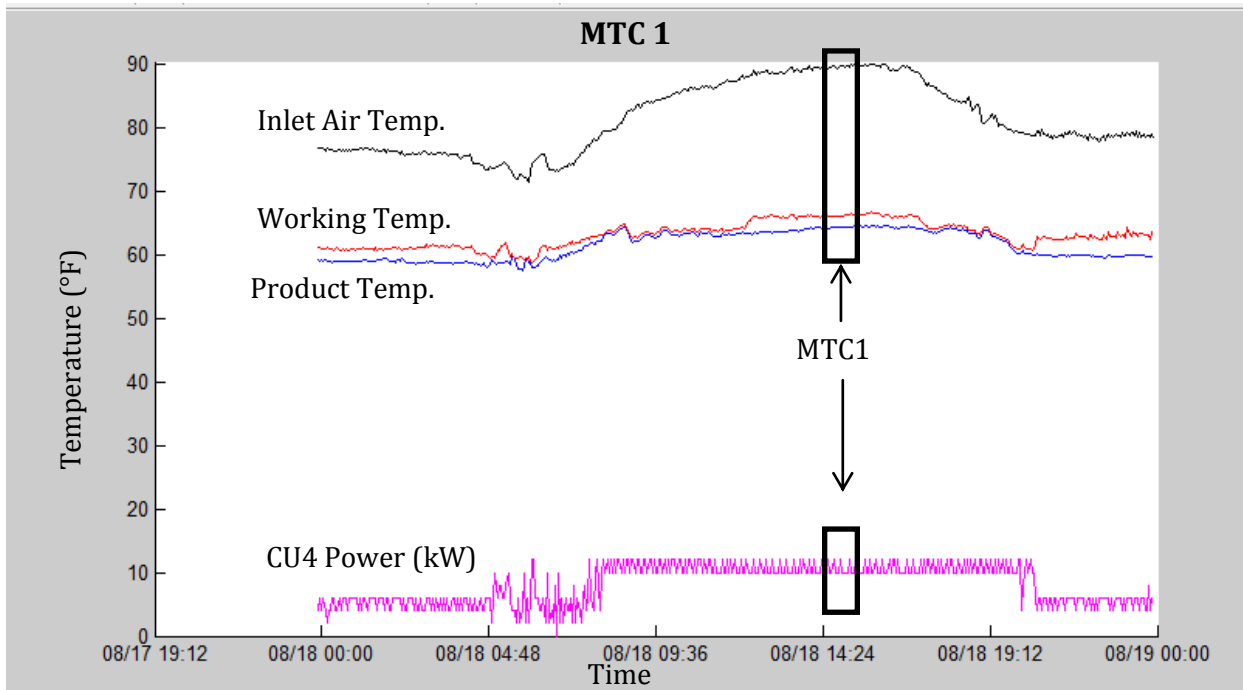


Figure 28. Example MTC plot of steady-state conditions.

Once a point was selected visually, MatLAB was used to calculate the 1-hour average values around that point (± 30 minutes from the selected point). Using average values eliminates most inconsistencies in the pre-selected data, and allows a more accurate derivation of the power consumption for those given air conditions. Due to the very low pulse frequency from the WattNodes, the power measurements have a resolution of 0.1 kW. This often results in oscillation between values (0.2 and 0.3 kW, for example) if the power consumption of CU4 is between the values (0.25 kW, for example). Calculating 1-hour averages gives a more accurate power consumption value to use in the model. These steady-state conditions are referred to as Model Test Conditions (MTC). A total of 23 conditions were selected. A table of the MTC's can be seen in Table 18 on pages 106-107 of the Appendix. Many of these conditions occurred in July or August of 2011 because this time period exhibited high outdoor air temperatures, conditions when the Coolerados were needed most to cool the data center (instead of the economizer mode in which the AHU handles most of the cooling throughout the cooler winter months). However, to test the model over a full range of HMX/Coolerado operation, some MTCs in October and November and March 2012 were included when the Coolerados were at partial load.

As discussed previously, a power and total airflow relationship was developed using the on-time measurement data. This relationship was then used to compare the model's predicted total airflow to the actual airflow. The CU4 total power vs. airflow regression from Figure 22 was used to predict the airflow for each MTC from the CU4 power measurement. The pressure differentials across the HMX also have a direct impact on the performance, as seen in Equation 15. Recall that pressure differences (product and working air) are an input to the model, and to simulate the correct airflows, the pressure differentials had to be derived from the calculated airflow. Switching the axes of Figure 21 results in Figure 29. The regression shown below was used to calculate the pressure differential input for both product air and working air in the model. Although the model allows the user to input different pressure differentials for the product and working air, because

the one-time data showed that these values were very similar, the same pressure was used for both air paths. Comparisons of the model outputs to CU4 field data at each given MTC can be seen in Figure 53 through Figure 56 on pages 120-121 in the Appendix.

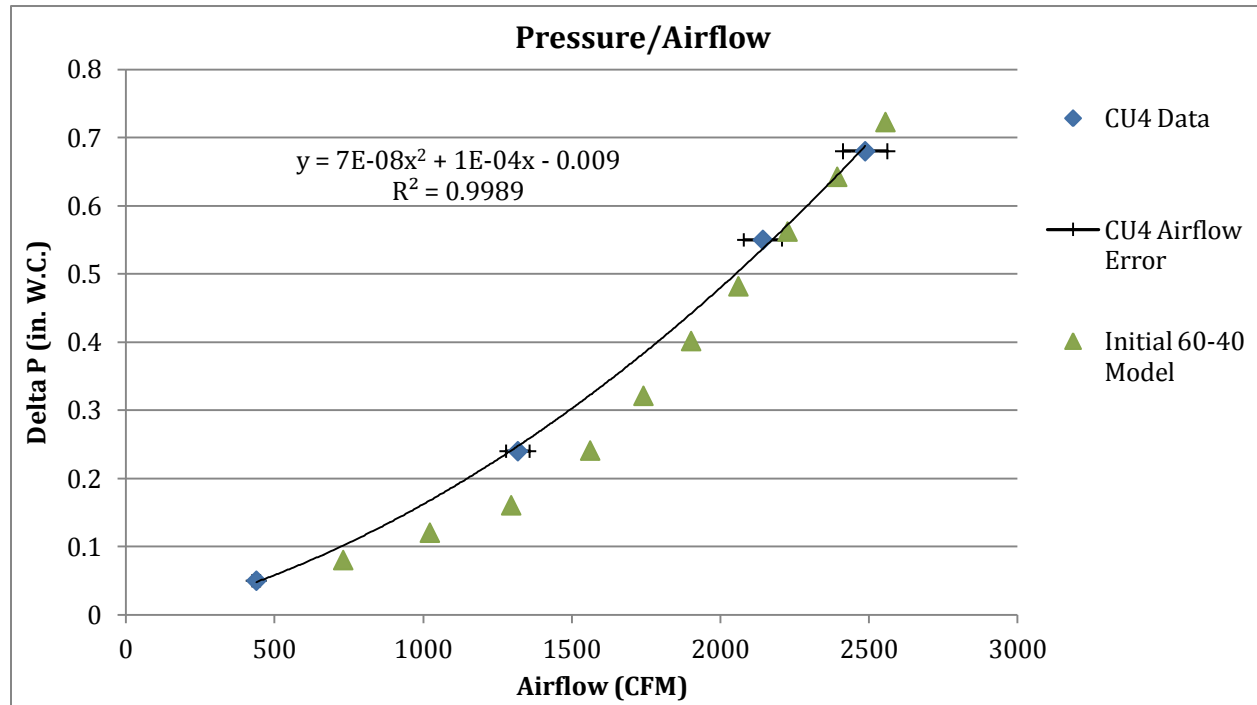


Figure 29. Airflow vs. pressure regression for an M50 unit.

ISSUES WITH MTC'S

Despite efforts to verify the model by comparing to over 20 MTC's, it became apparent that this was not going to be possible because of unknown, time-dependent temperature gradients in both the product and working air streams. (Note the very poor matches of thermodynamic performance in Figure 53 through Figure 56 on pages 120-121 in the Appendix). Recall that the product and working air temperatures are each measured at only 1 location within each outlet. The product air outlet is 14" wide by 40" tall. Measurement at only 1 location doesn't accurately capture the average temperature of the product air if there is a gradient. In theory, all product air outlets would have the same temperature. However, after attempting to verify that the product air is the

same across all vertical points, it was discovered that a gradient exists. To make matters worse, this gradient seemed to be dependent on the amount of water supplied to each HMX and the distribution within it. This conclusion was reached after measuring the vertical temperature profile before and after the NSIDC Coolerado units were “soaped”. All Coolerado units use dish detergent as a surfactant to help the working air channels in the HMX become fully wet out so that the wicking material is full of water. In theory, this soaping process only needs to be applied once at the startup of each unit; once a surface is wet and stays wet by constant addition of water, it should never dry out at any point. However, after some amount of time (or cumulative airflow), the product air temperature starts to increase, particularly in the HMX blocks at the top of the stack. The M50 units can be re-soaped by cycling the unit off and back on; upon a hard reboot, the unit runs the soap pump for 2 minutes. Within about an hour of soaping, the product air temperature gradient is significantly reduced. And it was noted that a day later, the gradient was non-existent. Data from this no-product-gradient day (3/23/12 11:30AM MST) was used to calibrate the model, although the input air temperature was not an optimal design condition (it was only 22°C or 72°F). This corresponds to MTC22a in the MTC list.

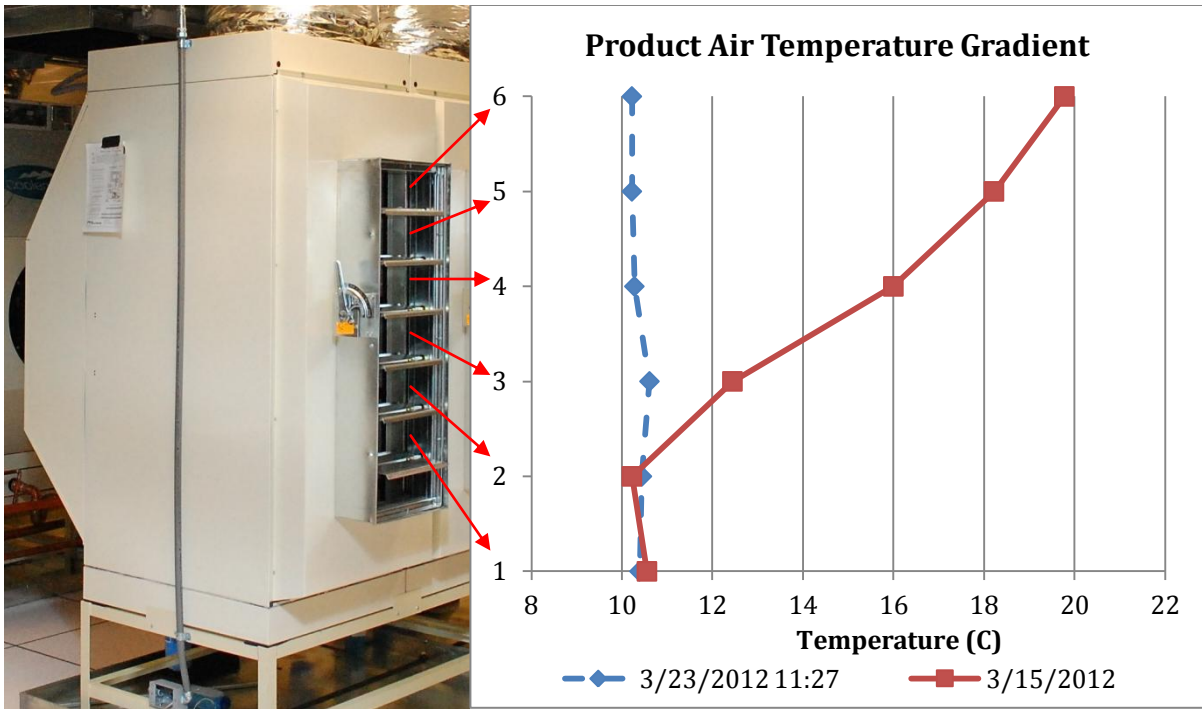


Figure 30. Product air temperature gradient.

Note that there are 6 openings in the product air outlet damper. These each correspond to one of the temperature data points on in Figure 30, as shown by the arrows. The temperature also varies horizontally across the HMX outlet by design. The temperatures in Figure 30 were all taken at the same location horizontally on the outlet of the HMX.

There was also a temperature gradient within the working air stream. CU4 is one of the 4 Coolerado units at the NSIDC that is equipped with a humid air damper (HAD). This damper controls the flow of humid air to the room as needed to maintain the ASHRAE humidity limits. The HAD is made of sheet metal, and was therefore an easy place to install a temperature and humidity probe for the working air. And being about 2 feet above the topmost HMX, it was assumed that all of the working air from the 20 individual channels (which each have a different temperature) would be fully mixed by the time the air reached the sensor location. However, after measuring the temperature at 12 points in a horizontal plane inside the HAD, it was found that the sensor location was 6.0°F (3.3°C) lower than the average temperature in the plane. This data can be seen in Figure

31 below. Note that the working air sensor is located at the same location as the low point at Center and 5.5”.

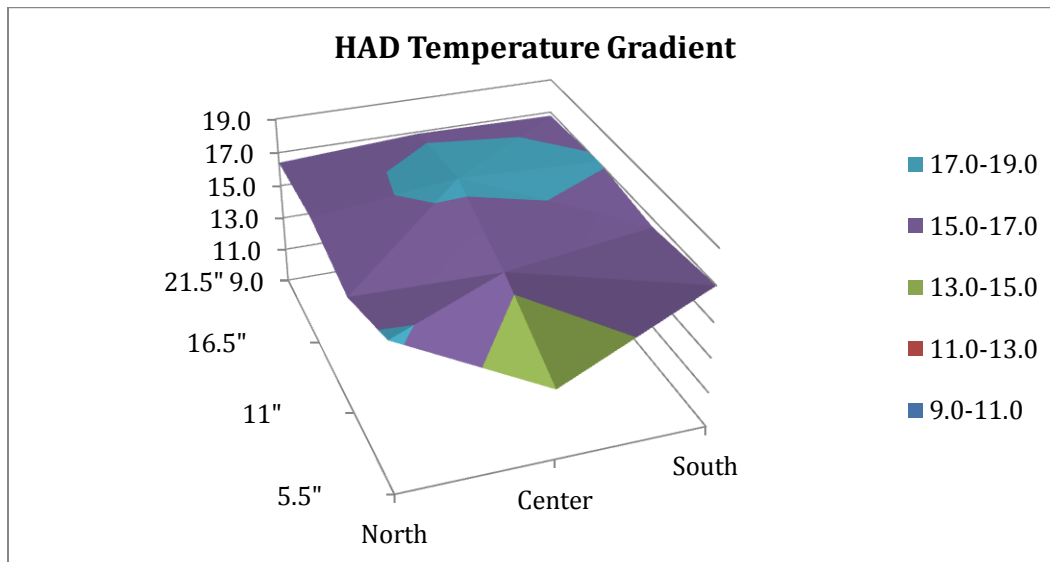


Figure 31. HAD temperature gradient plot.

To calibrate the working air temperature, 3.3°C was added to the recorded temperature value to account for the HAD gradient. Because the corresponding humidity measurement is a relative humidity (RH) value, the RH of the working air (not humidity ratio) was assumed to be the same with the new temperature value.

Unfortunately, even after adjusting for the gradient issues mentioned above, the model still didn't match well with CU4 data. The 60/40 split assumption is not valid. After compression into a complete HMX block, the inlet face is distorted from epoxy, and the HMX's in CU4 do not perform like a 60/40 split should. Two other models were simulated to determine the proper product and working air channel heights; a 55/45 split and a 65/35 split. The product air results from the 65/35 split were very close to the CU4 data. The divider widths were increased to 2.2mm and 2.0mm for the product and working air channels respectively, as seen in Table 11. Also, the water conductivity was reduced from 0.60 to 0.25 W/m-K; this this was an attempt to model the actual case in the CU4 HMX's if the wicking material in the working channel is not fully saturated or the effective

conductivity of the waterfilm is reduced by the presence wicking fibers. The results of the calibrated simulation can be seen in Figure 32. Note the error bars around the CU4 product data.

Table 11. Version 6 calibrated HMX design parameters; 65/35 split.

	Width (mm)	Height (mm)	Wall Thickness (mm)	Hole Diameter (mm)
Indirect Channel	23.2	3.5	2.2	4.75
Ind/Dir Channel	23.2	3.5	2.2	4.75
Direct Channel	23.4	1.88	2.0	4.75

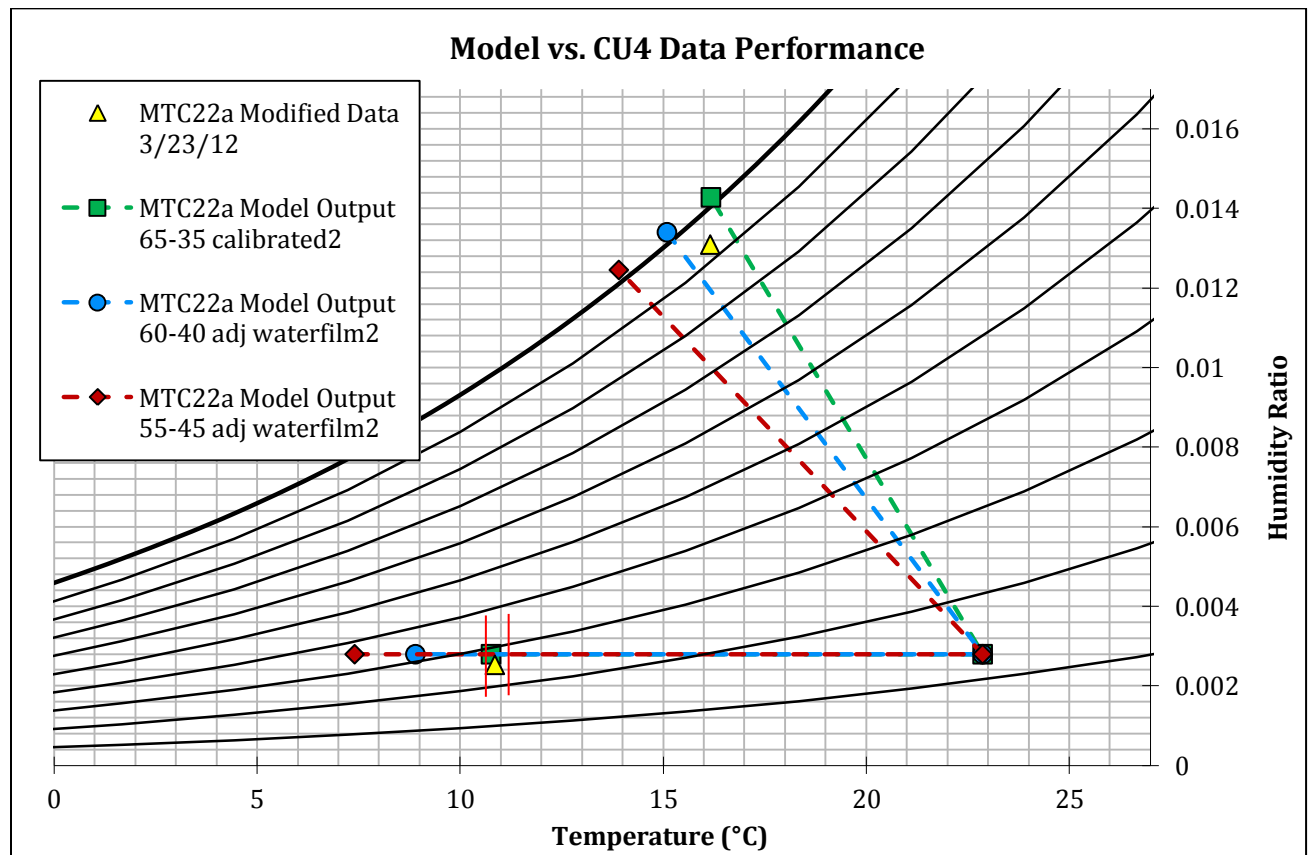


Figure 32. Model calibration with 3/23/12 CU4 data.

Note that the CU4 working air data point is very close to the same temperature as the 65/35 model (in fact the data is 16.16°C and the model predicts 16.18°C). The humidity level is not as close (93.5% data vs. 101.7% model). This is likely due to slight water deprivation in the CU4 unit, which would directly impact the achievable humidity ratio in the working air stream. The model assumes that there is enough water in each working air channel to fully saturate the wicking

surface. In reality, controlling the water flow with that degree of accuracy is very difficult, especially with other influencing factors like building water pressure, filter cleanliness (each Coolerado has a separate water filter), variable airflow and humidity ratio of incoming air. Based on a Coolerado technician’s professional maintenance during the week of April 16 (nearly 3 weeks after the MTC22a measurements were taken), the supply water pressure to the all of the NSIDC Coolerados was low; new filters and minor internal controls adjustments were made to attempt to account for this. Other less influential but still notable factors include the relative inaccuracy of RH sensors (especially near saturation) and the fact that this humidity was modified from its original absolute value.

However, on the product air end, the CU4 data and 65/35 model are very close, both in temperature and humidity. Data and model temperatures are less than 0.1°C apart, while humidities are about 0.0003 kg water/kg dry air apart (10.85°C data vs. 10.76°C model and 0.0025 data vs. 0.0028 kg water/kg dry air model).

Table 12. MTC22a calibration comparison between CU4 data and model output.

		Airflow (CFM)	Product Air Temp (°C)	Product RH (%)	Working Air Temp (°C)	Working Air RH (%)	Hydraulic Power (kW)
CU4 Data	MTC22a	2431	10.85	25.97%	16.16	93.48%	0.185
Model	MTC22a_calibrated2	2386	10.76	28.90%	16.18	101.70%	0.186
Error in Measurement		±135.4	±0.271	±2.46%	±0.219	±3.19%	- 0.026 to 0.029
Actual Deviation between CU4 Data and Model		45	0.09	-2.93%	-0.02	-8.22%	-0.001

It is apparent from Figure 32 above that the 65/35 model performance is the closest match to the CU4 data. For a numerical comparison, refer to Table 12 above. This suggests that the CU4 unit operates like a 65/35 HMX.

It should be noted that the model pressure and airflow correlations seen in Figure 21 and Figure 22 were both generated using an uncalibrated 60/40 split model. Changing the channel heights to a 65/35 split does affect the total and individual airflow, however, these slight changes

are very small and in fact improve the pressure and airflow correlations closer to the CU4 data. Therefore, it is still valid to use the regression from Figure 29 to calculate an approximate airflow through the CU4 unit from the power measurement, and then use this value to compare to the total airflow predicted by the model, as in Table 12. Figure 33 below is the same as Figure 29 except the calibrated 65/35 model correlation has been added to show that it actually improves the pressure vs. airflow correlation, making it closer to the actual CU4 data.

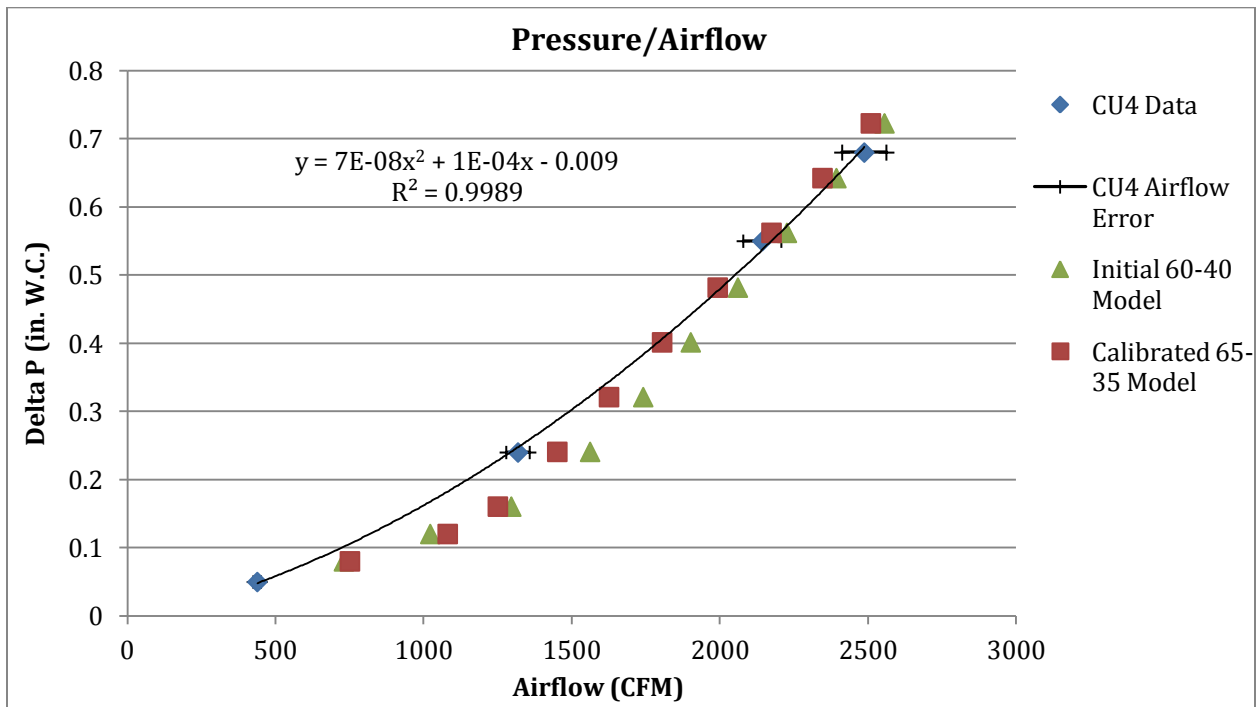


Figure 33. Pressure and asirflow relationships; CU4 data, initial 60-40 model, calibrated 65-35 model.

SENSITIVITY PROCEDURE

Once the model was calibrated to one point in time when CU4 operation was understood, it was used to determine the performance impact of adjusting different design parameters. To allow an equal comparison, a 40°C (104°F) design temperature and 10.1% relative humidity (17.2°C wet-bulb temperature) was selected as an inlet air state. This air condition represents a typical design condition used by Coolerado in their in-house testing, which Coolerado has determined to be an

ideal condition for the HMX system. It allows the working air stream plenty of capacity for humidity absorption, which in turn drives the product air temperature down. Ten percent RH is a relatively low humidity, but is common in the western U.S. Temperatures in this same region can reach 40°C in the heat of summer, particularly in the southwest, where cooling capacity is needed most. The key performance indicator used was the coefficient of performance (COP) which is defined in Equation 18. The COP is a robust performance metric that by definition incorporates cooling power, product air temperature, product air flow rate and total air flow rate. If any of these variables change, the COP will reflect that change. Note that only the product air mass flow rate, \dot{m}_{PA} , can be counted in the cooling power. Working air is very humid, almost saturated, and would be uncomfortable in an occupied space; therefore it is exhausted and not used to do any useful cooling.

$$COP = \frac{\text{Cooling Power}}{\text{Hydraulic Power}} = \frac{\dot{m}_{PA} C_{p,air} (T_{DB,PA,in} - T_{DB,PA,out})}{\frac{\dot{m}_{Total}}{\rho} (\Delta P)} \quad (18)$$

$$\text{Wet Bulb Effectiveness} = \frac{T_{DB,in} - T_{DB,out}}{T_{DB,in} - T_{WB,in}} \quad (19)$$

Wet bulb effectiveness is another common design comparison value, and is defined in Equation 19. As a measure of how close to the wet-bulb temperature a cooling system can reduce its supply air to, this metric is good for quantifying the temperature drop across a cooling system relative to the inlet condition. However, in the case of a Coolerado HMX which is purely sensible cooling, no humidity added or removed from the product air, wet bulb effectiveness is purely a function of the product air dry bulb temperature. Note that $T_{DB,out}$ is the only term in Equation 19 that will change depending on what changes are made to the design. The other three values are all constant as they are parameters of the constant inlet condition. Therefore, it is necessary to consider only wet bulb effectiveness or product air temperature when comparing different simulations. Because wet bulb effectiveness is a cooling equipment standard, it was used in

conjunction with COP for comparing different design sensitivities. Capacity and total airflow are also considered.

The constraints on the sensitivities that follow were employed to keep this analysis within some simple design considerations for Coolerado. These constraints were in effect for all simulations except those which specifically vary these variables. These constraints are outlined in Table 13.

Table 13. Sensitivity and optimization constraints.

Constraint	Reasoning
10.0" Tall, 8" Wide, 20" Deep	Current HMX frame size; Changing this would mean extensive modification to Coolerado's manufacturing line and Coolerado design.
25.4mm (1.0") Channel Width, O.C. divider to divider	Reducing this value while maintaining the HMX inlet face area would mean adding channels and/or widening dividers. This would decrease the effective area available for heat transfer on product and working air sheets. Increasing the channel width would improve performance by increasing the heat transfer area, however 1.0" is a structural maximum according to Coolerado.
Constant 170 Pa (0.68") Fan Pressure	Current maximum pressure differential achievable with the fan, at least the types installed in the NSIDC.
Constant 83.3 kPa (12.8psi) Atmospheric Pressure	Elevation of Boulder (the location of the NSIDC) is 5300 ft. and atmospheric pressure should be taken into account.

Initially, 19 sensitivity simulations were modeled. Various values for channel heights, hole location, hole size, water conductivity waterfilm thickness and divider width were input for different simulations. As trends became apparent, it was necessary to simulate a few more cases; in some cases the sensitivity range had to be expanded, and in others it had to be shifted up or down. In total, 45 useful sensitivity simulations were performed and are outlined in Table 14.

Table 14. Sensitivity simulations

Parameter changed	Description	Values	# Simulations
Channel Heights	± 10%, ± 5% Height Ratio & ±4 Inlet Channels	55, 60, 70, 75% Product Channel Height to Total Inlet Height	15
Divider Width	± 1.0mm	1.0, 1.5, 2.5, 3.0 mm	4
Hole Diameter	± 1.75mm, +2.25mm	4.0, 5.5, 6.25, 7.0 mm	4
Hole Location	± 1 hole, ± 2 holes, -3 holes	7, 8, 9, 11, 12 holes in first row	5
Waterfilm Thickness	± 30% of Base Case	0.34, 0.64 mm	2
Water Conductivity	± 50%, ± 25% of Base Case	0.3, 0.45, 0.75, 0.9 W/m-K	4
HMX Sheet Size	Adding Product and Working Channels	+2,4,6 Working Channels +2,4,6,8 Product Channels	11

The results of the sensitivities above all seemed reasonable and can be explained. The channel height sensitivities were the most complex because the product and working air heights are interrelated when it comes to the thermal performance of the HMX. Because the current HMX frame design has an inlet height limit of 10.0”, changing the height of either (or both) channel changes the number of inlet channels available within this 10.0” limit. And although changing one channel height has an effect, changing both channel heights has a different effect, meaning that the product height ratio (percentage of total inlet channel height that the product channel takes up) may also be important. For instance, a 75/25 split performs differently than a 55/45 split.

The following sections are dedicated to showing the results of these sensitivity simulations. The values boxed in red on the graphs represent the base case, the 65/35 split calibrated model under design inlet condition 40°C and 10% RH. Although only COP and cooling capacity are presented here, other graphs with airflow and wet-bulb effectiveness can be seen in Figure 57 through Figure 66 on pages 122-126 in the Appendix.

Channel Heights

Assuming the base case (65/35 split model, with dimensions as seen in Table 11; 39 inlet channels, effective inlet height of 5.38mm) as a middle ground, the product height ratio was varied from 55% to 75%. The results are seen in Figure 34, Figure 35 and Figure 36. The scales on each of these figures have been set constant for easier comparison.

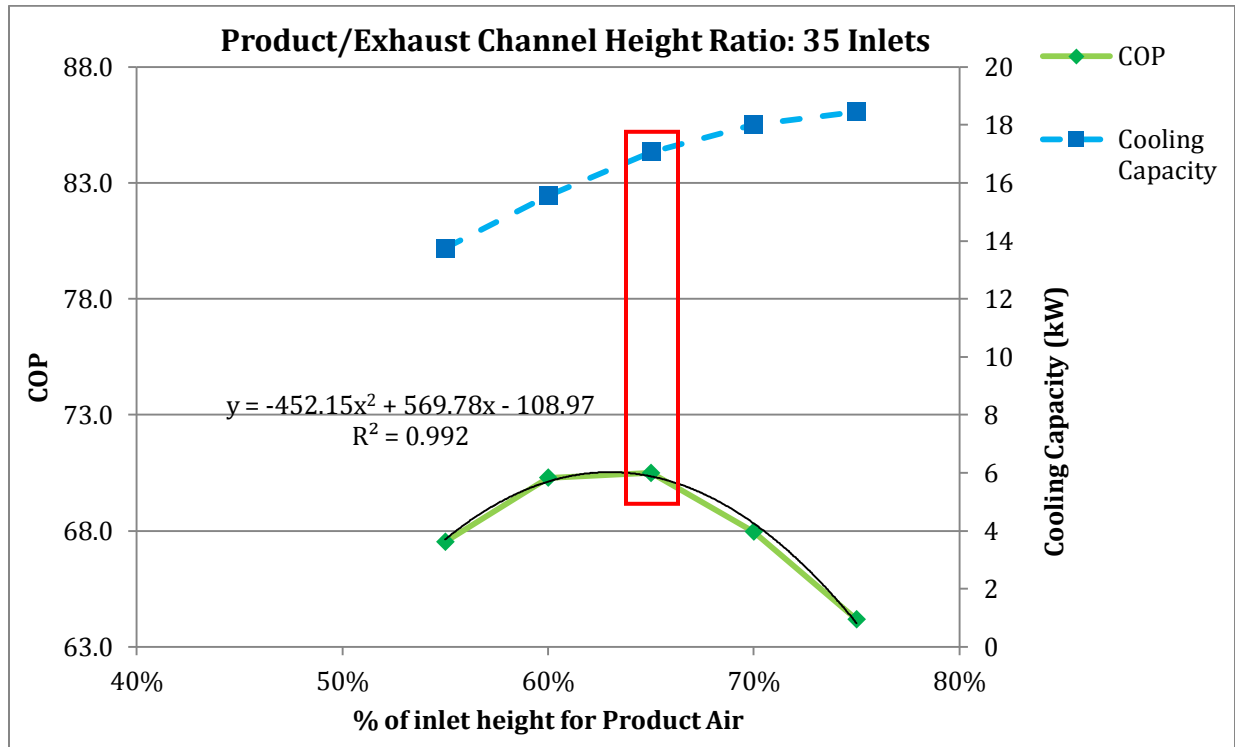


Figure 34. HMX performance sensitivity to product height ratio: 35 inlets

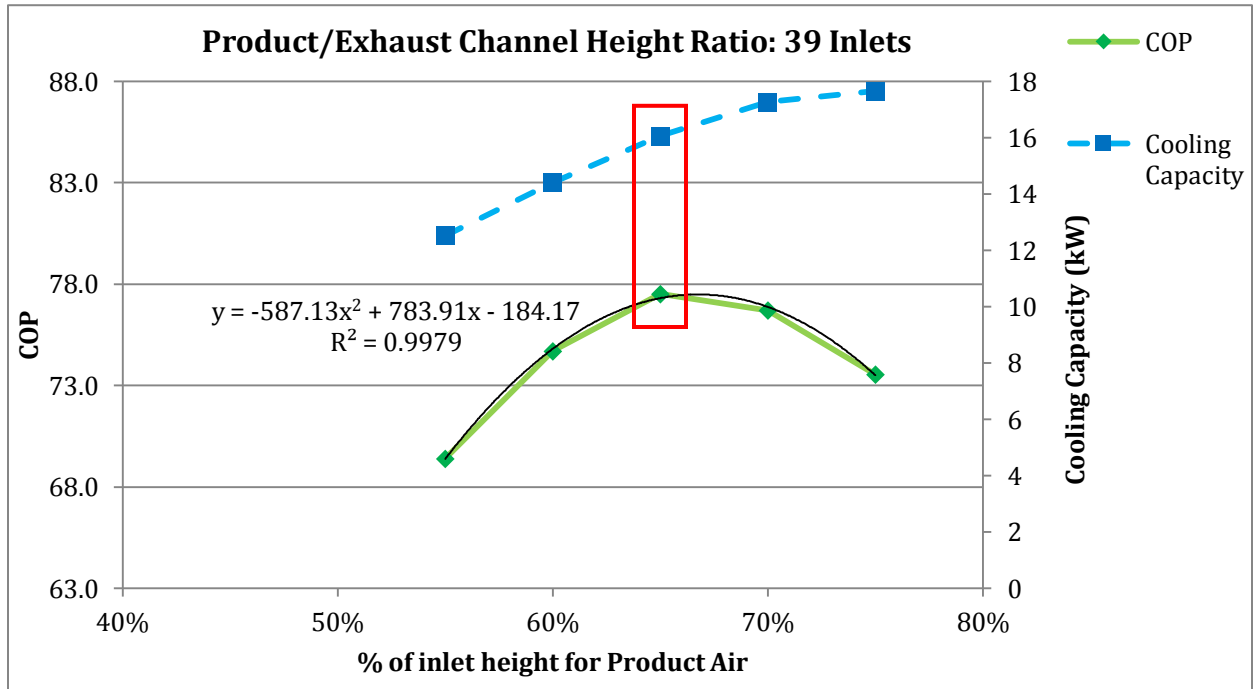


Figure 35. HMX performance sensitivity to product height ratio: 39 inlets

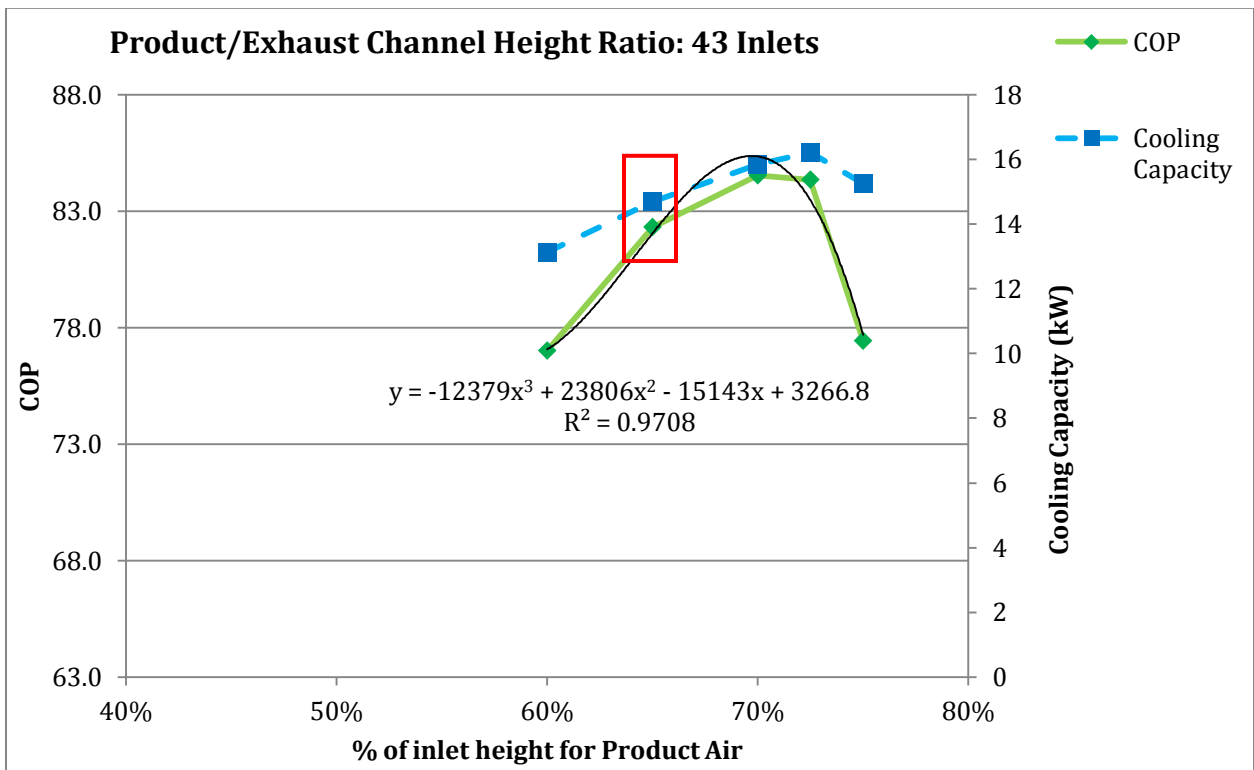


Figure 36. HMX performance sensitivity to product height ratio: 43 inlets

Varying the product height ratio from 55% to 75% was enough to capture the maximum COP value for these inlet channel counts. The regressions included on each graph represent a best-fit curve for calculating the maximum COP value in each scenario. Note that most of the curves are 2nd order, but the 43 inlet graph (Figure 36) uses a 3rd order equation; this cubic regression has a better correlation (higher R² value) than a 2nd order line.

The interesting feature from these figures is that the maximum COP value changes depending on the number of channels (or total inlet height). So depending on the number of sheets stacked into each HMX frame, the product height ratio should be different in order to maximize COP. This non-constant optimum product height ratio can be seen in the 3D image in Figure 37. The white arrow follows the “optimal ridgeline”.

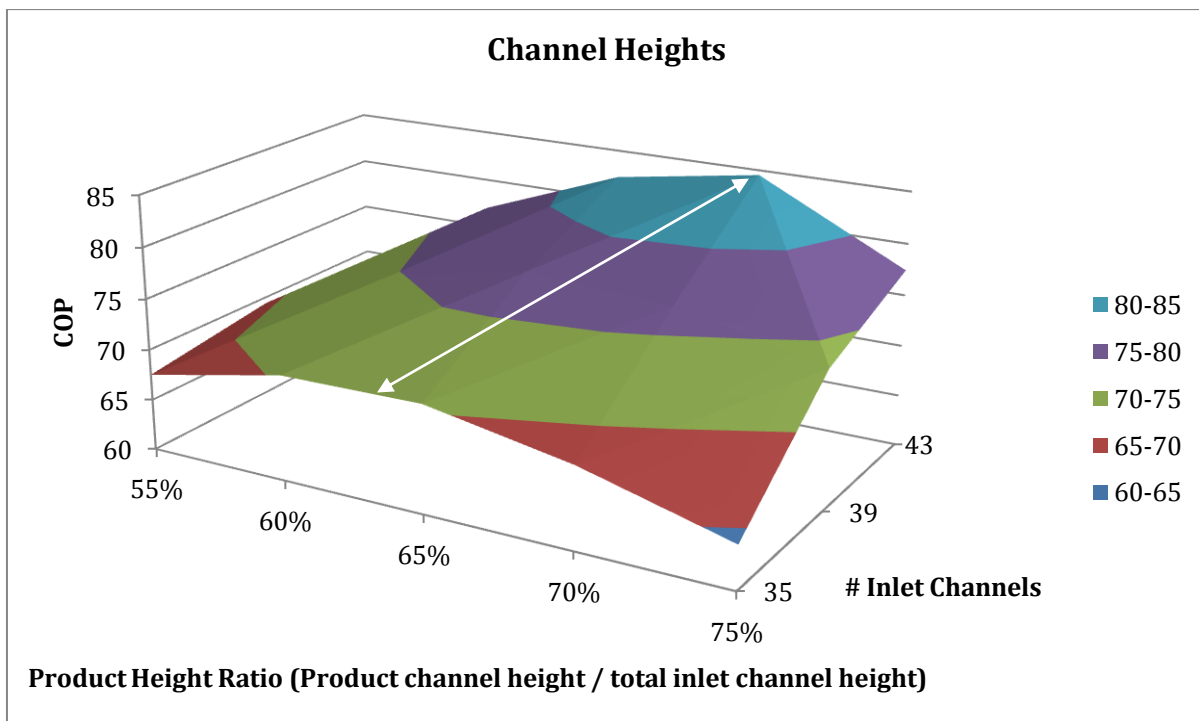


Figure 37. 3D surface HMX COP sensitivity to Product Height Ratio and # Channels.

The relationship between number of inlets and optimal product height ratio can be seen more clearly in Figure 38. The optimum product height ratio for maximizing COP increases linearly. With the design inlet condition of 40°C and 10% RH, at 35 inlets, the optimal product height ratio is

63%, at 39 inlets it's 66%, and at 43 inlets it's 69.7%. Note that the 65/35 model (which was calibrated using 39 inlet channels, the actual number in CU4) is reasonably close to the 66% optimum. These optimal ratios decrease by about 1% if the inlet air is cooler at 30°C.

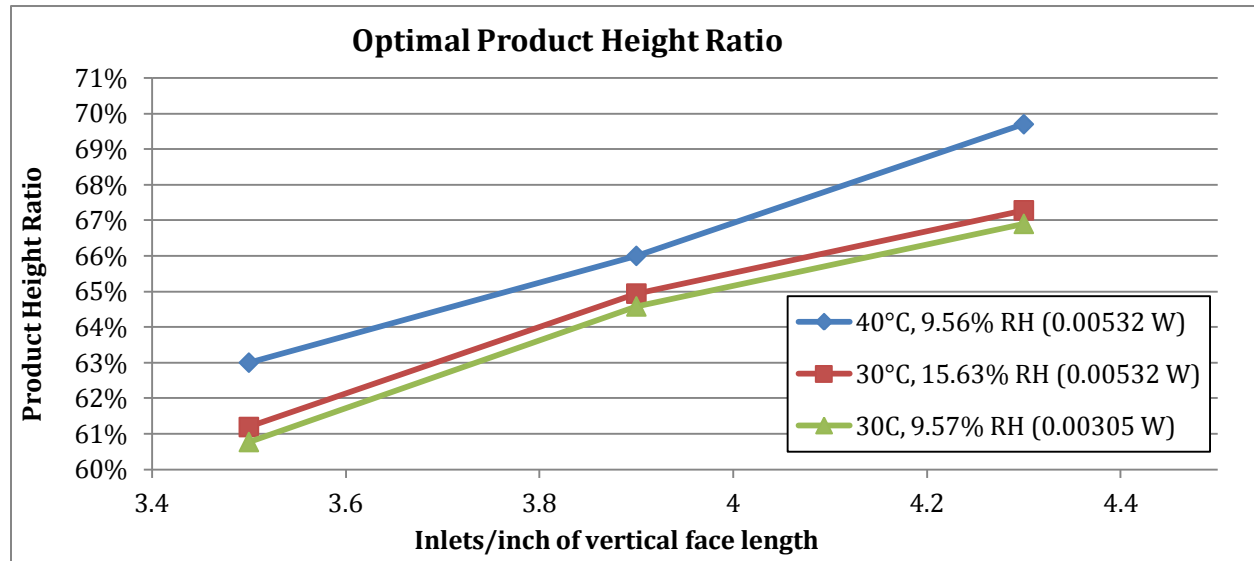


Figure 38. Optimal product height ratio as a function of inlets per inch.

Hole Diameter

The hole diameter was the next most sensitive parameter. From Figure 39, it is apparent that a smaller hole diameter results in higher COP, although slightly reduced cooling capacity relative to the base case (4.75mm). Effectively, the working airflow is reduced because of this smaller restriction in the air path. This decreases the required working air hydraulic power, and the wet-bulb effectiveness because there is less working air available to carry away heat from the product air stream. It should be noted that at the outset of this project, according to Coolerado, it was believed that the holes are currently oversized. But because of manufacturing limitations and high tolerances in the die-punched holes, the hole size could not be relied upon as a means of flow restriction; there is not enough fine control over the resulting hole size. Therefore, 4.75mm was used knowing it was oversized. It is better to error on oversizing than undersizing to help limit the

pressure drop across the working air path in the HMX, especially considering that the airflow resistance is likely more than is calculated in this model that assumes rigid sheet material.

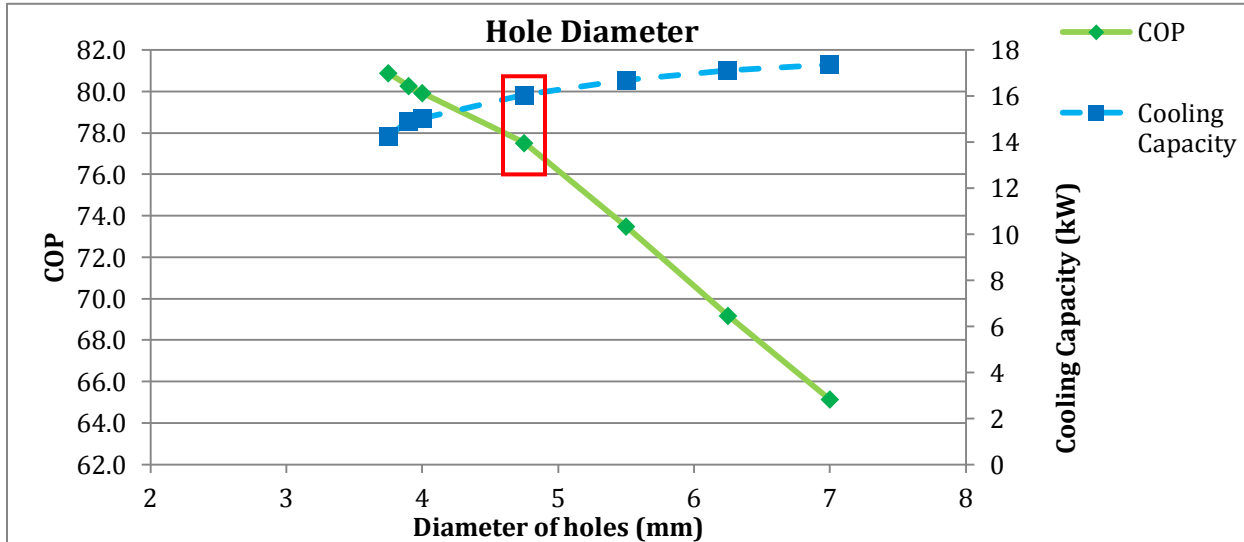


Figure 39. HMX performance sensitivity to hole diameter.

Divider Width

Varying the divider width has an approximately negative linear effect on the COP and wet-bulb effectiveness of the HMX. A wider channel divider means that less area is available for heat transfer and less airflow is allowed. Therefore increasing the width decreases the COP. This sensitivity varied both the product and working air dividers in unison. The exact values used can be seen in Table 19 on page 123 in the Appendix. Although it may be possible to increase the product divider and decrease the working divider (which would increase airflow in the working air channels), this is not recommended because the heat transfer is limited by the largest divider. The effect of divider width on COP and cooling capacity can be seen graphically in Figure 40. Note that cooling capacity decreases slightly, but relatively little, and COP decreases by about 3.75% from the base case.

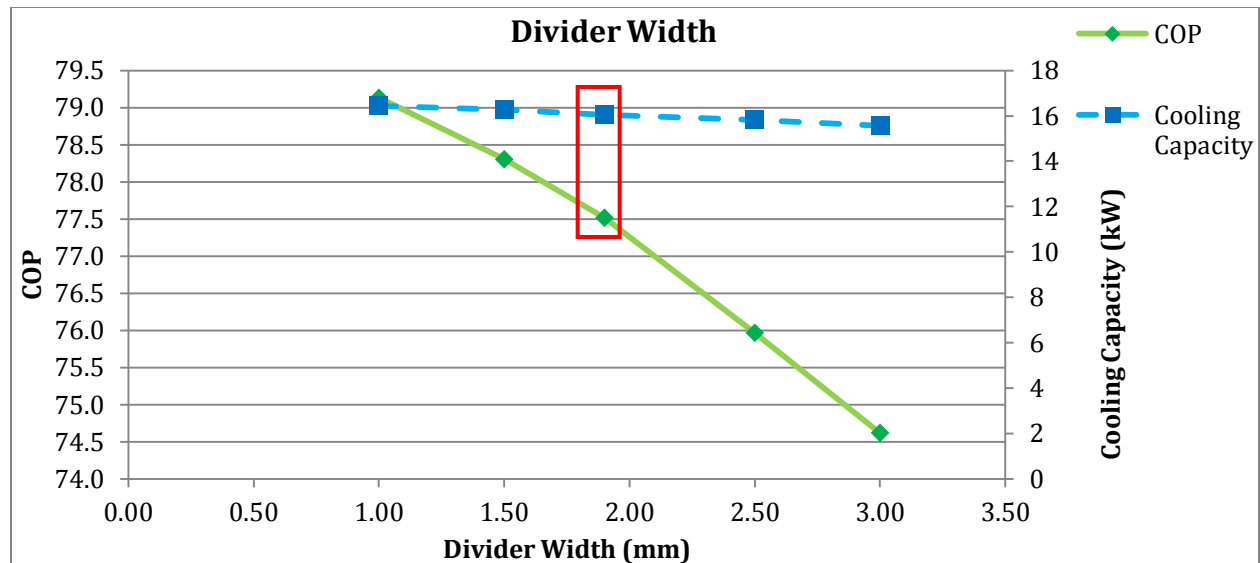


Figure 40. HMX performance sensitivity to divider width.

Hole Location

The placement of the holes in the indirect/direct working air channels was found to affect the performance of the HMX slightly, but not significantly. The figure below shows the impact of moving the first hole in the second channel forward or backward from the standard 10 holes. It is evident that 9 holes in the first channel is the optimum. However, the 10 hole model (the base case) is only 0.1% worse. The cooling capacity is relatively unaffected by changing the hole location because the total airflow (and therefore hydraulic power) is almost unchanged (see Figure 62 on page 124 in the Appendix). Adding more holes to the first channel has a more significant impact as the COP curve drops 1.45% with 12 holes. Overall, however, hole placement does not significantly affect HMX performance. See these effects in Figure 41.

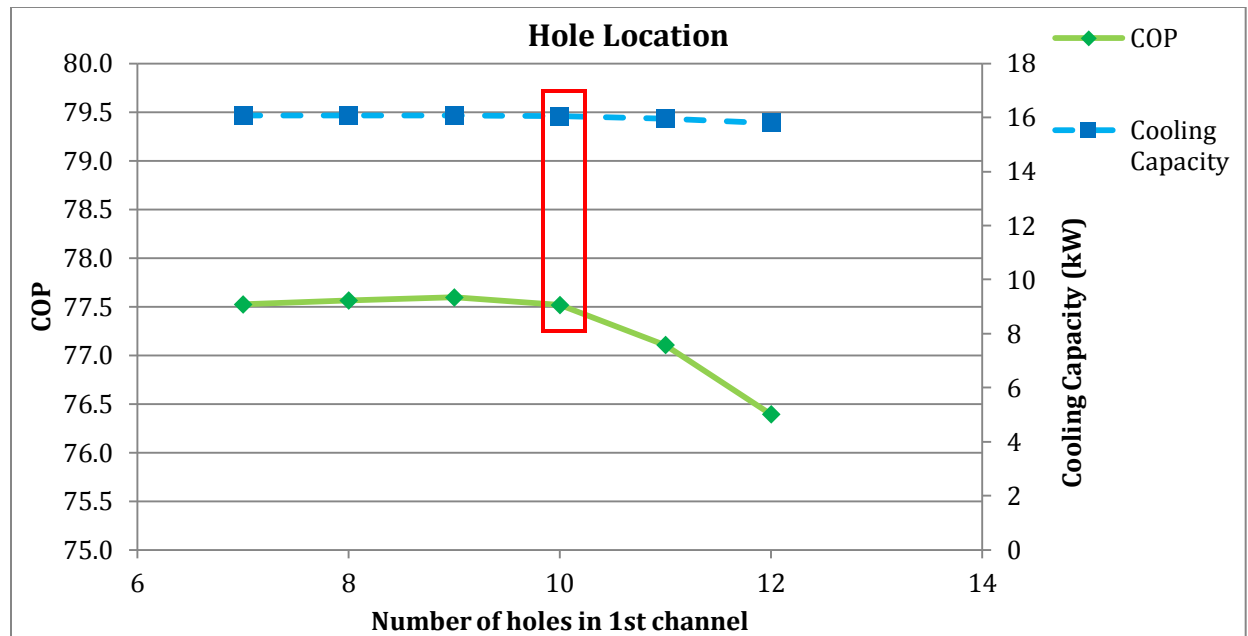


Figure 41. HMX performance sensitivity to hole placement.

Waterfilm Thickness

As discussed previously, assumptions for the waterfilm thickness were made to simulate the thickness of the wicking material that is fully saturated with water, or 0.49mm thick. However, if this were to change, it would have a direct and linear impact on the performance of the HMX, as seen in Figure 42. This is expected because the heat transfer process that cools the product air occurs exclusively through the waterfilm, whether it is evaporated or cooled by convection with the working air. In the model, the waterfilm thickness is simply multiplied by the conductivity and the temperature difference to determine the heat transfer; this results in the direct relationship. A thicker waterfilm means more resistance to heat transfer. Note that the model assumes there is always enough water available for evaporation; this is mostly a water control and dispersion issue which is arguably external to the heat and mass transfer that is theoretically possible inside the HMX. Only 2 more sensitivity simulations were performed because the relationship is linear and not expected to be different outside of the $\pm 30\%$ of base case waterfilm thickness range. Also note that like the hole location sensitivity, changing this thickness by fractions of a millimeter doesn't do

much to the COP (the scale is expanded only to show the linearity). There effect is negligible on the cooling capacity.

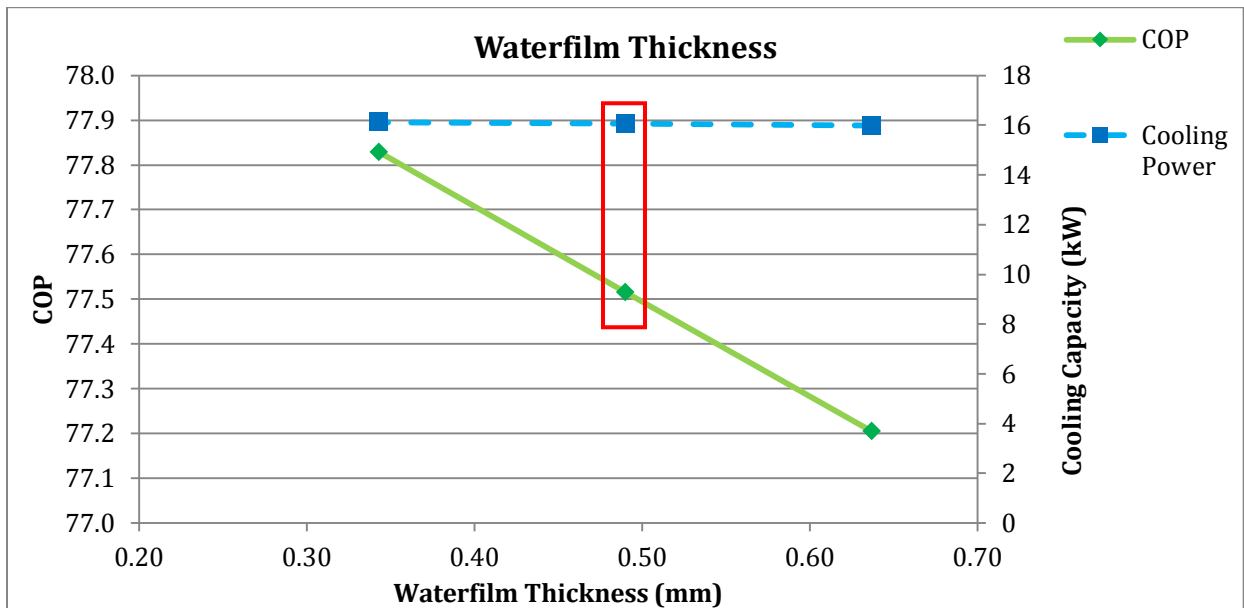


Figure 42. HMX performance sensitivity to waterfilm thickness.

Water Conductivity

Although water conductivity is simply a characteristic of the tap water that is used wherever the Coolerados are installed and not a parameter that could be easily actively adjusted, this sensitivity was performed to determine the effect of this value on the overall performance for two reasons. For one, the water quality may vary by location. Secondly, the exact conductivity of the saturated wicking material is not known, and may be less than that of just pure water. As expected, if the conductivity is decreased, the COP also decreases because all of the heat transfer has been reduced. See these effects in Figure 43.

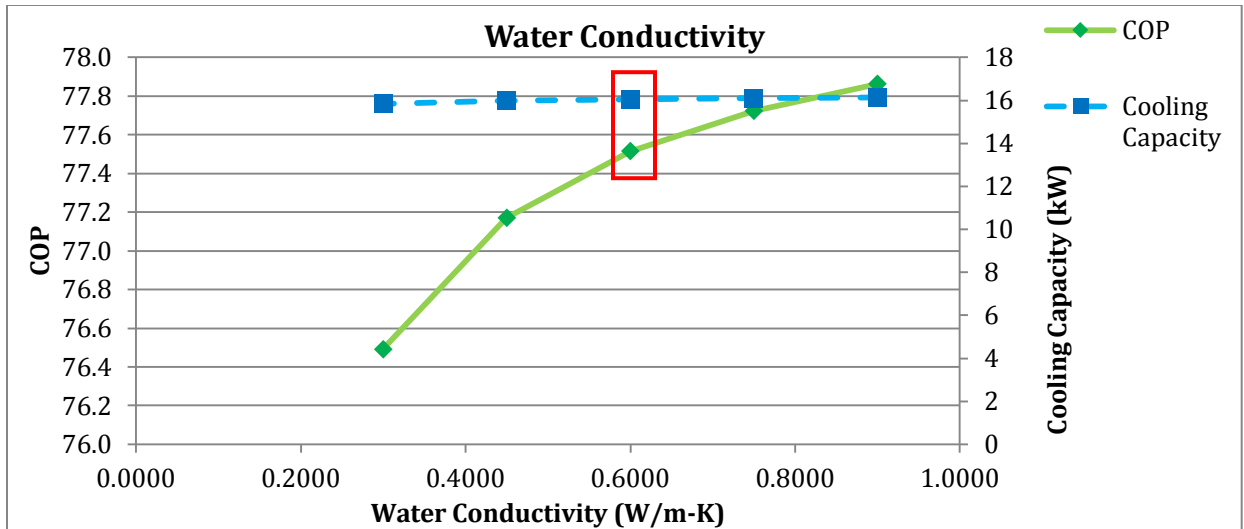


Figure 43. HMX performance sensitivity to water conductivity.

Elevation (Ambient Pressure)

For all of the above design sensitivities, the inlet air condition and pressure provided by the fan was constant. But in reality, the Coolerado air conditioners can be installed and used in many locations that may have lower elevations (higher atmospheric pressures), and all of the fans are equipped with internal VFD's to vary the airflow rates as necessary to meet a load. So it is necessary to characterize how these variables impact the performance of the HMX design.

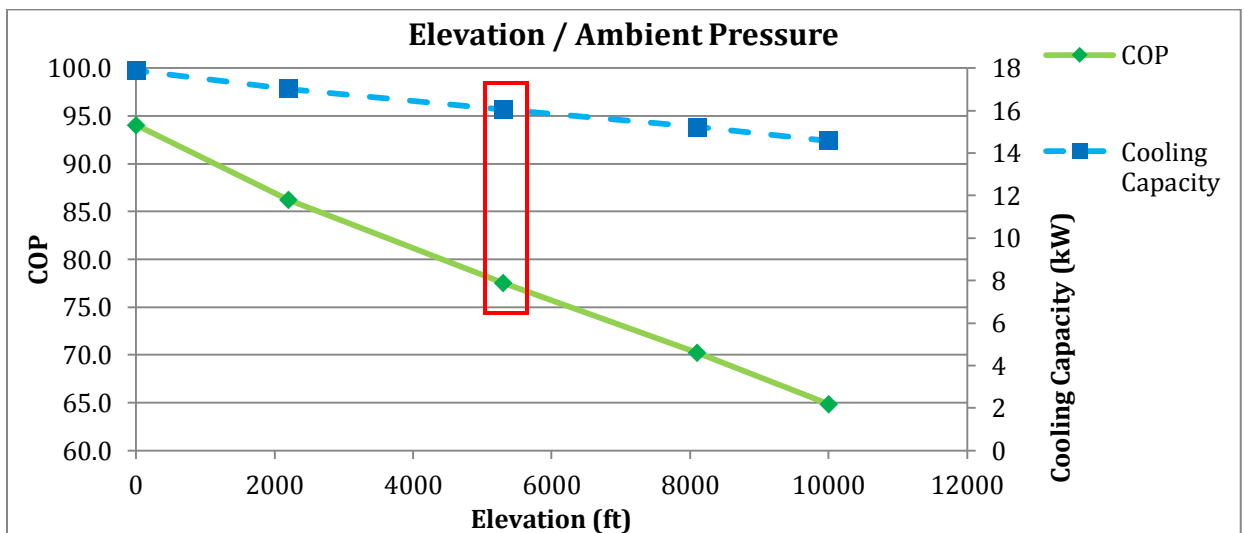


Figure 44. HMX performance sensitivity to Elevation (ambient pressure).

From Figure 44, it is apparent that the elevation has a significant impact on the performance of the HMX. As elevation increases, the COP decreases in a nearly linear fashion. This is expected because the air is thinner and has less heat capacity. This is typical of many heat and mass transfer processes.

Fan Pressure Differential

It is obvious that the pressure differential imposed across the HMX by the fan will vary as the VFD controls the fan speed. Cooling capacity increases linearly as the speed increases (see Figure 45); and because speed is directly proportional to flow, the airflow also rises linearly. See this in Figure 46 below. It is interesting that the product air temperature decreases by 1°C between 60 and 100 Pa, but then actually slightly increases again as pressure increases to 170 Pa. (See the reverse effect on wet-bulb effectiveness in Figure 46).

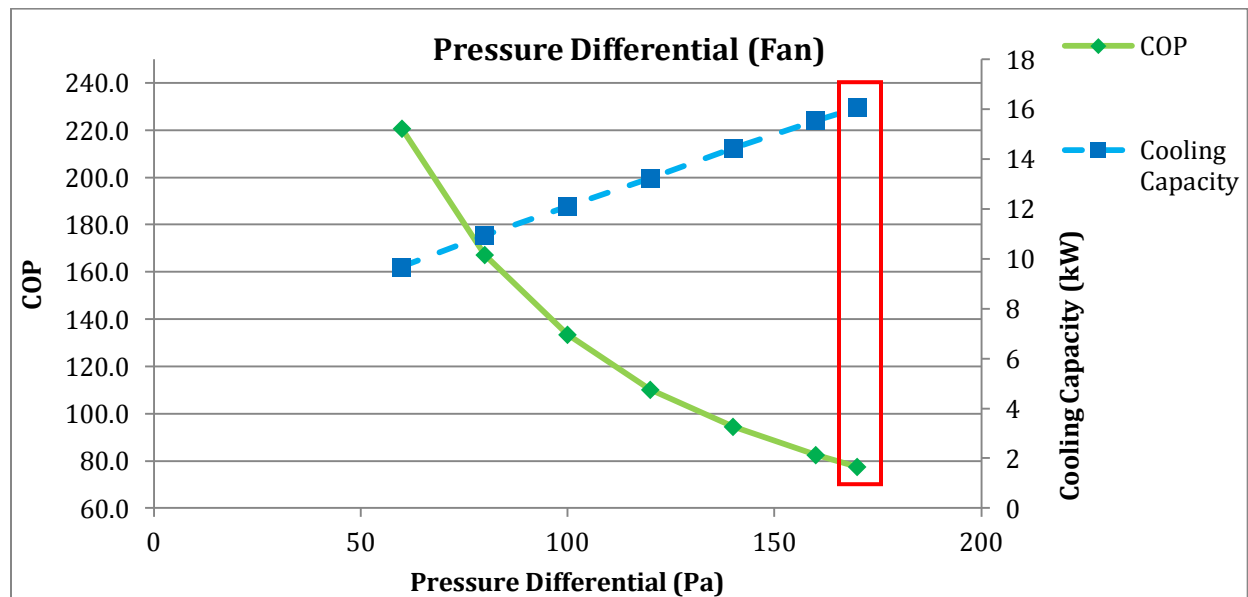


Figure 45. HMX performance sensitivity to Fan pressure.

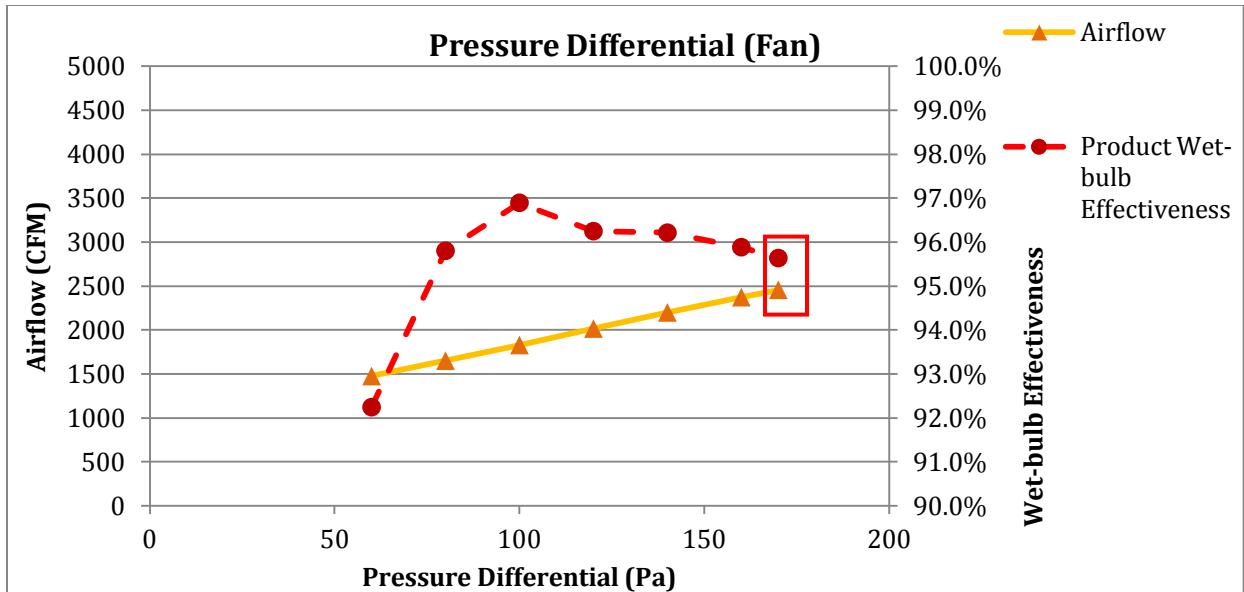


Figure 46. HMX airflow and product wet-bulb effectiveness sensitivity to fan pressure.

Additional Channels

The impact of adding various configurations of product and working channels does have a noticeable impact on HMX performance. Figure 47 shows that adding working air channels has a negligible effect on both cooling power and COP. And Figure 48 shows that although the total airflow doesn't change much, the wet-bulb effectiveness increases linearly with the number of channels. The cooling capacity doesn't increase also because the product airflow is reduced enough to balance out the increased wet-bulb effectiveness with each additional working channel.

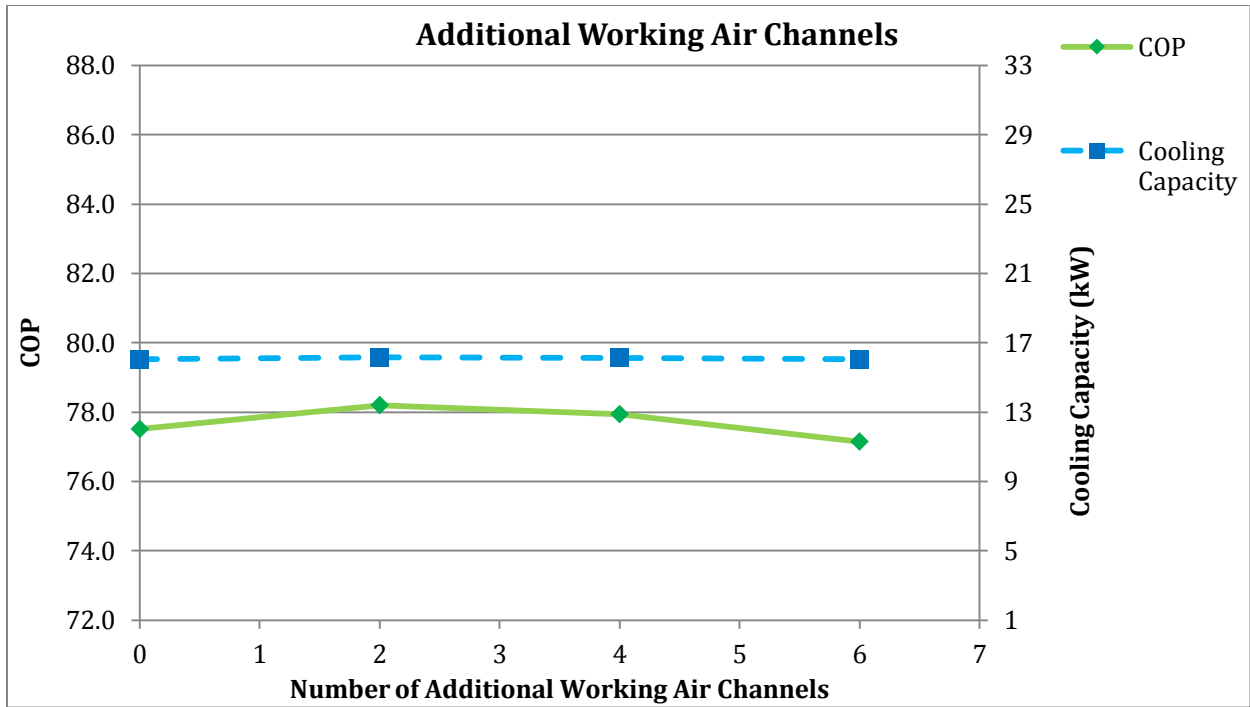


Figure 47. HMX performance sensitivity to additional working channels.

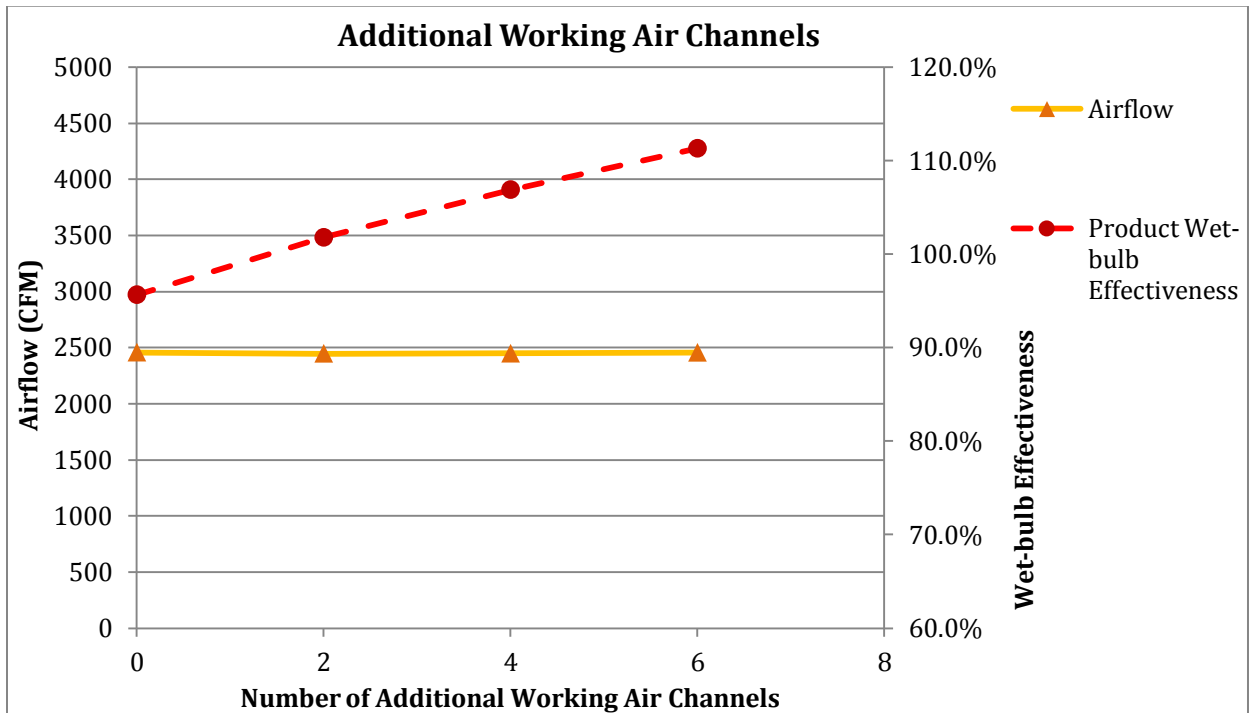


Figure 48. Airflow and wet-bulb effectiveness sensitivity to additional working channels..

Adding product channels has different impacts on the performance of the HMX. Because product airflow has a direct impact on the cooling capacity, in general, more channels results in

more airflow, and the cooling capacity increases. The COP, however, only increases for a limited number of additional product channels. More product channels also results in lower wet-bulb effectiveness because the added channels output warmer air than the first product channels, thereby increasing the average product air temperature. Depending on the number of additional *working channels*, adding *product channels* has a different impact on the COP, as seen in Figure 49. It is apparent that a 10% increase in COP is achievable by adding 6 working channels and 4 product channels.

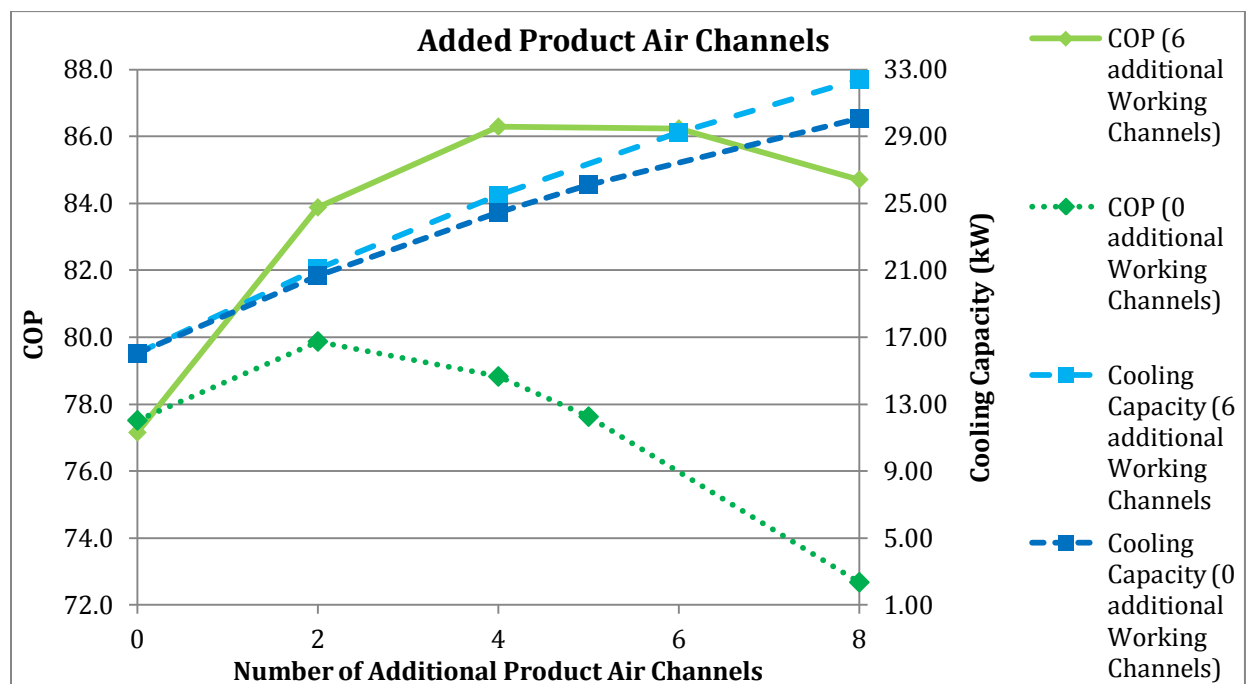


Figure 49. HMX performance sensitivity to additional product channels.

Sensitivity Summary

All of the above sensitivities can be seen below in Table 15. This table has them ordered by COP, the primary performance indicator. Note that the second column is the change in COP from the base case (the 65/35 split at design inlet condition). The remaining columns are self-explanatory. This table shows a lot of data, but most importantly it points out which variables have the greatest impact on the COP, relative to each other. Because the sensitivities were all performed with

approximately realistic ranges for each variable, comparing the simulations in this manner is reasonable.

Although it's not a design variable per se, the ambient pressure, or elevation, has the greatest impact on the performance, with over 11% increase at 2200 feet, and over 21% increase at sea level. It should be noted though, that the low channel heights sensitivity simulation ranks between these two elevation impacts, signifying that channel height is also a major performance driver. With over 14% increase in COP compared to the base case as both product and working air channel heights are decreased by 0.5mm (0.02"). This value was selected as a maximum change because Coolerado claims that changing the channel heights more than this amount requires some more time to dial in the proper flow and speed of the machine used in the manufacturing line. Also interesting to note, the Low Wet Wall simulation (reduced working air channel height) resulted in more than double the change that the Low Dry Wall simulation showed. This implies that it is more important for the working air channel height to be small and optimally sized for maximum evaporation rate than it is for the product channel height.

Adding working and product air channels also could have a significant impact on the performance, up to a 10% increase in COP. These simulations were performed assuming the channels added were the constant 25.4mm (1.0") in width. However, improving the performance of the HMX by adding channels and increasing the overall size of the sheet may not be possible in the near future because it would require significant adjustments be made to Coolerado's manufacturing process and Coolerado unit design. A feasibility analysis would need to be done that includes other factors such as capital costs of modifying the manufacturing line before this improvement should be implemented.

Table 15. All HMX sensitivity simulations; ordered by COP.

		COP	% ΔCOP	WB Effectiveness	Cooling Power	T_DB Product
Sea Level	1	94.0240	20.81%	95.21%	17.88	18.291
Low wet wall & low dry wall	2	88.6311	13.88%	108.59%	14.04	15.242
+ 6 WA Channels, + 4 PA Channels	3	86.2911	10.87%	98.12%	25.48	17.629
+ 6 WA Channels, + 6 PA Channels	4	86.2377	10.80%	92.11%	29.23	19.000
2200 Feet Elevation	5	86.2160	10.78%	95.19%	17.02	18.297
+ 6 WA Channels, + 8 PA Channels	6	84.7114	8.84%	86.44%	32.42	20.291
Low Wet Wall	7	84.2510	8.25%	91.75%	15.99	19.081
+ 6 WA Channels, +2 PA Channels	8	83.8784	7.77%	104.51%	21.11	16.172
4.0mm Holes	9	79.9322	2.70%	89.59%	15.04	19.574
+ 2 PA Channels	10	79.8727	2.63%	87.93%	20.67	19.951
1.0mm Divider	11	79.1313	1.67%	96.77%	16.45	17.937
+ 4 PA Channels	12	78.8274	1.28%	80.98%	24.47	21.536
Low Drywall	13	78.7079	1.13%	113.90%	13.44	14.031
1.5mm Divider	14	78.3040	0.61%	96.18%	16.27	18.071
+ 2 WA Channels	15	78.2049	0.48%	101.77%	16.17	16.797
+ 4 WA Channels	16	77.9436	0.15%	106.87%	16.14	15.633
High Water Conductivity	17	77.8640	0.05%	96.07%	16.13	18.097
0.34 waterfilm	18	77.8287	0.00%	96.02%	16.12	18.107
0.75 Water Conductivity	19	77.7240	-0.13%	95.89%	16.10	18.136
ch1-7 ch2-7	20	77.6590	-0.22%	95.90%	16.10	18.134
ch1-7 ch2-6	21	77.6480	-0.23%	95.84%	16.09	18.149
+ 5 PA Channels	22	77.6266	-0.26%	77.75%	26.11	22.272
ch1-9 ch2-6	23	77.5939	-0.30%	95.79%	16.08	18.161
ch1-8 ch2-7	24	77.5628	-0.34%	95.77%	16.08	18.164
ch1-12 ch2-3	25	77.5344	-0.38%	95.39%	16.01	18.252
ch1-7 ch2-8	26	77.5220	-0.39%	95.70%	16.07	18.181
BASE	27	77.5156	--	95.64%	16.12	18.195
ch1-4.0 ch2-4.75 ch3-5.5 Hole Dia	28	77.4461	-0.49%	93.49%	15.69	18.684
0.64 waterfilm	29	77.2053	-0.80%	95.25%	15.99	18.282
0.45 Water Conductivity	30	77.1710	-0.85%	95.21%	15.98	18.292
+ 6 WA Channels	31	77.1539	-0.87%	111.29%	16.06	14.626
ch1-11 ch2-4	32	77.1054	-0.93%	95.04%	15.95	18.331
Low Water Conductivity	33	76.4910	-1.72%	94.37%	15.84	18.483
ch1-12 ch2-4	34	76.3930	-1.84%	94.13%	15.80	18.539
2.5mm Divider	35	75.9660	-2.39%	94.59%	15.82	18.433
2.5mm Holes	36	75.9020	-2.48%	85.89%	14.42	20.416
High drywall, Low wetwall	37	75.6445	-2.81%	76.08%	14.04	22.653
3.0mm Divider	38	74.6180	-4.13%	93.58%	15.56	18.655
5.5mm Holes	39	73.4900	-5.57%	99.42%	16.69	17.332
High drywall	40	72.8849	-6.35%	81.50%	17.12	21.418
+ 8 PA Channels	41	72.6795	-6.62%	68.94%	30.09	24.282
High wetwall	42	72.1184	-7.34%	98.55%	14.72	17.530
3.0mm Holes	43	71.4580	-8.19%	66.56%	11.17	24.825
Low drywall, High wetwall	44	70.2429	-9.75%	113.87%	12.48	14.037
8100 Feet Elevation	45	70.2170	-9.78%	96.30%	15.22	18.043
High drywall, High wetwall	46	69.2492	-11.02%	83.60%	16.59	20.940
6.25mm Holes	47	69.1810	-11.11%	101.91%	17.11	16.765
7.0mm Holes	48	65.1460	-16.30%	103.53%	17.38	16.396
10000 Feet Elevation	49	64.8340	-16.70%	96.39%	14.57	17.966

OPTIMIZED DESIGN

The sensitivity analysis presented above varied each design parameter separately and compared the result to the base case design. Once those simulations were run, an optimum design can be simulated using more than just one improved variable. For instance, if an HMX is designed with a 1.0mm divider, 3.2mm product channel height, 1.5mm working channel height (68% product height ratio) and 43 inlets, the COP would be 85.3. The 1.5mm is thought to be a reasonable minimum channel height; below this number may not be practical to manufacture or push air through, considering the undulating nature of the pliable sheets.

INLET CONDITION VARIANCE

As shown in Figure 44 above, the ambient pressure, which is largely defined by the location of the Coolerado units, has a significant impact on the HMX performance. Typical climate and weather also has a significant impact. Figure 50 below shows a portion of a psychrometric chart with a COP surface created from 20 simulations: 4 humidity ratios (0.001, 0.005, 0.009, 0.013) at 5 different temperatures (20°, 25°, 30°, 35° and 40°C). The humidity range minimum was 0.001 instead of actually zero because simulations with no humidity resulted in many wet-bulb convergence and mass transfer errors. Practically speaking, it is reasonable to use 0.001 as a minimum humidity ratio because the outdoor humidity ratio in Colorado (which is one of the driest States) is rarely below this level (based on EPW weather data for Broomfield, CO) [14]. The humidity range was capped at 0.013 because above this level is typically considered outside the thermal comfort range, according to ASHRAE Standard 55. And because the Coolerado is an evaporative cooling system, humidity cannot be removed from the product airstream; product air has the same humidity ratio as the inlet air. The temperature range was limited by a lower limit of

20°C because if inlet air is below this level, not much cooling will be needed. The upper limit, 40°C (104°F), is the main design condition that Coolerado uses to rate their system.

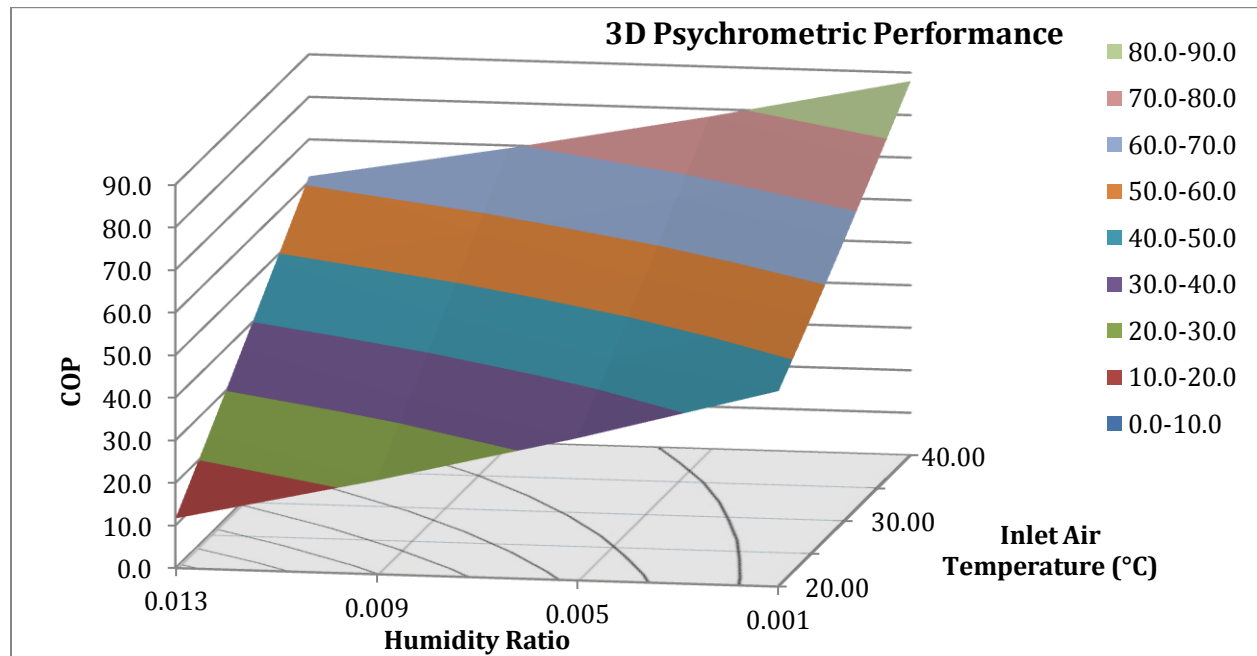


Figure 50. 3D HMX performance sensitivity to different inlet conditions (locations).

It is evident that hotter and drier inlet conditions significantly increase the COP of the HMX. This is reasonable because higher temperatures at the same humidity ratio have a greater vapor and heat carrying capacity. The HMX system relies upon the working air being able to absorb heat in the form of moisture and conduction. Therefore, the COP significantly decreases as temperature decreases. While humidity does also affect the performance, temperature has more of an effect; this is evident by the steeper gradient from 20 to 40°C at a constant humidity ratio (0.001) than the COP gradient between 0.001 and 0.013 humidity ratio at a constant temperature (20°C). This can be seen more clearly in Table 16.

Table 16. HMX performance sensitivity to different inlet conditions data.

COP		Humidity Ratio				
		0.001	0.005	0.009	0.013	
Temp. (°C)	20	45.9	33.4	22	11.6	Δ COP = 49.6
	25	55.7	44	33.4	23.7	
	30	66.2	55.2	45.2	36.1	
	35	76.9	66.6	57.2	48.7	
	40	88	78.3	69.4	61.3	
		Δ COP = 18.7				

Table 16 was created from the 20 simulation outputs. In theory, it could be used to predict the performance of a Coolerado system based on an average inlet condition. Although there is a slight curvature to the surface in Figure 50, it is relatively flat, and extrapolation within one interval of temperature or humidity ratio should give reasonable results. Based on Figure 50, Coolerado air conditioners would operate most efficiently in climates with very hot and dry conditions.

NSIDC COOLERADO SYSTEM OPERATION

The results of the inlet condition sensitivity simulations are applied to the NSIDC to determine when the Coolerado system can be used to cool the data center. As seen in Figure 50, the performance of the HMX degrades significantly in cooler and very humid conditions. This is largely due to decreased cooling power. Although the wet-bulb effectiveness is about the same, at higher humidity ratios, the dew-point is also higher. And because the Maistosenko cycle is driven by the dew-point of inlet air, this results in less available heat transfer and difference between product and working air enthalpies. Because of this effect, the cooling capacity of the Coolerados at the NSIDC is not enough to cool the constant heat load (servers) for some inlet air conditions. The current server load of the NSIDC is about 33 kW and is supplied power from the UPS. The UPS is also in the room and contributes to the heat load of the space. Assuming that the power consumed by the UPS efficiency is completely dissipated as heat, this also must be cooled by the cooling system. 33 kW of power requires 37.63 kW of input to the UPS. The

rooftop AHU is also run off the UPS, and on a peak cooling day, the AHU fan consumes about 6 kW of power. This fan power accounts for 0.84 kW of power loss through the UPS. Rearranging Equation 2, Equations 20 and 21 show this algebraically.

$$\text{Total Cooling Load} = \text{Total Power Consumption in Room} \quad (20)$$

$$\text{Total Cooling Load} = \frac{\text{IT Power}}{\text{UPS Efficiency}} + (\text{AHU Power})(1 - \text{UPS Efficiency}) \quad (21)$$

$$= \frac{33 \text{ kW}}{87.7\%} + (6 \text{ kW})(100\% - 87.7\%) \quad (22)$$

$$= 37.63 \text{ kW} + 0.84 \text{ kW} = 38.47 \text{ kW} \approx 40 \text{ kW} \quad (23)$$

Therefore, the total cooling load is about 40 kW. The Coolerados must be able to meet this load. By interpolating linearly between the inlet condition sensitivity simulations (and a few other simulations run just for this purpose), a line can be drawn on a psychrometric chart showing the limits of where the Coolerados can and can't be exclusively used to cool the data center. Outside of this range, the CRAC must be used to dehumidify the space. Figure 51 shows the operation modes. Note that the curved line between the CRAC and Coolerado operations is steeper than the relative humidity lines. This is a similar trend as seen in Figure 50, and is reasonable because cooling capacity has a direct impact on COP. The ASHRAE allowable upper humidity limit defines the limit of the Coolerado use above about 27.2°C (81°F); if there is more moisture in the air than this limit at the inlets to the Coolerados, the CRAC must be used to dehumidify the air. The Coolerados cannot remove moisture from the air. If the recommended limit is the target operation for the data center, then the CRAC may need to be run more often. Below an AHU supply air temperature of 18.3°C (65°F), the economizer mode can be used exclusively to meet the cooling load.

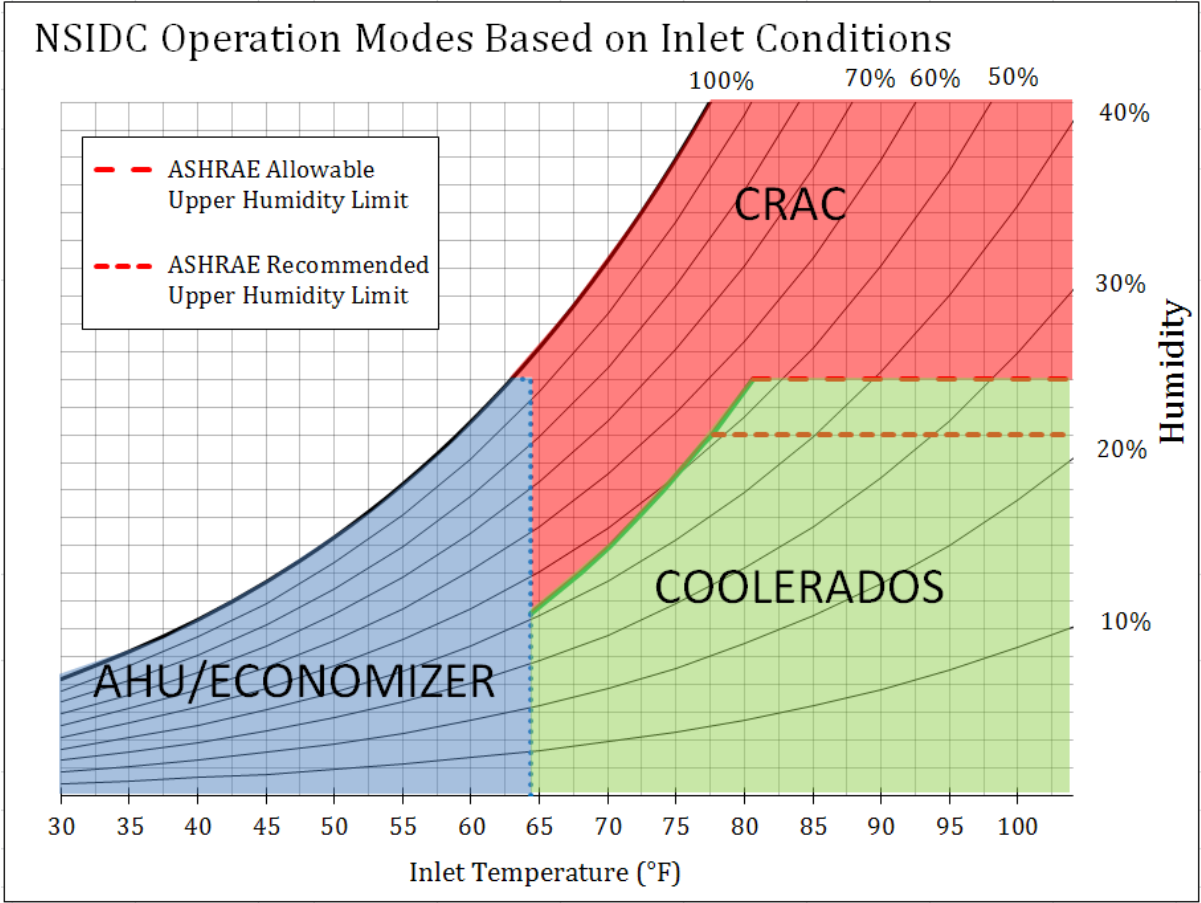


Figure 51. NSIDC new system operation based on inlet conditions.

VI. CONCLUSION

ENERGY USE

Since the installation of the new cooling system in June 2011, the Coolerado units and the AHU have reduced the energy required to cool the data center by almost 90% in winter months and over 70% in hot summer months. One of Coolerado's early projections was 80% savings in energy [8]; the NSIDC has certainly demonstrated that this is achievable and even beatable. These reductions directly impact the PUE or efficiency of the data center. The average annual PUE is now around 1.30, where as it used to be 2.03. The new PUE shows that the NSIDC could now be considered a high performance data center as it requires significantly less energy to support its IT infrastructure.

The new cooling system is relatively simple and has fewer extensive maintenance requirements. The lower maintenance and energy savings translates to significant operational cost reduction for the NSIDC. This results in a very reasonable payback period. The Coolerado air conditioner uses a unique technology that has demonstrated savings potential, and is a great addition to the NSIDC's facility to further their vision of reduced environmental impact as the center continues its research on climate related issues.

SUGGESTED HMX DESIGN IMPROVEMENTS

It is evident that the Coolerado system is very efficient at delivering cooling power to an environment with a high heat load. However, there is always room for improvement and a portion of this research was devoted to sensitivity analysis to better understand how the HMX performance relates to each of the design variables. It was found that channel heights and the ratio between them have a significant impact on HMX performance. Divider width was the parameter with the

next biggest practical impact, but the COP increase associated with decreasing divider width is very small. Hole diameter reduction had a greater impact, however, this design variable may not be a practical way to change the performance because current manufacturing tolerances limit the precision needed to adjust this dimension accurately. Other parameters, hole location, water conductivity and waterfilm thickness, were found to have insignificant effects on the performance. Table 17 shows some suggested design improvements, based on the sensitivity simulations as well as general observations of the Coolerado units at the NSIDC. Some of these items are small and may only account for fractional increases in performance. However, from an academic point of view, it is prudent to document all potential fixes and improvements to increase the theoretical performance of the Coolerado HMX system. It is understood that some of these issues may have already been addressed in newer versions of the HMX design. The theoretical MatLAB model, developed by NREL, has been validated at one point in time through this research, and can be applied to the actual design process in predicting the performance of the Coolerado units under a specified set of conditions. Sensitivity analysis was performed to determine which design parameters have the most impact on Coolerado performance.

Table 17. Summary of suggested design improvements.

	Issue	Description	Suggested Improvement
1)	Water Flow and Dispersion	It is understood that for the HMX system to perform to its theoretical best, the working air channel must remain fully wet, on top and bottom, at all times during operation. It was evident that there is a connection between product air temperature and the time since the last "soaping" of the unit. Over a few months, product air temperature will start to rise, with the top HMX blocks becoming warm first. Although water deprivation of the whole Coolerado unit would cause the unit to dry out, the temperature gradient may point to a different issue: water dispersion to each HMX block is different. The Version 6 design has 1 water inlet in the middle of each HMX block on the front face.	Put water inlet for each HMX block at the top of the block instead of the center, to ensure complete water dispersion in the vertical direction in each HMX.
2)	Rough and Irregular air inlets	The epoxy used to seal the front (and back) faces of the HMX appears to spread out the sheets sometimes, which reduces the actual opening height for the surrounding channels. (See Figure 24). It is unknown how much this affects the overall performance, but in theory it would increase the fan power required to overcome inlet turbulence.	Consider including a little extra sheet area on the front side of the HMX or simply using a thinner adhesive between the working air sheets to seal the front edge of them into a wedge or point. This would more effectively help guide the air smoothly into the dry channels.
3)	Channel Heights	Reducing channel heights (product or working air) reduces the product air temperature, which increases the COP of the HMX. The channel heights and the ratio between them have the greatest impact on the performance because they directly affect airflow and heat transfer. Lowering the wet channel height by 0.5mm (0.02") could increase the COP by 8%. Lowering both the working channel height and the product channel height could increase the COP by 14%.	If it is possible to more precisely control the number of sheets stacked in an HMX frame, use the Optimum Product Height Ratio chart to determine what the height ratio should be based on a given number of sheets. In general, more sheets results in higher efficiency. <i>But the height setup should be tested to ensure the expected airflows are attained.</i> Because the model assumes rigid sheets, the actual pliable sheets may impede flow.
4)	Divider Width	The channel divider is required to maintain the structure of the HMX and the channel heights. However, its width directly reduces the available heat transfer surface area on a sheet. Sensitivity analysis showed that reducing the width from 2mm to 1mm could increase the COP by 2%.	If this can be done at reasonably low expense, refine divider bead manufacturing techniques to allow thinner beads of equal height to be deposited onto the sheet. Maybe consider other stiffer materials that could be formed thinner or come pre-shaped in a specified cross sectional dimension.
5)	Hole Diameter	Hole diameter does have a noticeable effect on COP. Reducing the hole diameter limits the flow, allowing more heat transfer into the working air stream, thereby increasing COP. However cooling capacity decreases, so a compromise must be made.	None. It seems that the current (V6) value of 4.75mm is reasonable and a good compromise between COP and cooling capacity. Also, it is understood that current manufacturing tolerances are too wide to accurately control hole diameter.
6)	Hole Locations	Adjusting the number of holes in the first working air channel does have an impact on the airflow and pressure drop along the working air paths. However, the impact is insignificant, increasing the COP by less than 0.2% if 9 holes are used in the first channel. And fewer than 9 or greater than 10 holes performs no better than the base case of 10 holes.	None. The current design with 10 holes in the first channel performs very close to the optimal performance, as far as this variable goes. 9 holes is optimal, however the COP is nearly the same.

CHALLENGES

One challenge of this project, and is often overlooked in research, is data collection. Any research or experimental data can only be as good as the system that is used to collect it. In this project in particular, the CU4 unit was not operating as designed; and air temperatures across the product and working air outlets were not consistent. Therefore, the list of Model Test Conditions could not be used for model verification. Because the water flow and dispersion has a significant impact on the Coolerado unit performance and it was not constant, there was a performance dynamic that was independent from the fan speed dynamic. If the data logging system had multiple sensors in each CU4 outlet, the temperature gradient could have been captured by the system and conditions of high gradient could be discarded from the MTC list.

Another “behind the scenes” aspect of this project was the extensive amount of time and effort that went into developing data consolidation strategies and algorithms. The data collected is also only as useful as its presentation. Because multiple different types of data were collected from multiple different sources, the data had to be consolidated into one common file with similar timestamps. This was not an easy task, especially considering that over 12 months of data was used throughout this report. This data consolidation required more time than initially expected.

FUTURE WORK

An extensive amount of time was put into this project from installing the datalogging system, collecting and consolidating data, validating that the model has enough theoretical detail and proving its relative accuracy, and using the model to simulate improved design strategies. However, there is still a lot of work that can be done to further the understanding of the applicability of the Maisotsenko Cycle and the Coolerado system to the built environment. First of all, although good agreement was found between simulated and actual performance at one point in time, the original intent of this research was to validate the model over a range of actual operating

conditions. Due to datalogging system limited capabilities, not enough measurements were taken at every point in time to properly characterize the thermal performance of the M50 units. More data that includes multiple sensor location in both outgoing airstreams should be collected for a range of inlet conditions. Once the model is more thoroughly validated, there would be more confidence in its results.

A formal optimization simulation was not developed for the model. Although the sensitivity simulations show the effects that each individual parameter has the performance of the HMX, changes in more than one parameter require many more simulations to be performed. To find the optimum values for each parameter requires an optimization algorithm. Because the model is completely based in MatLAB, developing an optimization engine should be possible and within the scope of further graduate student work. One challenge to this will be determining how to interface with the complex and robust GUI that is already in use. There is a "Run DOE" option on the model that prompts the user to select which design parameters to vary and then how much to vary them. Perhaps this feature could be used as a starting point. However, the results from this parametric simulation were not consistent or easy to decipher, so it may take some code integration work.

Once more completely validated, the model could be used to simulate annual performance, based on a given set of inlet conditions (from a weather file like TMY3) and operating times (occupancy schedule). Ultimately, this research may prove useful in populating equipment libraries of whole-building energy simulation tools with theoretically accurate and experimentally validated components, namely the Coolerado air conditioner. As sustainable and integrated building design becomes more prevalent, tools to validate low-energy systems like Coolerados are necessary for proof of concept.

REFERENCES

1. EPA Energy Star Program. "Report to Congress on Server and Data Center Efficiency." August 2, 2007.
2. J. Koomey, "Growth in data center electricity use 2005 to 2010," Analytics Press. Table 1 p. 20. August 1, 2011.
3. ASHRAE publication. "2008 ASHRAE environmental guidelines for datacom equipment." pp. 1-8. 2008.
4. Rasmussen, Neil. "Guidelines for Specification of Data Center Power Density." American Power Conversion. 2005.
5. Seaton, Ian. "The Biggest Opportunity for Data Center Energy Savings." Chatsworth Products, Inc. 2009.
6. Rawson, Andy et al. "Green Grid Data Center Power Efficiency Metrics: PUE and DCiE." The Green Grid. 2008.
7. Carmichael, Ben. "Data centers set to outpace airlines in GHG emissions." onearth magazine. May 12, 2008. <http://www.onearth.org/blog/whats-happening-on-earth/data-centers-set-to-outpace-airlines-in-ghg-emissions>
8. UC Davis News Service. "UC Davis challenge produces a better air conditioner." UC Davis News and Information. Aug. 13, 2009. http://www.news.ucdavis.edu/search/news_detail.lasso?id=9200. Accessed Jan. 30, 2012.
9. Wicker, Ken. "Life below the wet-bulb: the Maisotsenko Cycle." Power Magazine. Noember/December 2003.
10. Threlkeld, James L. "Thermal Environmental Engineering. Second Edition." Prentice-Hall, Inc., Englewood Cliffs, NJ. p254-256. 1970.
11. "WattNode Pulse Installation and Operation Manual." Continental Control Systems LLC. Boulder, CO. p24-29. 2011.
12. Zube, Daniel. "Flow Rate vs. HMX Pressure Drop - Coolerado M50 Equipped with Stack of V6 HMXs (02.17.2012)." Coolerado Corporation. Denver, CO. February 17, 2012.

13. Moffat, Robert J. "Describing the Uncertainties in Experimental Results." *Experimental Thermal and Fluid Science*. Elsevier Science Publishing, Co, Inc. New York, NY. pp. 3-17. 1988.
14. Wilcox, S. and W. Marion. 2008. *User's Manual for TMY3 Data Sets*, NREL/TP-581-43156. April 2008. Golden, Colorado: National Renewable Energy Laboratory.

APPENDIX

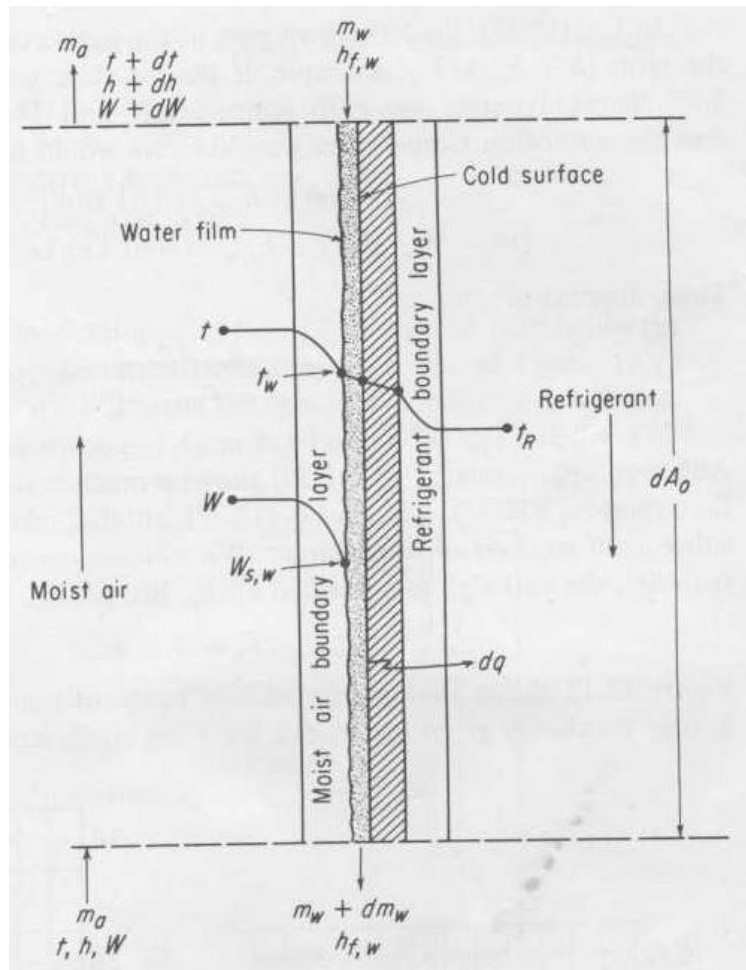


Figure 52. Discrete portion of cooling coil; heat transfer schematic from Threlkeld [10].

Actual Data from Campbell:									
Description	Date/Time cu4data_condensed #	Airflow				Prod			
		(6) TOTAL CFM	1/8 or 1/4 of AHU	My data: power regression	Error ±CFM	(7) T (°F)	Error ±T(°C)		
1a Hottest INPUT T	19736 8/18/2011 15:51	20925	2615.6	2431.3	135.4	64.460	18.033	0.210	
1b 8 hour steady state power	19580:198 8:00-20:00	20197	2524.6	2471.3	136.6	63.470	17.483	0.213	
1c ± 30 min	19726:19746	20258	2532.3	2461.9	136.4	64.390	17.994	0.215	
Minimum INPUT RH/SA_RH	46442 11/11/2011 13:00	8418	2104.5	1931.7	120.5	51.830	11.017	0.245	
2 hour steady state power	46434:464 12:12-14:24	8190	2047.5	1793.6	116.3	52.130	11.183	0.244	
2 ± 30 min	46437:46447	8172	2043.0	1748.1	114.9	51.882	11.046	0.245	
Warm INPUT T, high RH	12259 8/3/2011 3:00	19960	2495.0	2493.4	137.3	65.450	18.583	0.207	
3 ± 30 min (12251-12255 DRY)	12249:12269	17055	2131.9	2267.3	130.5	67.122	19.512	0.202	
4 ± 30 min (29589 DRY)	29583 9/8/2011 8:12	9543	2385.8	2431.3	135.4	59.518	15.288	0.224	
	29575:29593	12585	3146.3	2886.7	137.1	59.338	15.188	0.224	
5 ± 30 min	34119 9/21/2011 4:12	10294	2573.5	2431.3	135.4	52.809	11.561	0.242	
Hottest CU4_IN_T	34109:34129	10040	2510.0	2207.1	128.7	53.868	12.149	0.239	
6 ± 30 min	11051:11071	20347	2543.4	2493.4	137.3	67.720	19.844	0.201	
Medium CU4_IN_T & low RH	42147 10/24/2011 16:18	20260	2532.5	2469.8	136.6	67.723	19.846	0.201	
7 ± 30 min	42137:42157	8764	1095.5	1494.2	107.3	57.118	13.954	0.230	
	37927 10/7/2011 2:12	11165	1395.6	1675.6	112.8	57.220	14.011	0.230	
8 ± 30 min	37917:37937	8966	2241.5	1494.2	107.3	52.545	11.414	0.243	
	4326 7/17/2011 14:21	9154	2288.5	1241.9	99.8	52.559	11.422	0.243	
9 ± 30 min	4316:4336	20224	2528.0	2473.3	136.7	70.034	21.130	0.206	
	6351 7/21/2011 18:36	19810	2476.3	2431.3	135.4	66.200	19.000	0.205	
10 ± 30 min	6341:6361	19868	2483.5	2465.9	136.5	66.359	19.088	0.205	
	6471 7/22/2011 0:36	14940	1867.5	1494.2	107.3	61.390	16.328	0.218	
11 ± 30 min	6461:6481	15539	1942.4	1494.2	107.3	60.900	16.055	0.220	
12 ± 30 min	1419 7/11/2011 12:00	20020	2502.5	2431.3	135.4	67.840	19.911	0.200	
	24879 8/29/2011 9:00	19933	2491.6	2431.3	135.4	66.432	19.129	0.204	
13 ± 30 min intermittent DRY	24869:24889	19754	2469.3	2482.1	137.0	66.597	19.221	0.204	
	25293 8/30/2011 5:42	15763	1970.4	931.5	90.4	57.451	14.139	0.229	
14 ± 30 min	25283:25303	15755	1969.4	1494.2	107.3	57.978	14.432	0.228	
	30218 9/9/2011 15:57	13971	1746.4	1494.2	107.3	58.700	14.833	0.226	
15 ± 30 min	30208:30228	14476	1809.5	1541.1	108.7	59.094	15.052	0.225	
16 ± 30 min ALL DRY	35530 9/27/2011 2:18	16190	4047.5	2444.1	129.8	61.193	16.218	0.219	
	36602 10/1/2011 12:36	15042	3760.5	2244.1	129.8	61.068	16.149	0.219	
17 ± 30 min	36592:36612	15985	1998.1	2431.3	135.4	60.642	15.912	0.220	
	36638 10/1/2011 16:12	16001	2000.1	2390.6	134.2	60.500	11.933	0.240	
18 ± 30 min	36628:36648	15335	1916.9	2232.0	129.5	60.746	12.070	0.240	
	36689 10/1/2011 21:18	12723	1590.4	1494.2	107.3	60.792	15.996	0.220	
19 ± 30 min	36679:36699	12151	1518.9	1421.4	105.1	60.651	12.017	0.240	
20 101,2012,801,1330,22,635,7781,3,52,772,47.: 3/20/2012 13:30	7781 1945.3 2244.1	8294	2073.5	1494.2	107.3	52.183	8.213	0.259	
21 101,2012,81,1330,20:184,8644,8,52,586,38.: 3/21/2012 13:30	8644 2161.0 1931.7	8551	2137.8	1931.7	120.5	52.586	11.437	0.243	
± 30 min		12139	3034.8	2431.3	135.4	51.538	10.854	0.246	
22 101,2012,83,1206,13,449,13424,NOGRAD 3/23/2012 12:06									

```

% EnergyCalc_CRAC
% Ben Weerts
% Calculates Energy Used over specified period.
% (Pre 6/2011)
%
% IMPORT CRAC_data.dat!

% CRACdata:
% 1 20 ton Liebert CRAC
% 2 30 ton Liebert CRAC
% 3 UPS Power

% textdata:
% 1 Date (mm/dd/yyyy)
% 2 Time (HH:MM PM)

format long

% r=1;
L20_Energy = zeros(13,1);
L30_Energy = zeros(13,1);
UPS_Energy = zeros(13,1);

% % To convert date to datenum:
% year_month_day = zeros(3030784,6);
% time = zeros(3030784,6);
% temp = zeros(3030784,6);
% timestamp = zeros(3030784,1);
%
% year_month_day = datevec(textdata(:,1));
% time = datevec(textdata(:,2));
%
% temp = [year_month_day(:,1:3),time(:,4:6)];

% j = 0;
% for j = 1:3030784
%     timestamp(j,1) = datenum(temp(j,:));
% end

% % Annual Energy Consumption:
% for i = 53852:2821848
%     L20_temp = (data(i,1)+data(i+1,1))/2*(timestamp(i+1,1)-
timestamp(i,1))*24;
%     L20_Energy = L20_temp + L20_Energy;
%     L30_temp = (data(i,2)+data(i+1,2))/2*(timestamp(i+1,1)-
timestamp(i,1))*24;
%     L30_Energy = L30_temp + L30_Energy;
%     UPS_temp = (data(i,3)+data(i+1,3))/2*(timestamp(i+1,1)-
timestamp(i,1))*24;
%     UPS_Energy = UPS_temp + UPS_Energy;
% end

% Monthly Energy Consumption
for i = 53852:3030783

```

```

L20_temp = (data(i,1)+data(i+1,1))/2*(timestamp(i+1,1)-timestamp(i,1))*24;
L30_temp = (data(i,2)+data(i+1,2))/2*(timestamp(i+1,1)-timestamp(i,1))*24;
UPS_temp = (data(i,3)+data(i+1,3))/2*(timestamp(i+1,1)-timestamp(i,1))*24;

% June 2010
if timestamp(i,1) < 734320
    if timestamp(i,1) > 734290
        L20_Energy(1,1) = L20_temp + L20_Energy(1,1);
        L30_Energy(1,1) = L30_temp + L30_Energy(1,1);
        UPS_Energy(1,1) = UPS_temp + UPS_Energy(1,1);
    end
end
% July 2010
if timestamp(i,1) < 734351
    if timestamp(i,1) > 734320
        L20_Energy(2,1) = L20_temp + L20_Energy(2,1);
        L30_Energy(2,1) = L30_temp + L30_Energy(2,1);
        UPS_Energy(2,1) = UPS_temp + UPS_Energy(2,1);
    end
end
% August 2010
if timestamp(i,1) < 734382
    if timestamp(i,1) > 734351
        L20_Energy(3,1) = L20_temp + L20_Energy(3,1);
        L30_Energy(3,1) = L30_temp + L30_Energy(3,1);
        UPS_Energy(3,1) = UPS_temp + UPS_Energy(3,1);
    end
end
% September 2010
if timestamp(i,1) < 734412
    if timestamp(i,1) > 734382
        L20_Energy(4,1) = L20_temp + L20_Energy(4,1);
        L30_Energy(4,1) = L30_temp + L30_Energy(4,1);
        UPS_Energy(4,1) = UPS_temp + UPS_Energy(4,1);
    end
end
% October 2010
if timestamp(i,1) < 734443
    if timestamp(i,1) > 734412
        L20_Energy(5,1) = L20_temp + L20_Energy(5,1);
        L30_Energy(5,1) = L30_temp + L30_Energy(5,1);
        UPS_Energy(5,1) = UPS_temp + UPS_Energy(5,1);
    end
end
% November 2010
if timestamp(i,1) < 734473
    if timestamp(i,1) > 734443
        L20_Energy(6,1) = L20_temp + L20_Energy(6,1);
        L30_Energy(6,1) = L30_temp + L30_Energy(6,1);
        UPS_Energy(6,1) = UPS_temp + UPS_Energy(6,1);
    end
end
% Decemebr 2010
if timestamp(i,1) < 734504
    if timestamp(i,1) > 734473

```



```

        L20_Energy(7,1) = L20_temp + L20_Energy(7,1);
        L30_Energy(7,1) = L30_temp + L30_Energy(7,1);
        UPS_Energy(7,1) = UPS_temp + UPS_Energy(7,1);
    end
end
% January 2011
if timestamp(i,1) < 734535
    if timestamp(i,1) > 734504
        L20_Energy(8,1) = L20_temp + L20_Energy(8,1);
        L30_Energy(8,1) = L30_temp + L30_Energy(8,1);
        UPS_Energy(8,1) = UPS_temp + UPS_Energy(8,1);
    end
end
% February 2011
if timestamp(i,1) < 734563
    if timestamp(i,1) > 734535
        L20_Energy(9,1) = L20_temp + L20_Energy(9,1);
        L30_Energy(9,1) = L30_temp + L30_Energy(9,1);
        UPS_Energy(9,1) = UPS_temp + UPS_Energy(9,1);
    end
end
% March 2011
if timestamp(i,1) < 734594
    if timestamp(i,1) > 734563
        L20_Energy(10,1) = L20_temp + L20_Energy(10,1);
        L30_Energy(10,1) = L30_temp + L30_Energy(10,1);
        UPS_Energy(10,1) = UPS_temp + UPS_Energy(10,1);
    end
end
% April 2011
if timestamp(i,1) < 734624
    if timestamp(i,1) > 734594
        L20_Energy(11,1) = L20_temp + L20_Energy(11,1);
        L30_Energy(11,1) = L30_temp + L30_Energy(11,1);
        UPS_Energy(11,1) = UPS_temp + UPS_Energy(11,1);
    end
end
% May 2011
if timestamp(i,1) < 734655
    if timestamp(i,1) > 734624
        L20_Energy(12,1) = L20_temp + L20_Energy(12,1);
        L30_Energy(12,1) = L30_temp + L30_Energy(12,1);
        UPS_Energy(12,1) = UPS_temp + UPS_Energy(12,1);
    end
end
% June 2011 (
if timestamp(i,1) < 734685
    if timestamp(i,1) > 734655
        L20_Energy(13,1) = L20_temp + L20_Energy(13,1);
        L30_Energy(13,1) = L30_temp + L30_Energy(13,1);
        UPS_Energy(13,1) = UPS_temp + UPS_Energy(13,1);
    end
end
end
% End EnergyCalc_CRAC.m

```

```

% EnergyCalc_CR10X
% Ben Weerts
% Calculates Energy Used over specified period.
% (Post 9/16/2011)
%
% IMPORT EnergyCalc_CR10X.csv! (using MatLAB 2011b spreadsheet importer which
% automatically converts date/time field to datenum)

% CR10X_power:
% 1 datenum
% 2 AHU Power
% 3 CU4 Power
% 4 UPS Power
% 5 L3M Power
% 6 CRAC Power

format long

AHU_Energy = zeros(8,1);
L3M_Energy = zeros(8,1);
UPS_Energy = zeros(8,1);
L30_Energy = zeros(8,1);

for i = 1:98861

    % The 2 IF statements below account for midnight format discrepancy
    % (24:00 became 00:00 when shifting between 102 and CR10X program
    versions on the datalogger)
    if CR10X_power(i+1,1)-CR10X_power(i,1) > 0
        AHU_temp =
(CR10X_power(i,2)+CR10X_power(i+1,2))/2*(CR10X_power(i+1,1)-
CR10X_power(i,1))*24;
        UPS_temp =
(CR10X_power(i,4)+CR10X_power(i+1,4))/2*(CR10X_power(i+1,1)-
CR10X_power(i,1))*24;
        L3M_temp =
(CR10X_power(i,5)+CR10X_power(i+1,5))/2*(CR10X_power(i+1,1)-
CR10X_power(i,1))*24;
        L30_temp =
(CR10X_power(i,6)+CR10X_power(i+1,6))/2*(CR10X_power(i+1,1)-
CR10X_power(i,1))*24;
    end
    if CR10X_power(i+1,1)-CR10X_power(i,1) > .00694444
        AHU_temp = (CR10X_power(i-
1,2)+CR10X_power(i+1,2))/2*(CR10X_power(i+1,1)-CR10X_power(i-1,1))*24;
        UPS_temp = (CR10X_power(i-
1,4)+CR10X_power(i+1,4))/2*(CR10X_power(i+1,1)-CR10X_power(i-1,1))*24;
        L3M_temp = (CR10X_power(i-
1,5)+CR10X_power(i+1,5))/2*(CR10X_power(i+1,1)-CR10X_power(i-1,1))*24;
        L30_temp = (CR10X_power(i-
1,6)+CR10X_power(i+1,6))/2*(CR10X_power(i+1,1)-CR10X_power(i-1,1))*24;
    end
    if CR10X_power(i+1,1)-CR10X_power(i,1) < 0
        AHU_temp =
(CR10X_power(i,2)+CR10X_power(i+1,2))/2*(CR10X_power(i+2,1)-
CR10X_power(i,1))*24;

```

```

        UPS_temp =
(CR10X_power(i,4)+CR10X_power(i+1,4))/2*(CR10X_power(i+2,1)-
CR10X_power(i,1))*24;
        L3M_temp =
(CR10X_power(i,5)+CR10X_power(i+1,5))/2*(CR10X_power(i+2,1)-
CR10X_power(i,1))*24;
        L30_temp =
(CR10X_power(i,6)+CR10X_power(i+1,6))/2*(CR10X_power(i+2,1)-
CR10X_power(i,1))*24;
    end

% September 2011 (ONLY FROM 9/16-9/30!)
if CR10X_power(i,1) < 734777
    if CR10X_power(i,1) > 734747
        AHU_Energy(1,1) = AHU_temp + AHU_Energy(1,1);
        L3M_Energy(1,1) = L3M_temp + L3M_Energy(1,1);
        UPS_Energy(1,1) = UPS_temp + UPS_Energy(1,1);
        L30_Energy(1,1) = L30_temp + L30_Energy(1,1);
    end
end

% October 2011
if CR10X_power(i,1) < 734808
    if CR10X_power(i,1) > 734777
        AHU_Energy(2,1) = AHU_temp + AHU_Energy(2,1);
        L3M_Energy(2,1) = L3M_temp + L3M_Energy(2,1);
        UPS_Energy(2,1) = UPS_temp + UPS_Energy(2,1);
        L30_Energy(2,1) = L30_temp + L30_Energy(2,1);
    end
end

% November 2011
if CR10X_power(i,1) < 734838
    if CR10X_power(i,1) > 734808
        AHU_Energy(3,1) = AHU_temp + AHU_Energy(3,1);
        L3M_Energy(3,1) = L3M_temp + L3M_Energy(3,1);
        UPS_Energy(3,1) = UPS_temp + UPS_Energy(3,1);
        L30_Energy(3,1) = L30_temp + L30_Energy(3,1);
    end
end

% December 2011
if CR10X_power(i,1) < 734869
    if CR10X_power(i,1) > 734838
        AHU_Energy(4,1) = AHU_temp + AHU_Energy(4,1);
        L3M_Energy(4,1) = L3M_temp + L3M_Energy(4,1);
        UPS_Energy(4,1) = UPS_temp + UPS_Energy(4,1);
        L30_Energy(4,1) = L30_temp + L30_Energy(4,1);
    end
end

% January 2012
if CR10X_power(i,1) < 734900
    if CR10X_power(i,1) > 734869
        AHU_Energy(5,1) = AHU_temp + AHU_Energy(5,1);
        L3M_Energy(5,1) = L3M_temp + L3M_Energy(5,1);
    end
end

```

```

        UPS_Energy(5,1) = UPS_temp + UPS_Energy(5,1);
        L30_Energy(5,1) = L30_temp + L30_Energy(5,1);
    end
end

% February 2012
if CR10X_power(i,1) < 734929
    if CR10X_power(i,1) > 734900
        AHU_Energy(6,1) = AHU_temp + AHU_Energy(6,1);
        L3M_Energy(6,1) = L3M_temp + L3M_Energy(6,1);
        UPS_Energy(6,1) = UPS_temp + UPS_Energy(6,1);
        L30_Energy(6,1) = L30_temp + L30_Energy(6,1);
    end
end

% March 2012
if CR10X_power(i,1) < 734960
    if CR10X_power(i,1) > 734929
        AHU_Energy(7,1) = AHU_temp + AHU_Energy(7,1);
        L3M_Energy(7,1) = L3M_temp + L3M_Energy(7,1);
        UPS_Energy(7,1) = UPS_temp + UPS_Energy(7,1);
        L30_Energy(7,1) = L30_temp + L30_Energy(7,1);
    end
end

% April 2012
if CR10X_power(i,1) < 734990
    if CR10X_power(i,1) > 734960
        AHU_Energy(8,1) = AHU_temp + AHU_Energy(8,1);
        L3M_Energy(8,1) = L3M_temp + L3M_Energy(8,1);
        UPS_Energy(8,1) = UPS_temp + UPS_Energy(8,1);
        L30_Energy(8,1) = L30_temp + L30_Energy(8,1);
    end
end
end

% End EnergyCalc_CR10X.m

```

```

% cu4data_creation.m
% Ben Weerts
%
% IMPORT cu4data_monthly.mat FIRST!!!
%
% cu4data_monthly:
% 1 datenum
% 2 year
% 3 day
% 4 time
% 5 SA_RH
% 6 CFM
% 7 Product Air Temp
% 8 Product Air RH
% 9 Working Air Temp
% 10 Working Air RH
% 11 CU4 Power
% 12 L3M Power
% 13 Water
% 14 CU4_IN_T
% 15 INPUT-T
% 16 INPUT-RH
% 17 S-COOL-T
% 18 INPUT-DP

cu4data = zeros(417422,18);

for i = 1:417423
    if i < 33776
        cu4data(i,:) = CU4_Jul(i,:);
    end

    if i < 78416
        if i > 33775
            cu4data(i,:) = CU4_Aug(i-33775,:);
        end
    end

    if i < 121616
        if i > 78415
            cu4data(i,:) = CU4_Sep(i-78415,:);
        end
    end

    if i < 166256
        if i > 121615
            cu4data(i,:) = CU4_Oct(i-121615,:);
        end
    end

    if i < 209456
        if i > 166255
            cu4data(i,:) = CU4_Nov(i-166255,:);
        end
    end
end

```

```

if i < 254096
    if i > 209455
        cu4data(i,:) = CU4_Dec2(i-209455,:);
    end
end

if i < 298736
    if i > 254095
        cu4data(i,:) = CU4_Jan(i-254095,:);
    end
end

if i < 340496
    if i > 298735
        cu4data(i,:) = CU4_Feb(i-298735,:);
    end
end

if i < 385135
    if i > 340495
        cu4data(i,:) = CU4_Mar2(i-340495,:);
    end
end

if i < 417422
    if i > 385134
        cu4data(i,:) = CU4_Apr(i-385134,:);
    end
end

end

for i = 1:417422
    if cu4data(i,5) < 0
        cu4data(i,5) = 0;
    end
    if cu4data(i,6) < 0
        cu4data(i,6) = 0;
    end
    if cu4data(i,8) < 0
        cu4data(i,8) = 0;
    end
    if cu4data(i,10) < 0
        cu4data(i,10) = 0;
    end
    if cu4data(i,16) < 0
        cu4data(i,16) = 0;
    end
end

cu4data_condensed = zeros(85772,18);

```

```

r = 1;

for j = 2:417422
    if j == 2
        cu4data_condensed(r,1:5) = cu4data(j,1:5);
        cu4data_condensed(r,6) = mean(cu4data(j-1:j,6));
        cu4data_condensed(r,7:10) = cu4data(j,7:10);
        cu4data_condensed(r,11) = mean(cu4data(j-1:j,11));
        cu4data_condensed(r,12) = mean(cu4data(j-1:j,12));
        cu4data_condensed(r,13) = sum(cu4data(j-1:j,13));
        cu4data_condensed(r,14) = mean(cu4data(j-1:j,14));
        cu4data_condensed(r,15) = mean(cu4data(j-1:j,15));
        cu4data_condensed(r,16) = mean(cu4data(j-1:j,16));
        cu4data_condensed(r,17) = mean(cu4data(j-1:j,17));
        cu4data_condensed(r,18) = mean(cu4data(j-1:j,18));
        r = r + 1;
    end

    if j > 2
        if cu4data(j,2) > 2000
            if cu4data(j,14) > 0
                if cu4data(j-1,14) > 0
                    cu4data_condensed(r,1:5) = cu4data(j,1:5);
                    if cu4data(j-1,6) > 0
                        cu4data_condensed(r,6) = mean(cu4data(j-2:j,6));
                        cu4data_condensed(r,11) = mean(cu4data(j-2:j,11));
                        cu4data_condensed(r,12) = mean(cu4data(j-2:j,12));
                    elseif cu4data(j-1,6) == 0
                        cu4data_condensed(r,6) = cu4data(j,6);
                        cu4data_condensed(r,11) = cu4data(j,11);
                        cu4data_condensed(r,12) = cu4data(j,12);
                    end
                    cu4data_condensed(r,7:10) = cu4data(j,7:10);
                    cu4data_condensed(r,13) = sum(cu4data(j-2:j,13));
                    cu4data_condensed(r,14) = mean(cu4data(j-2:j,14));
                    cu4data_condensed(r,15) = mean(cu4data(j-2:j,15));
                    cu4data_condensed(r,16) = mean(cu4data(j-2:j,16));
                    cu4data_condensed(r,17) = mean(cu4data(j-2:j,17));
                    cu4data_condensed(r,18) = mean(cu4data(j-2:j,18));
                    r = r + 1;
                end
                if cu4data(j-1,14) == 0
                    cu4data_condensed(r,1:5) = cu4data(j,1:5);
                    if cu4data(j-1,6) > 0
                        cu4data_condensed(r,6) = mean(cu4data(j-2:j,6));
                        cu4data_condensed(r,11) = mean(cu4data(j-2:j,11));
                        cu4data_condensed(r,12) = mean(cu4data(j-2:j,12));
                    elseif cu4data(j-1,6) == 0
                        cu4data_condensed(r,6) = cu4data(j,6);
                        cu4data_condensed(r,11) = cu4data(j,11);
                        cu4data_condensed(r,12) = cu4data(j,12);
                    end
                    cu4data_condensed(r,7:10) = cu4data(j,7:10);
                    cu4data_condensed(r,13) = sum(cu4data(j-5:j,13));
                    cu4data_condensed(r,14) = mean([cu4data(j,14), cu4data(j-
2,14), cu4data(j-4,14)]);
                end
            end
        end
    end
end

```

```

                cu4data_condensed(r,15) = mean([cu4data(j,15),cu4data(j-
2,15),cu4data(j-4,15)]);
                cu4data_condensed(r,16) = mean([cu4data(j,16),cu4data(j-
2,16),cu4data(j-4,16)]);
                cu4data_condensed(r,17) = mean([cu4data(j,17),cu4data(j-
2,17),cu4data(j-4,17)]);
                cu4data_condensed(r,18) = mean([cu4data(j,18),cu4data(j-
2,18),cu4data(j-4,18)]);
                r = r + 1;
            end
        end
    end
end

end

% End cu4data_creation.m

```



```

% cu4plot.m
% Ben Weerts
%
% IMPORT cu4data4.mat FIRST!!!
%
% cu4data_condensed:
% 1 datenum
% 2 year
% 3 day
% 4 time
% 5 SA_RH
% 6 CFM
% 7 Product Air Temp
% 8 Product Air RH
% 9 Working Air Temp
% 10 Working Air RH
% 11 CU4 Power
% 12 L3M Power
% 13 Water
% 14 CU4_IN_T
% 15 INPUT-T
% 16 INPUT-RH
% 17 S-COOL-T
% 18 INPUT-DP

% INPUT START AND STOP DATES FOR PLOT (must be between 7/8/2011 13:06 and
% 4/23/2012 10:06):
Start = '7/20/2011';
Stop = '4/23/2012';

% Search cu4data_condensed for the above timestamps:
temp1 = datenum(Start);
temp2 = datenum(Stop);

for i = 1:85771
    if cu4data_condensed(i+1,1) < temp1
        beg = i;
    end
    if cu4data_condensed(i+1,1) < temp2
        finish = i;
    end
end

% beg = 35520;
% finish = 35540;

hold off
figure(1)
hold on

% COMMENT (Ctrl+R) or UNCOMMENT (Ctrl+T) for whichever variables you want
% to plot:

% % Supply Air Relative Humidity
% plot(cu4data_condensed(beg:finish,1),cu4data_condensed(beg:finish,5),'k')

```

```

% % CFM (airflow)
% plot(cu4data_condensed(beg:finish,1),cu4data_condensed(beg:finish,6),'k')
%
% CU4 Product Air Temperature (F)
plot(cu4data_condensed(beg:finish,1),cu4data_condensed(beg:finish,7),'b')
%
% % CU4 Product Air Relative Humidity
% plot(cu4data_condensed(beg:finish,1),cu4data_condensed(beg:finish,8),'k')
%
% CU4 Working Air Temperature (F)
plot(cu4data_condensed(beg:finish,1),cu4data_condensed(beg:finish,9),'r')
%
% % Difference between Product and Working air temperatures (F) (requires
% % dryout.m to be run beforehand)
% plot(cu4data_condensed(beg:finish,1),dryout(beg:finish,2),'g')
% plot(cu4data_condensed(beg:finish,1),0,'g')
%
% % CU4 Working Air Relative Humidity
% plot(cu4data_condensed(beg:finish,1),cu4data_condensed(beg:finish,10),'g')
%
% CU4 Power
plot(cu4data_condensed(beg:finish,1),cu4data_condensed(beg:finish,11)*20,'m')
%
% % L3M (Coolerado Panel) Power
%
plot(cu4data_condensed(beg:finish,1),cu4data_condensed(beg:finish,12)*10,'b')
%
% % Water Use (all Coolerados) (quarts/6min interval)
% plot(cu4data_condensed(beg:finish,1),cu4data_condensed(beg:finish,13))

% CU4 Input Temperature (F)
plot(cu4data_condensed(beg:finish,1),cu4data_condensed(beg:finish,14),'k')

% % AHU Supply Air Temperature (F)
% plot(cu4data_condensed(beg:finish,1),cu4data_condensed(beg:finish,15),'c')

% % AHU Supply Air Relative Humidity
% plot(cu4data_condensed(beg:finish,1),cu4data_condensed(beg:finish,16),'g')

% % South Cool Aisle Temperature (CU8) (F)
% plot(cu4data_condensed(beg:finish,1),cu4data_condensed(beg:finish,17),'g')

% % AHU Supply Air Dewpoint (calculated) (F)
% plot(cu4data_condensed(beg:finish,1),cu4data_condensed(beg:finish,18),'k')

datetick('x','mm/dd HH:MM','kepticks')
% set(figure(1),'Position',[10,500,1110,437])

% End cu4plot.m

```

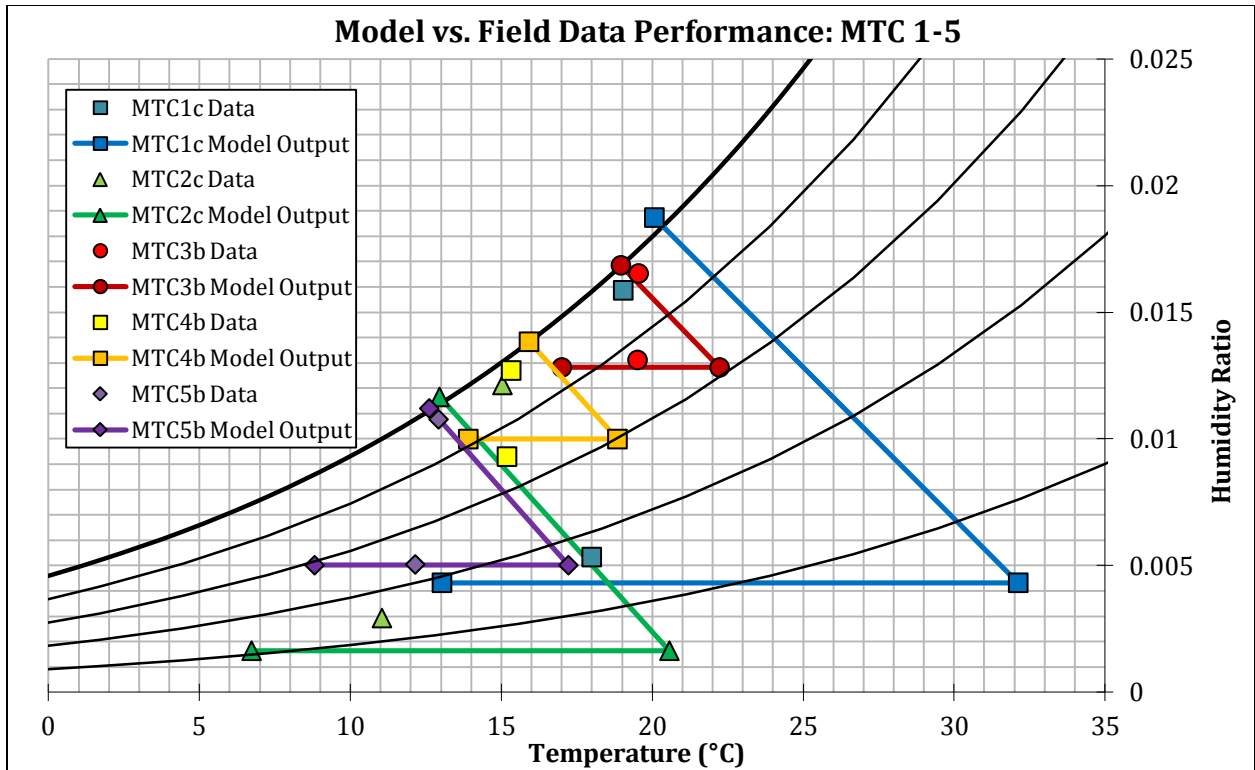


Figure 53. Model vs. Field Data Comparison: MTC 1-5

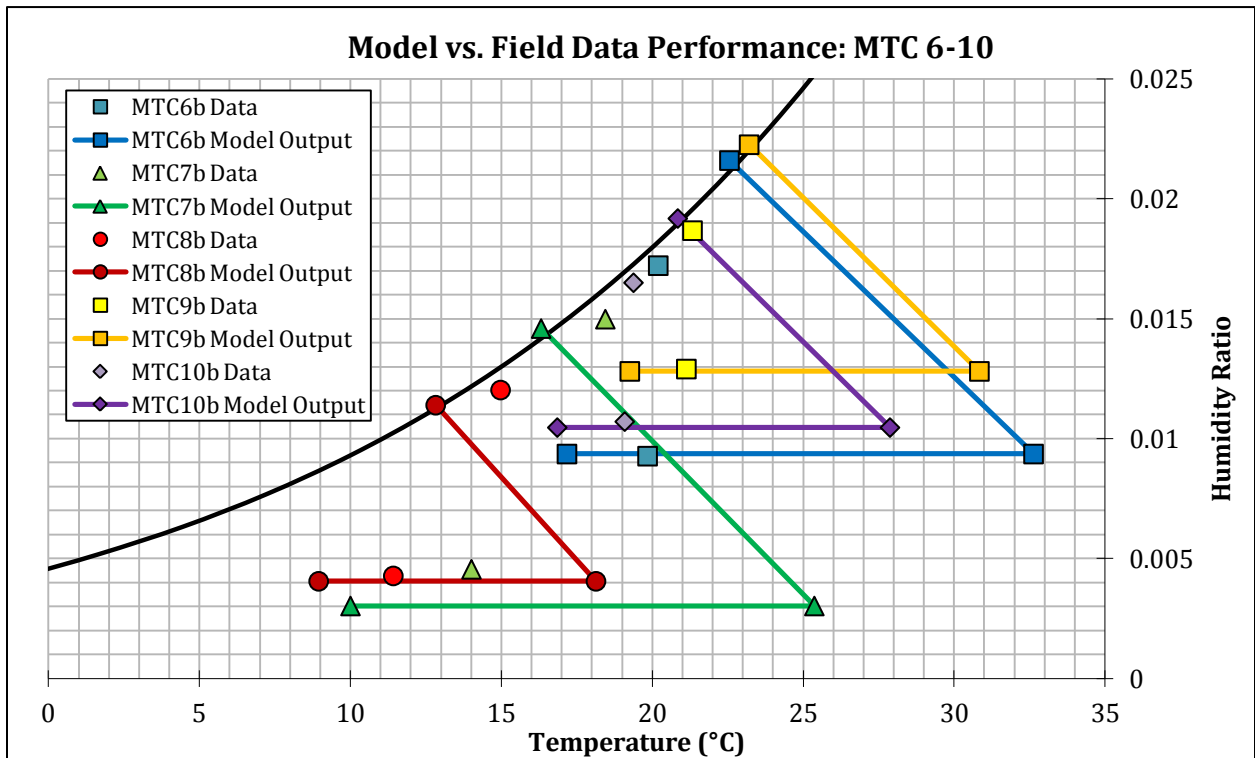


Figure 54. Model vs. Field Data Comparison: MTC 6-10

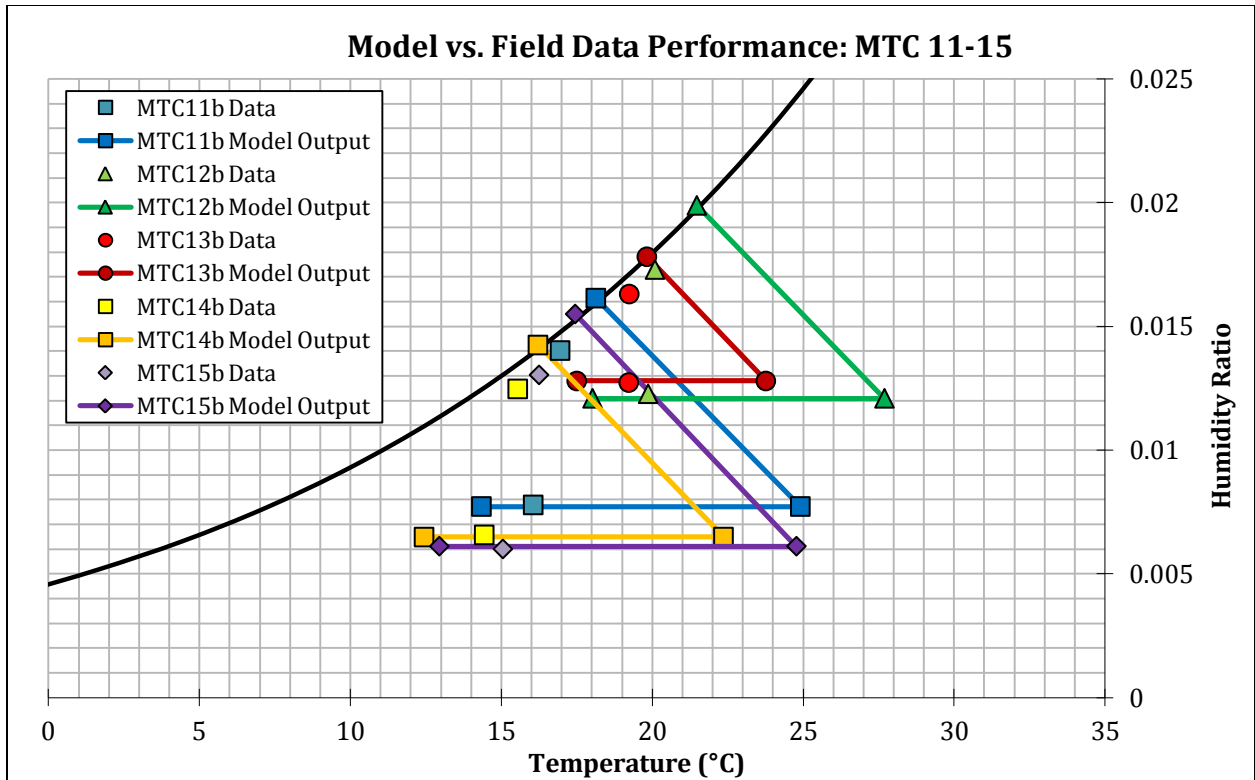


Figure 55. Model vs. Field Data Comparison: MTC 11-15

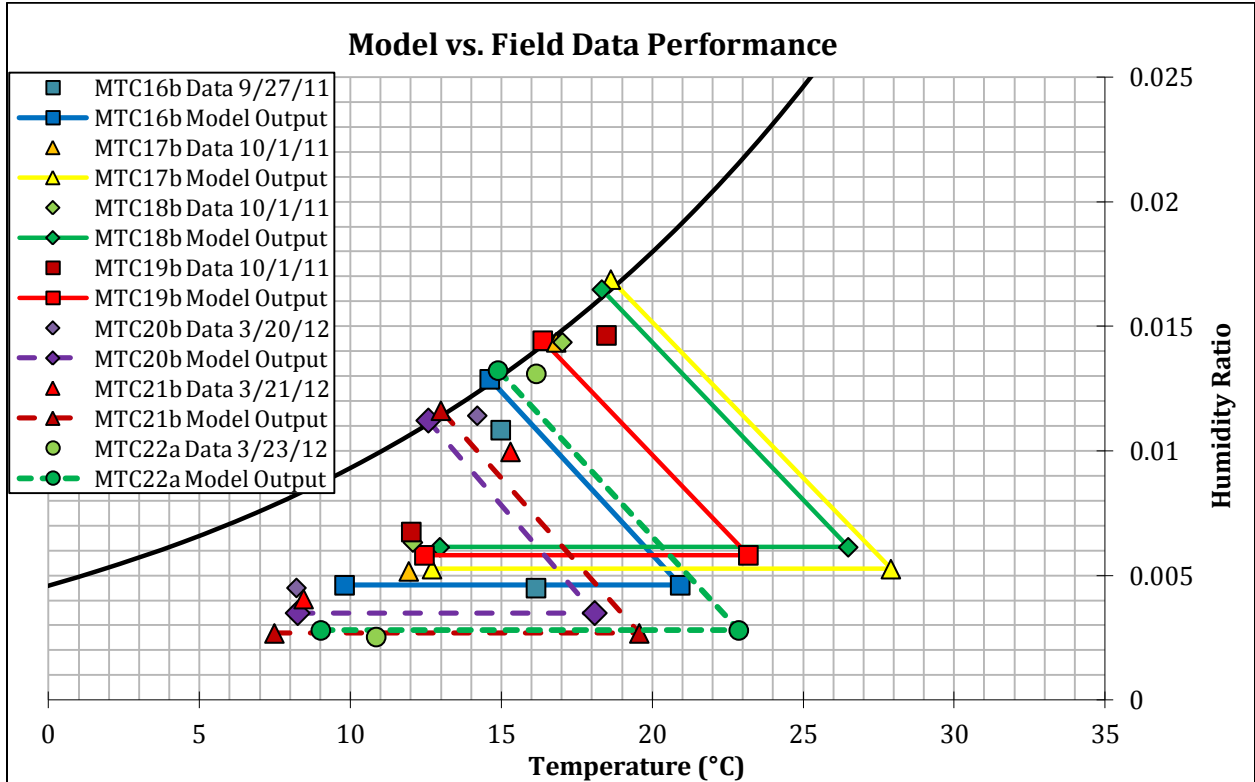


Figure 56. Model vs. Field Data Comparison: MTC 16-22

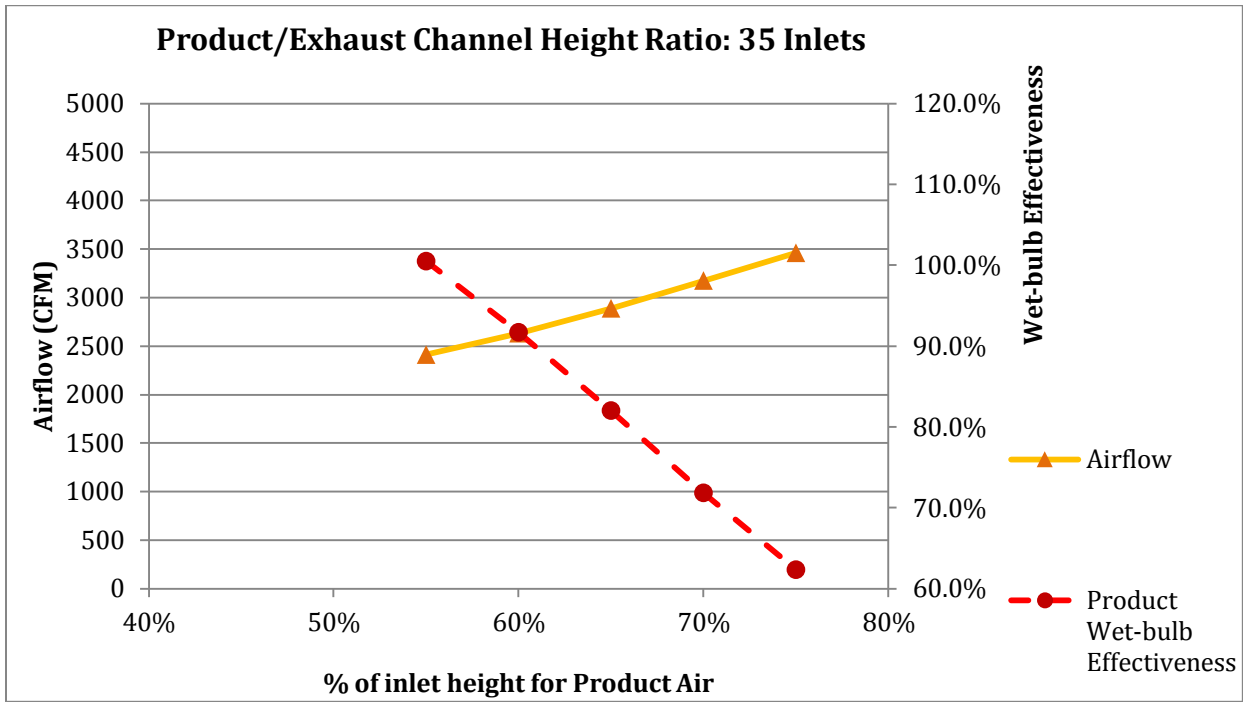


Figure 57. Airflow and wet-bulb effectiveness sensitivity to product height ratio; 35 inlets.

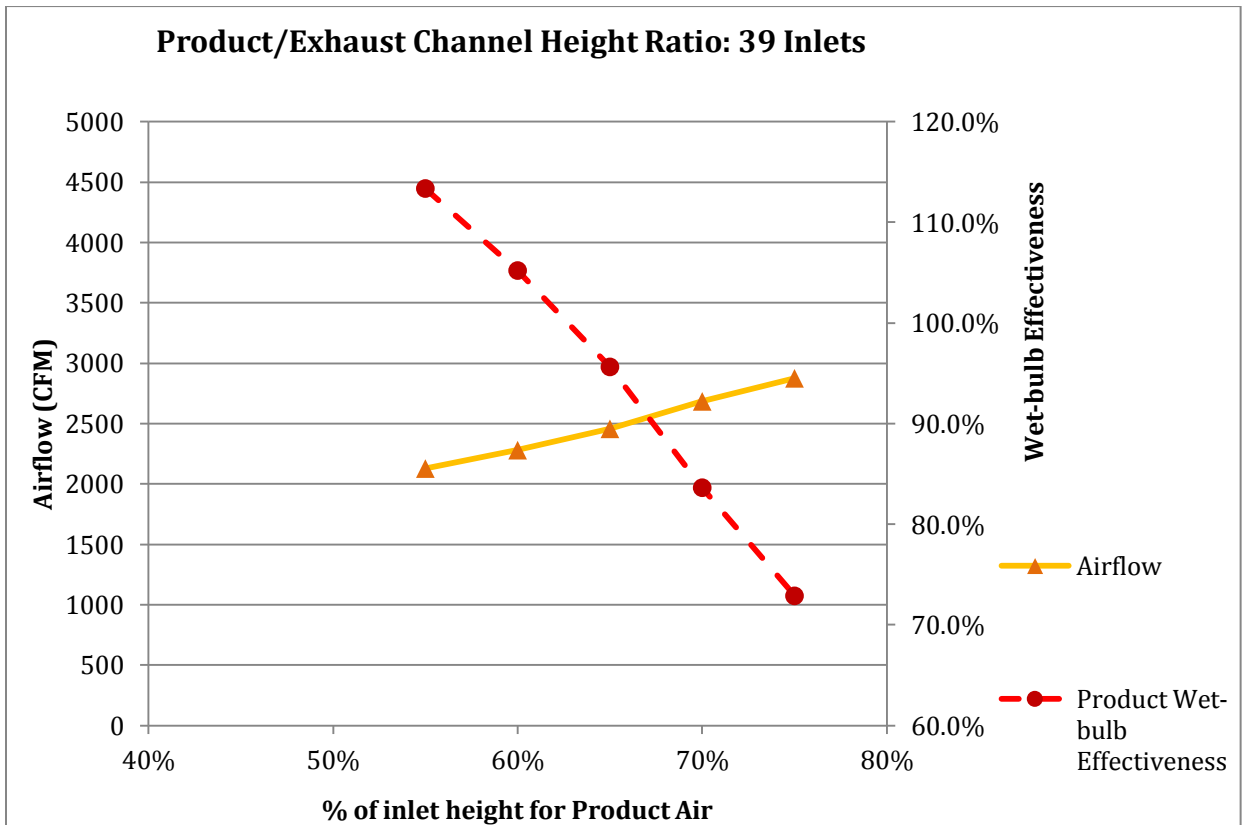


Figure 58. Airflow and wet-bulb effectiveness sensitivity to product height ratio; 39 inlets.

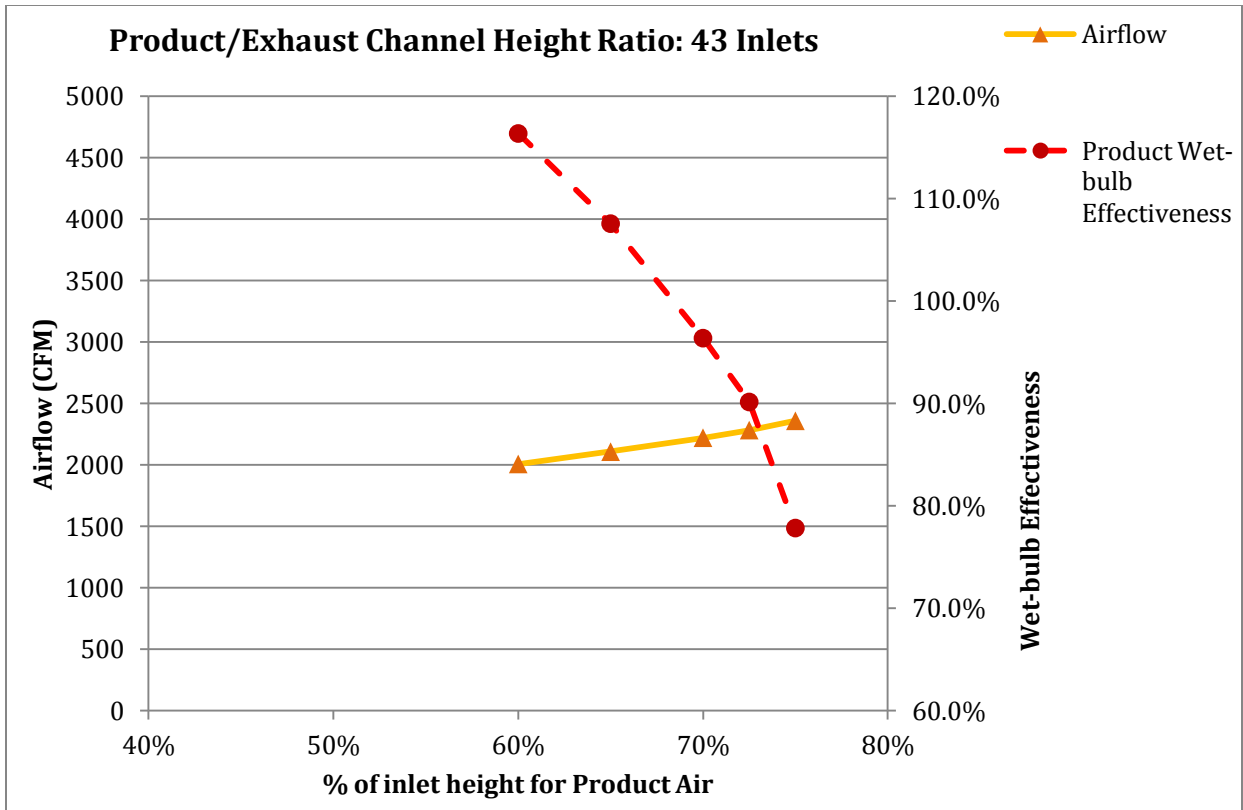


Figure 59. Airflow and wet-bulb effectiveness sensitivity to product height ratio; 43 inlets.

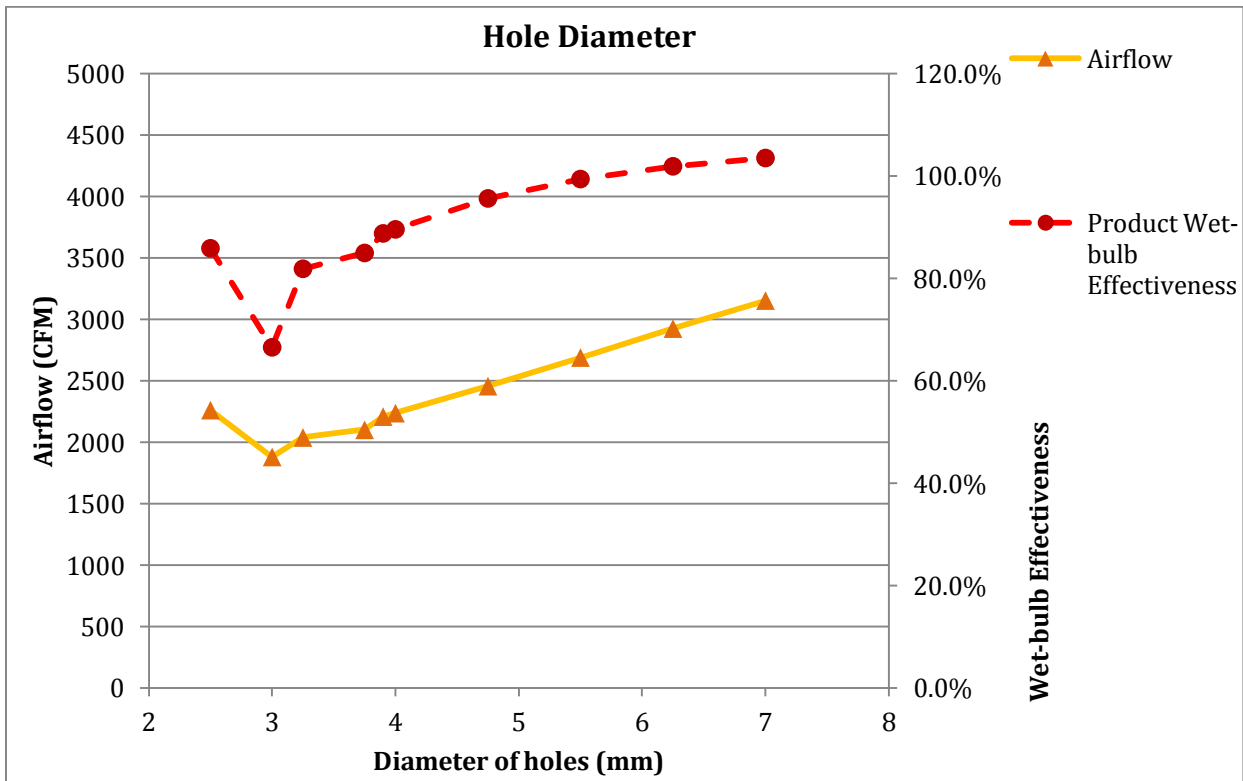


Figure 60. Airflow and wet-bulb effectiveness sensitivity to hole diameter.

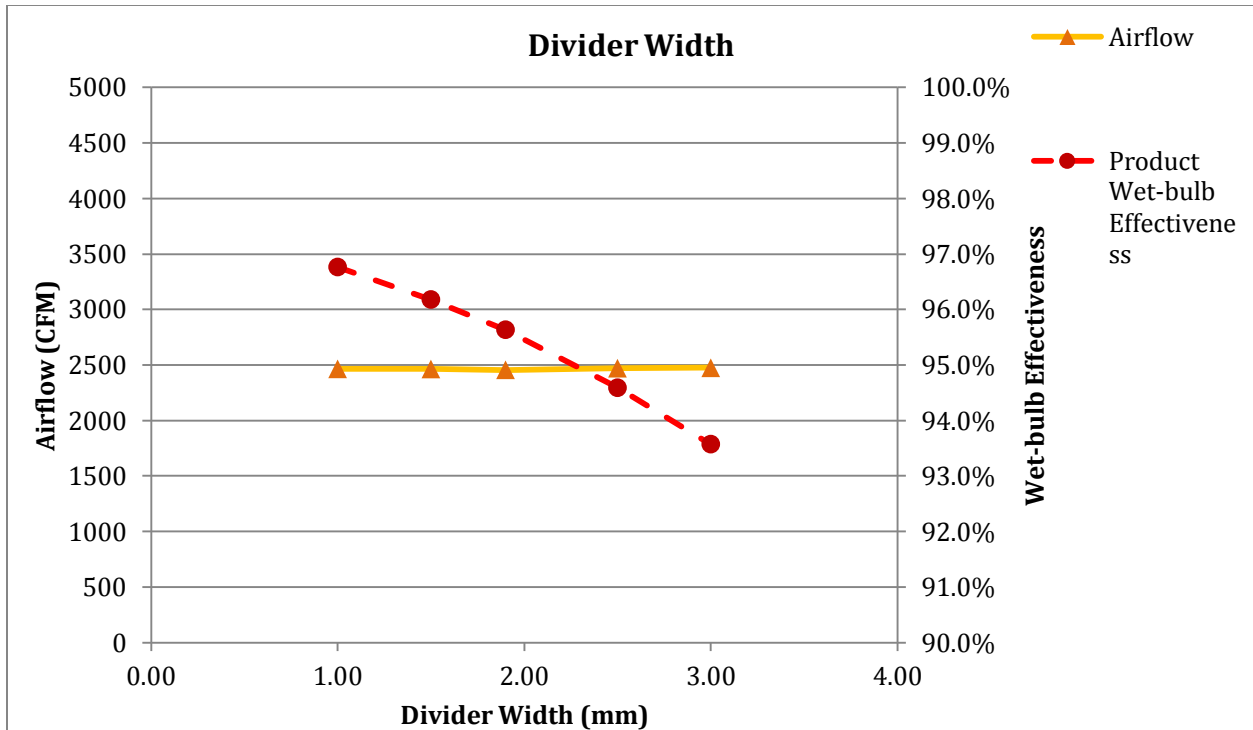


Figure 61. Airflow and wet-bulb effectiveness sensitivity to divider width.

Table 19. Divider widths used for sensitivity simulations.

Product Channel Divider Width (mm):	1.0	1.5	1.9	2.5	3.0
Working Channel Divider Width (mm):	0.8	1.3	1.6	2.3	2.8

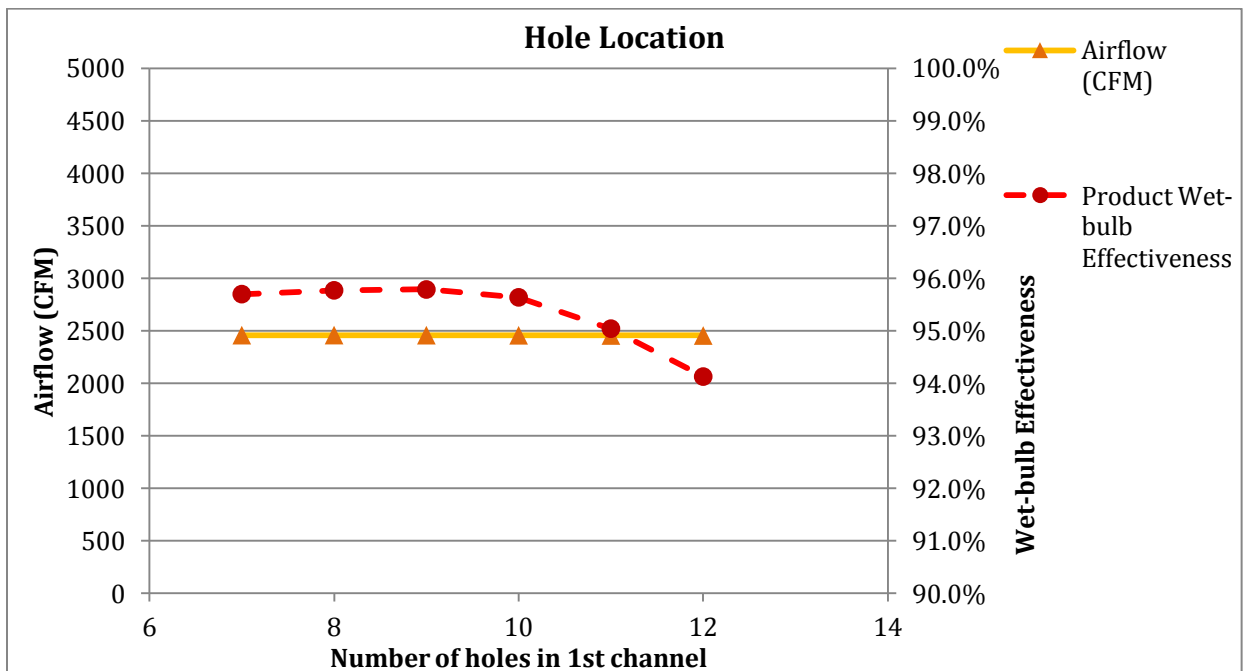


Figure 62. Airflow and wet-bulb effectiveness sensitivity to hole location.

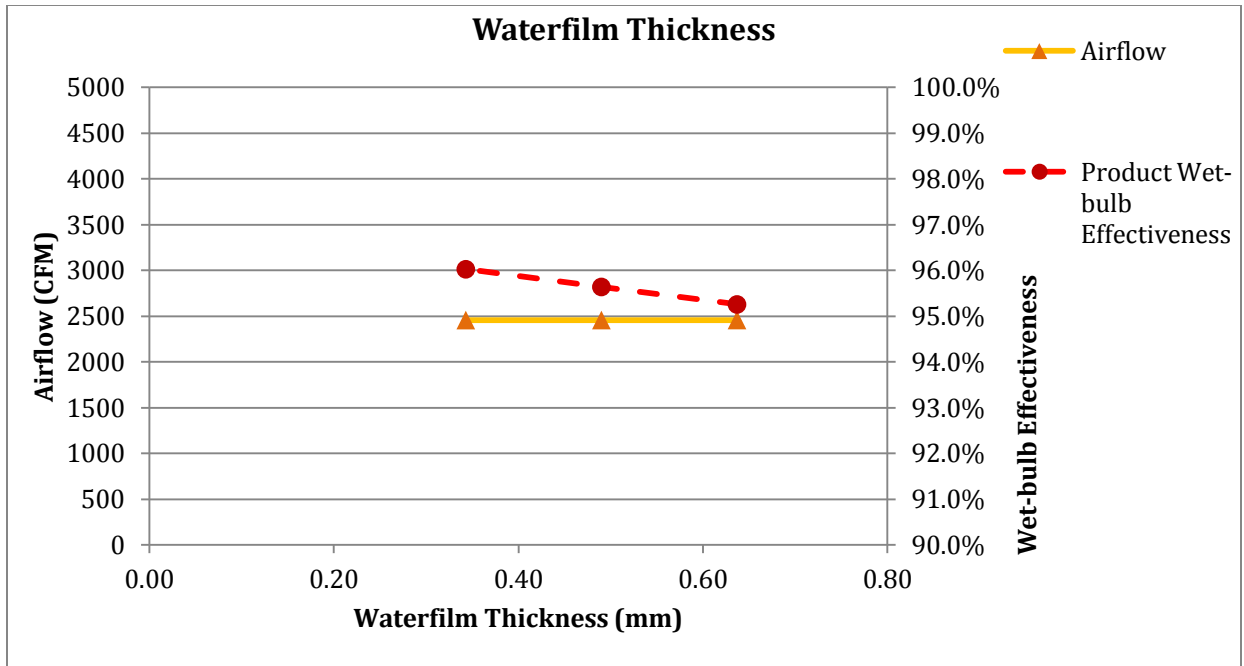


Figure 63. Airflow and wet-bulb effectiveness sensitivity to waterfilm thickness.

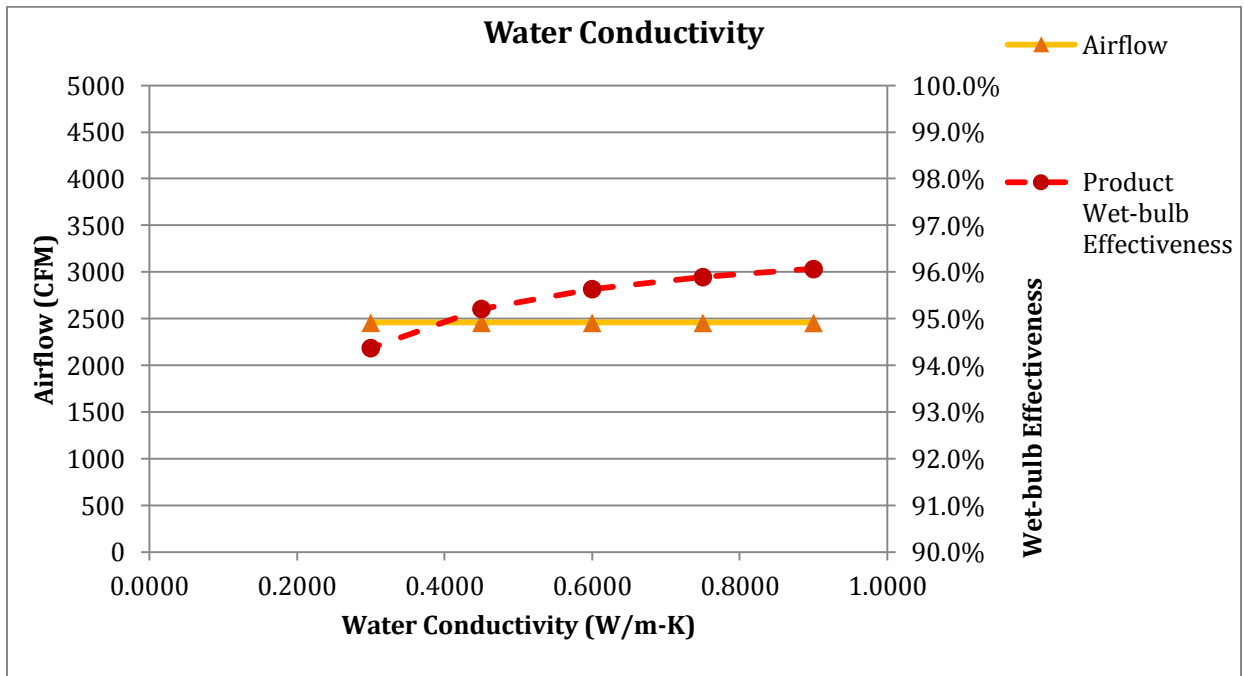


Figure 64. Airflow and wet-bulb effectiveness sensitivity to water conductivity.

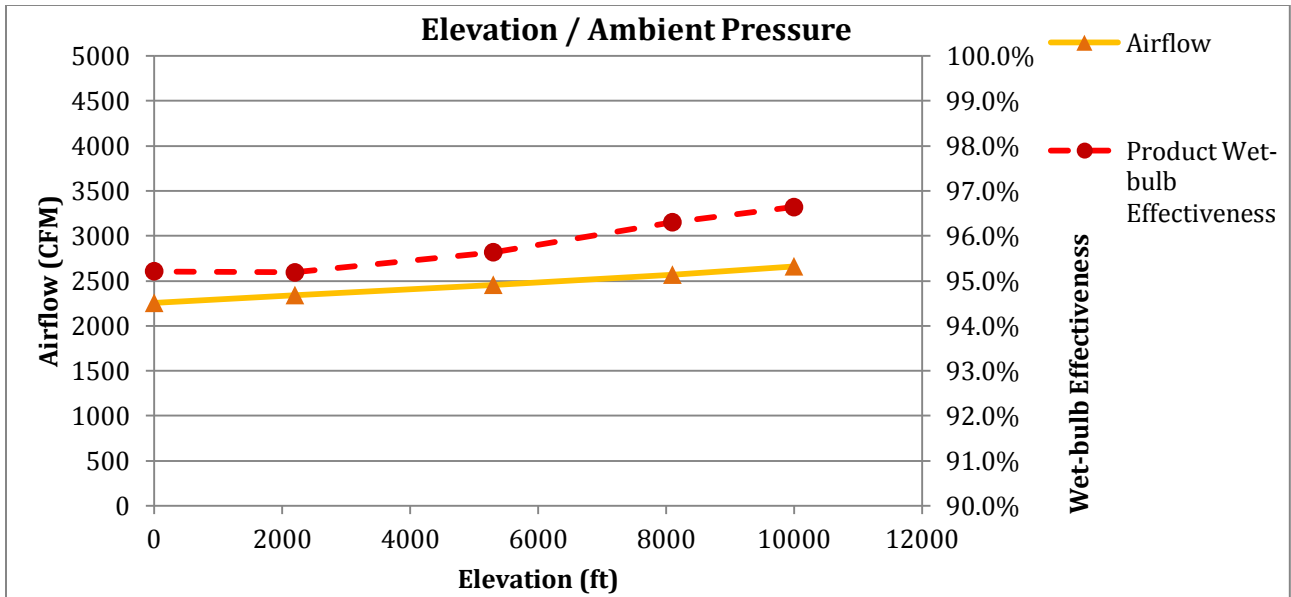


Figure 65. Airflow and wet-bulb effectiveness sensitivity to elevation.

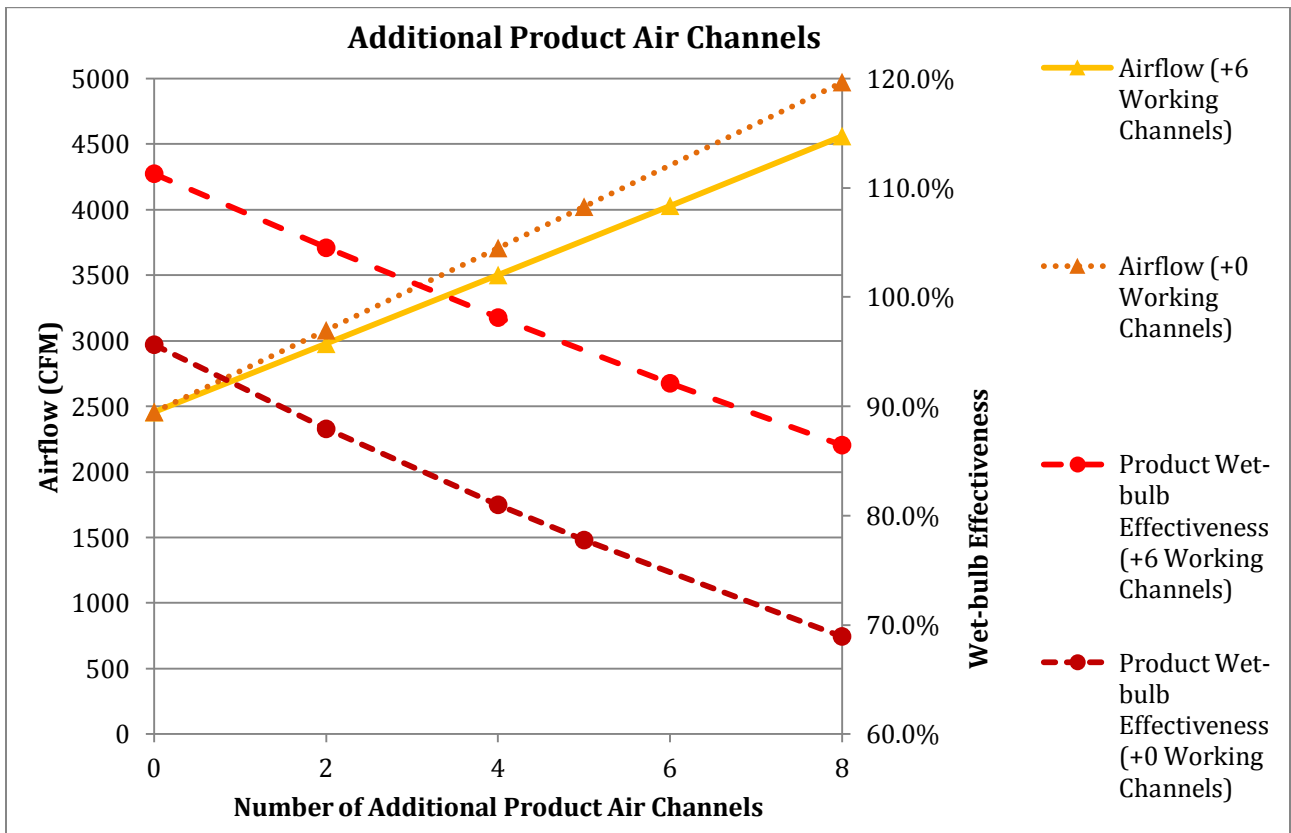


Figure 66. Airflow and wet-bulb Effectiveness sensitivity to additional product channels.